UNIVERSITEIT VAN PRETORIA
UNIVERSITY OF PRETORIA
YUNIBESITHI YA PRETORIA
Faculty of Natural and Agricultural Sciences

Genetic manipulation of *Plasmodium falciparum* for conditional knockdown of potassium channels

---

Fiona Els

13024133

Submitted in partial fulfilment of the requirements of the degree

Magister Scientiae

(Specialisation in Biochemistry)

In the Faculty of Natural and Agricultural Sciences
Department of Biochemistry, Genetics and Microbiology
University of Pretoria
Pretoria
South Africa

January 2021

UNIVERSITEIT VAN PRETORIA
UNIVERSITY OF PRETORIA
YUNIBESITHI YA PRETORIA
Faculty of Natural and Agricultural Sciences

SUBMISSION DECLARATION

I, Fiona Els, declare that the dissertation, which I hereby submit for the degree *Magister Scientiae* in the department of Biochemistry, Genetics and Microbiology at the University of Pretoria, is my own work and has not previously been submitted by me for a degree at this or any other tertiary institution.

SIGNATURE: 

DATE: 12/01/2021

UNIVERSITEIT VAN PRETORIA
UNIVERSITY OF PRETORIA
YUNIBESITHI YA PRETORIA
Faculty of Natural and Agricultural Sciences

DECLARATION OF ORIGINALITY

UNIVERSITY OF PRETORIA

FACULTY OF NATURAL AND AGRICULTURAL SCIENCES

DEPARTMENT OF BIOCHEMISTRY, GENETICS AND MICROBIOLOGY

DIVISION OF BIOCHEMISTRY

Full names of student: Fiona Els

Student number: 13024133

Title of work: Genetic manipulation of *Plasmodium falciparum* for conditional knockdown of potassium channels

Declaration:

1. I understand what plagiarism is and am aware of the University's policy in this regard.

2. I declare that this dissertation (e.g. essay, report, project, assignment, dissertation, thesis, etc.) is my own original work. Where other people's work has been used (either from a printed source, Internet or any other source), this has been properly acknowledged and referenced in accordance with departmental requirements.

3. I have not used work previously produced by another student or any other person to hand in as my own

4. I have not allowed, and will not allow, anyone to copy my work with the intention of passing it off as his or her own work

SIGNATURE 

DATE: 12/01/2021

Acknowledgements

First, I would like thank God for giving me the strength, determination and ambition to do this degree. He has been with me every step of the way, and I could not have done it without Him.

To the most important people in my life, my mom and sister, thank you. Mom, Dorothy Robinson, I struggle to find words to describe my gratitude towards you. You have supported me, motivated me and you have always been my biggest cheerleader. Without you, none of this would be possible. You are the strongest, and most beautiful person, and I am so grateful God chose you to be my mother. My sister and ultimate best friend, Megan. Thank you for your motivational words throughout the years. You make life fun and worthwhile! Thank you for being my forever best friend and that I can always count on you.

To my grandparents, Robbie and Dollie Robinson, without you, none of this would've been possible. You are my role models, and I only hope to be as kind, loving and compassionate as you are. Thank you for always being ready to help, and playing such an integral part in my life.

To my friends in M^2PL, Janie, Meta, Tayla and Michel. Thank you for crying with me if an experiment failed. Thank you for the coffee and cake dates and always being a pillar of support. Janie and Meta, I never thought I would find such ambitious people to share MSc with. Thank you for supporting me when I was at my lowest, and helping me pick up the pieces. I will be forever grateful to you. Tayla and Michel, thank you for stepping in when I couldn't go back to the lab during a pandemic, and always sharing experiences in the lab. Thank you for your trouble, I appreciate you!

To the ultimate lab guru, Dr Elisha Mugo, thank you for your endless amount of patience, advice and wisdom. Your opinion has and will always be highly appreciated and valued.
I would also like to thank the UP ISMC and NRF-Grantholder linked bursary (from Professor Birkholtz) for funding my studies the past two years.

Lastly, I would like to thank my supervisor, Dr Niemand (Department of Biochemistry, Microbiology and Genetics), for giving me the opportunity to do this degree. Your advice and support means the world to me, and I will be forever grateful for your caring heart and kind words. I would also like to thank my co-supervisor, Prof. Birkholtz (Department of Biochemistry, Microbiology and Genetics) for her input and assistance during my research.

Summary

Malaria is a devastating disease with the most severe cases caused by the *Plasmodium falciparum* parasite. Despite it being a preventable disease, mortality rates remain a concern due to emerging drug resistance. Ion channels have been recognized as important therapeutic targets for treating numerous illnesses, since the maintenance of the ion concentration gradient regulates a wide range of physiological processes. Studies on Na^+ transporter PfATP4 have revealed its potential as an effective drug target, and disrupts the K^+ gradient with an ionophore, such as salinomycin, kills the parasite throughout the intra-erythrocytic stages.

K^+ channels are essential to maintain the electrochemical gradient in a eukaryotic cell. In *P. falciparum*, two K^+ channels, PF3D7_1227200 (K1) and PF3D7_1465500 (K2), have been identified. Both K^+ channels are expressed throughout the asexual intra-erythrocytic stages, whereas only K2 is expressed in the sexual intra-erythrocytic stages. However, the essentiality and localisation of these channels throughout intra-erythrocytic development is unknown.

In this study, it was attempted to genetically modify K1 and K2 by adding a green fluorescent protein tag and conditional knockdown mechanism to investigate localisation and prove their essentiality in *P. falciparum* in future studies. This was done by cloning C-terminal gene fragments into two plasmid systems that contain an inducible riboswitch which regulates the level of mRNA and ultimately leads to reduced levels of protein produced, thus knocking down the protein. An original *glmS* and a modified SLI *glmS* system was compared. The modified SLI *glmS* system use a double selection mechanism and thus produces modified parasites at a faster rate than the original *glmS* system.

Recombinant parasite lines were produced for K2, but not for K1. The original *glmS* system proved to integrate faster into the genome compared to the modified SLI *glmS* system. The successful construction of these recombinant lines allows for subsequent studies to determine essentiality and localisation of K2 in *P. falciparum* during intra-erythrocytic development. This study provides the basis for future studies that may develop K^+ homeostasis as an intra-erythrocytic drug target.

Table of Contents

List of figures

List of tables

List of abbreviations

ACT	Artemisinin combination therapy
AID	Auxin-inducible degron
ATc	Anhydrotetracycline
BK K^+ channel	Large conductance potassium channel
CRISPR	Clustered regularly interspaced short palindromic repeats
DD	Destabilisation domain
DHFR	Dihydrofolate reductase
DiCre	Dimerisable Cre
E_m	Membrane potential
FKBP	FK506 binding protein
FRB	FKBP-rapamycin binding domain
GFP	Green fluorescent protein
GlcN6P	Glucosamine-6-phosphate
glmS gene	Glucosamine-6-phosphate synthethase
glmS ribozyme	Glucosamine-6-phosphate riboswitch ribozyme
GOI	Gene of interest
GTS	Global Technical Strategy
HA	Heamaggluttin
HEPES	4-(2-hydroxyethyl)-1-piperazineethanesulfonic acid
HMM	Hidden Markov Model
IDC	Intra-erythrocytic developmental cycle
IPTG	Isopropyl β- d-1-thiogalactopyranoside
IPTp	Intermittent preventive treatment of malaria in pregnancy
IRS	Indoor residual spraying
ITN	Insecticide treated net
K1	*Plasmodium falciparum* potassium channel 1
K2	*Plasmodium falciparum* potassium channel 2
MTP	Membrane transport protein
NPP	New permeation pathway
PfATP4	*P. falciparum* Na^+ ATPase
PfvapA	Vacuole (V-type) H^+ ATPase
RE	Restriction enzyme
SDS	Sodium dodecyl sulfate
TCP	Target candidate profile
TetO	*tet* operator sequences
TetRep	Tetracycline transcription repressor
TMD	Transmembrane domain
TMHMM	Transmembrane Helices; Hidden Markov Model
TPP	Target product profile
UTR	Untranslated region
WHO	World Health Organisation

1 Chapter 1: Introduction

1.1 Malaria as a global burden

Malaria is one of the most infectious parasitic diseases, affecting millions of people around the world. In 2019, there were 229 million malaria cases, with approximately 409 000 deaths [1]. People from disadvantaged and poor communities without access to quality health care facilities are most affected by malaria. Pregnant women and children under five years of age are most vulnerable and 35 % of pregnant women were exposed to malaria in the African region in 2019 [1].

Plasmodium parasites, are single-cell eukaryotes in the apicomplexa phylum. They are the causative agent of malaria, spread by female *Anopheles* mosquitos. Six different species of the genus *Plasmodium*, namely *P. vivax*, *P. knowlesi*, *P. ovale*, *P. malariae, P. cynomolgi* and *P. falciparum* all cause for human malaria [2, 3]. *P. vivax* is the most common in humans living in dense tropical and temperate environments [4]. *P vivax* is phylogenetically similar to *P. knowlesi* and morphologically similar to *P. ovale and P. malariae*. A unique feature of the *P. vivax* life cycle is the latent hepatic form, or hypnozoites, that can lead to relapse of the disease when the parasite re-enters the bloodstream. *P. knowlesi* is found in south east Asia. Its natural host is *Macaca fascicularis* (‘kra’ monkey). Whether *P. ovale* also forms hypnozoites is still under debate [5], malaria caused by this species however rarely results in death [6]. *P. malariae* often results in kidney disorders [7]. *P. falciparum* is responsible for most malaria cases in humans and has developed partial resistance to existing drugs [1]. The WHO African Region accounted for about 94 % of cases globally. Countries with the highest number of malaria cases include Nigeria (27 %), Democratic Republic of the Congo (12 %), Uganda (5 %), Mozambique (4 %), and Niger (3 %) [1].

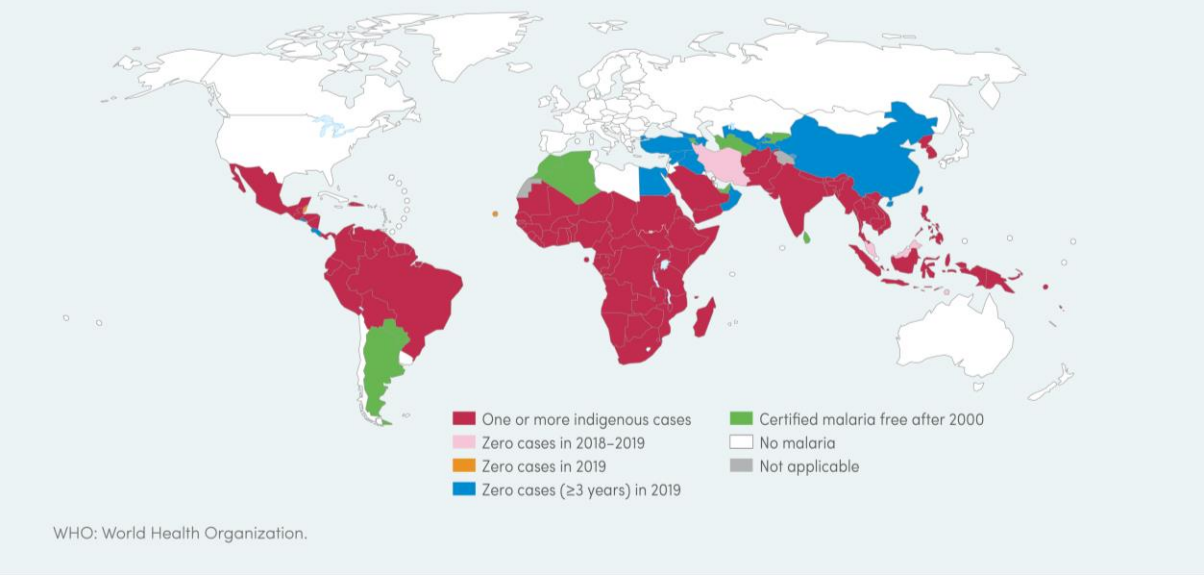

Figure 1: The 2018 global malaria case incidence status by country. Global malaria case profiles of countries where malaria is present (maroon), no new cases in 2018-2019 (pink), no new cases in 2019 (orange) and no new cases in the past three years (blue). Several countries have been certified malaria free (green) or have no malaria cases (white). Source: WHO World Malaria Report 2020 [1] (URL: https://www.who.int/teams/global-malaria-programme/reports/world-malaria-report-2020).

From 2000 to 2019, ten countries eliminated malaria, and 21 countries achieved three consecutive years of zero indigenous malaria cases [1] (Figure 1). This led to the World Health Organisation (WHO) Global Technical Strategy (GTS) for Malaria. Here, an ambitious goal was set to reduce both the malaria case incidence and the mortality rates by 90 %, prevent malaria resurgence in all malaria-free countries, and eliminate malaria in at least 35 countries [8]. Unfortunately, due to a recent resurgence in malaria case numbers, the GTS interim goals for 2020 on morbidity and mortality were not achieved. To achieve the GTS goal for 2030 (90 % reduction in malaria case incidence and mortality rate, compared to 2015), urgent interventions such as innovative and sustained malaria control strategies are required.

1.2 The *P. falciparum* life cycle

The *P. falciparum* life cycle (Figure 2) occurs in two organisms; the mosquito plasmid and the human host [9]. A female *Anopheles* mosquito transmits the *P. falciparum* parasite by taking up sexual stage parasites (gametocytes) from an infected human host during a blood meal and after development in the mosquito gut, the sporozoites are injected into the blood vessels of a new human host [9]. During the pre-erythrocytic cycle, the sporozoites migrate to the liver and invade hepatocytes where, after five to eight days they develop into multinucleated schizonts. The schizonts bursts, releasing merozoites into the bloodstream where they invade erythrocytes.

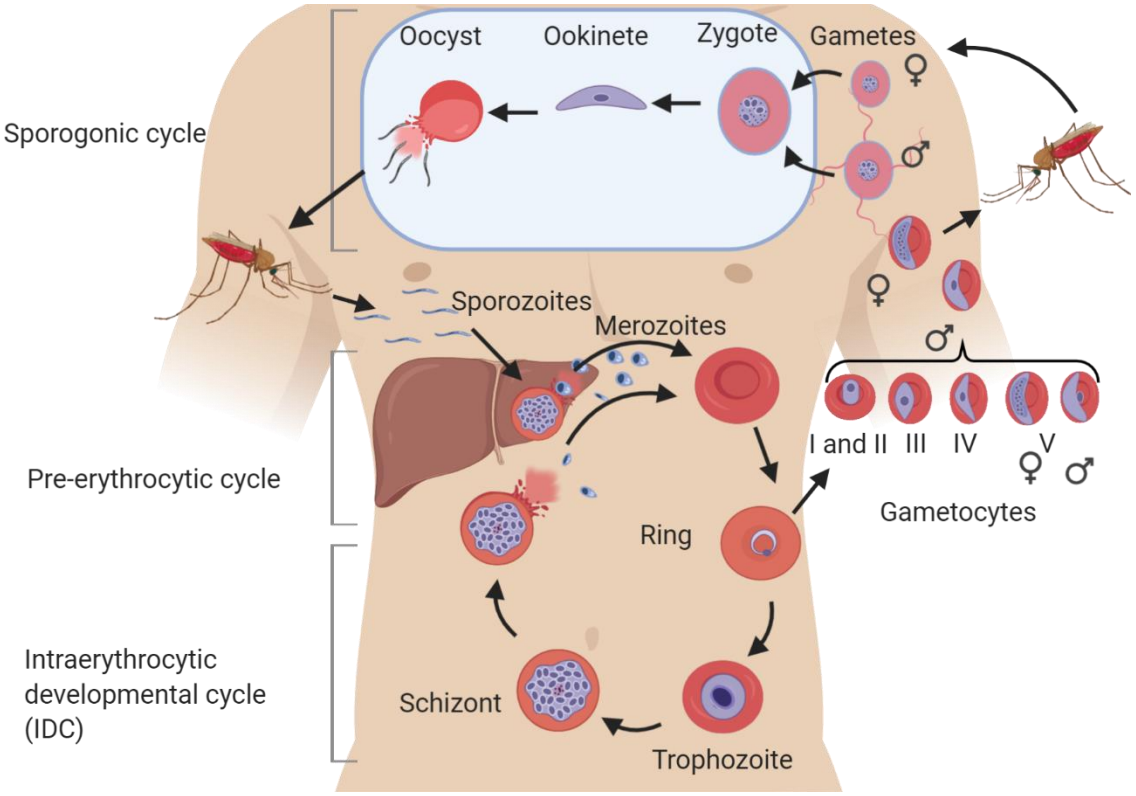

Figure 2: The life cycle of *P. falciparum* parasites. During a blood meal, the female *Anopheles* mosquito injects sporozoites into the blood vessel of a human, where the parasite develops through the pre-erythrocytic cycle in the liver, followed by the intra-erythrocytic cycle. In the intra-erythrocytic cycle, the parasite develops into a ring, trophozoite and schizont stage parasite, after which the erythrocyte bursts releasing merozoites into the blood stream. Merozoites invade erythrocytes repeating the asexual intra-erythrocytic cycle. A small portion of parasites commit to differentiate into gametocytes, of which stage V gametocytes can be taken up by a mosquito. This leads to the sporogonic cycle that occurs in the mosquito plasmid where the gametocytes develop into gametes. Gametes form a zygote which elongates into an ookinete and develops into an oocyst. The oocyst then bursts, releasing sporozoites that travel to the mosquito salivary glands. The entire life cycle is repeated when an infected *Anopheles* mosquito feeds again injecting sporozoites stage parasites into the human host. This work 'The life cycle of *P. falciparum*' was compiled using graphic components from BioRender. (https://app.biorender.com/).

The intra-erythrocytic developmental cycle (IDC) is observed over 48 h in *P. falciparum* [9, 10]. Upon entering the erythrocyte, a merozoite develops into three main stages that are morphologically distinct from each other: the ring-stage parasite, followed by the trophozoite- and schizont-stage parasites [11]. Trophozoites are the most metabolically active with roles such as ingesting erythrocyte cytoplasm via the cytostome, digesting haemoglobin and forming haemozoin (malaria pigment) to avoid the toxicity of the free haem that results from haemoglobin digestion [9, 12]. As a trophozoite parasite develops, the nucleus divides and schizogany commences [9]. The schizont undergoes asexual nuclear division and bursts, releasing between six and thirty daughter merozoites that invade other erythrocytes and repeat the IDC [11]. This repeated erythrocytic invasion and bursting of erythrocytes results in malaria symptoms such as anaemia, fever and chills [2]. Within the first 20 h of each IDC, a

fraction of the ring-stage parasites will commit to gametocytogenesis, the process of differentiation into sexual intra-erythrocytic parasites [13].

Gametocytogenesis is an irreversible step in the life cycle of malaria parasites resulting in differentiated gametocytes, the long-lived sexual forms of the parasite [14]. Gametocytogenesis produces male and female gametocytes that take eight to ten days to reach morphological maturity. This is crucial for parasite survival and ensures malaria transmission [15, 16]. Gametocyte maturation has been classified in five morphologically recognisable stages: the early gametocyte stages (stage I-III) and late gametocyte stages (stage IV-V).

The morphology of stage I and II gametocytes closely resembles that of the trophozoite stage parasite, except that they have a single nucleus and occupy most of the erythrocyte. The gametocytes remain roughly spherical in these stages [15]. From stage II-III, *P. falciparum* gametocytes form a characteristic crescent shape [15, 17]. By stage III, the parasite adopts a D-shape and has one region that is straightened and extended. The sex of gametocytes can morphologically be determined when the parasite enters stage III. In stage IV further elongation is observed and the host cell is visible only as a thin layer around the gametocyte. Stage I-IV gametocytes sequester in bone marrow and are absent in blood circulation [16]. Stage V gametocytes appear in a characteristic crescent shape [18] and reappear in blood circulation to be taken up by the mosquito plasmid and initiate the sporogonic cycle. Within the sporogonic cycle, male and female gametocytes further develop into gametes. The genome replicates three times in male gametocytes, producing 8 flagellated microgametes that seek out the female macrogametes [2, 14, 18]. This is essential for diploid zygote formation in the mosquito in the subsequent stages of the life cycle. Male and female gametes fuse to form a diploid zygote, which elongates into an ookinete [2, 9]. The ookinete moves through the mosquito gut membrane, and forms a cyst-like body called the oocyst [16]. Sporozoites are produced within the oocyst, which bursts releasing thousands of sporozoites. The sporozoites migrate to the salivary gland of the mosquito and are injected into the human host when the mosquito takes a blood meal, thus repeating the cycle [9]. This combination of asexual development in the human host and sexual development in the mosquito vector is mediated by biological processes that may be targeted to control the disease transmission and development.

1.3 Malaria control strategies

To eliminate malaria both the mosquito vector and the malaria parasite are essential must be controlled [19]. Both infections and transmissions would need to be reduced, while also treating existing malaria patients.

1.3.1 *Anopheles* vector control

The overall goal of vector control is to reduce the vector population to below the critical threshold for transmission. Vector control can contribute to the eradication of malaria by i) reducing the rate at which future infections arise from currently infected vectors; ii) targeting vector species not affected by the current vector control strategies and iii) improving the effectiveness of current insecticide interventions [20]. The four classes of insecticides used in vector control include pyrethroids, organochlorides, carbamates and organophosphates [21]. Pyrethoids are the only class approved for use in insecticide-treated mosquito nets (ITNs) [22] that prevent transmission by physically blocking human-mosquito interaction [23]. Due to emerging resistance to pyrethoid, indoor residual spraying (IRS) depend on organochlorides, carbamates and organophosphates for vector control [24]. IRS involves the annual application of an insecticide to surfaces where the mosquito vector might rest after a blood meal, and is the main vector control strategy used in South Africa [25]. However, the efficacy of vector control is reduced by insecticide resistant *Anopheles* mosquitos [26, 27]. Simultaneous *Plasmodium* parasite control is thus needed for malaria elimination.

1.3.2 *Plasmodium* parasite control

Parasite control aims to target different *Plasmodium* parasite life stages to disrupt the parasite development cycle and/or transmission [28]. The parasite can be controlled in the different life stages such as the pre-erythrocytic stage where the infection is first established in the liver. The intra-erythrocytic stage is where the parasite enters erythrocytes and starts asexual replication. Lastly, the sexual stage parasites transmitted to the mosquito can be targeted. Parasite control can thus refer to prevent infections or to clear established infections and preventing transmission within a population.

1.3.2.1 Strategies to prevent the *Plasmodium* parasite from establishing an infection

1.3.2.1.1 Vaccine development

Vaccines are used to prime the immune system against a specific pathogen. Four vaccine approaches have been explored to prevent malaria infections: i) vaccines against whole sporozoite or sporozoite proteins, ii) liver-stage vaccine iii) intra-erythrocytic stage vaccine and iv) transmission-blocking vaccine [29]. Vaccine development has a particular challenge because of the adaptable nature of the parasite, parasite complexity, antigenic variation and the limited information on human immune response to parasite infection [30].

An advanced vaccine candidate RTS,S/AS01, targets the *P. falciparum* circumsporozoite protein [11]. RTS,S/AS01 is the first vaccine to be tested in Phase III clinical trials and the first to be assessed in routine vaccination programs in malaria-endemic areas [31]. It has an efficacy of 30 % protection against clinical malaria and 26 % protection against severe malaria [32]. Whole sporozoites vaccines contain live attenuated sporozoites such as by radiation. The PfSPZ vaccine of this category protects African adults for an entire malaria season [33]. ChAd63 MVA ME-TRAP is a liver-stage vaccine in Phase IIb field trials that use $CD8^+$ T cell responses to target infected liver cells by using a viral plasmid [34]. Vaccines that target intra-erythrocytic stage parasites target proteins such as PfRH5 on the merozoite surface induce antibodies [35], but proved ineffective in clinical trials [29]. Another pre-erythrocytic vaccine has recently been reported and has shown 77 % efficacy under 450 participants in a clinical trial in Burkina Faso [36]. This vaccine (R21/MM) is administered prior to the malaria season and has a favourable safety profile [36]. Transmission-blocking vaccines target sexual stage parasites. For example, antibodies against antigens Pfs48/45 and Pfs230 on the surface of sexual stage parasite has been investigated in pre-clinical trials, which can be used in the treatment of malaria [37].

1.3.2.1.2 Chemoprophylaxis

In the absence of an effective vaccine, liver-stage *Plasmodium* parasites may instead be targeted by chemoprophylaxis. Appropriate drugs are presribed to people planning to visit a high transmission area for less than 4 months. In South Africa, mefloquine, doxycycline and atovaquone-proguanil are used. Mefloquine binds to the cytoplasmic ribosome (Pf80S) inhibiting protein synthesis [38]. It is the only drug recommended for pregnant women [11, 39]. Doxycycline also inhibits protein synthesis by binding to the 30S ribosomal subunit [40]. Doxycycline is not used in children under eight years of age due to the risk of yellow tooth discolouration and dental enamel hypoplasia [41]. Atovaquone inhibits ATP synthesis and the

parasite mitochondrial electron transport, whereas the active proguanil metabolite, cycloguanil, inhibits *P. falciparum* dihydrofolate reductase (DHFR) [42]. Proguanil works with atovaquone, by lowering the concentration of the latter needed to collapse the mitochondrial potential [42].

1.3.2.2 Chemotherapies to clear established *Plasmodium* infections and prevent transmission within a population

Three families of antimalarial drugs developed to block intra-erythrocytic parasites include quinolines (quinine, primaquine, chloroquine and mefloquine), artemisinin derivatives and antifolates (sulfadoxine and pyrimethamine) [43]. Intra-erythrocytic stage parasites degrade haemoglobin for parasite proliferation [11, 44], and quinolines interfere with this haem degradation process in the food vacuole. Artemisinin is an endoperoxide and uses free radicals to eliminate the parasite. Artemisinin is activated by the haem-iron in the intra-erythrocytic parasite, and cleaves the endoperoxide of the artemisinin to form a free radical which target malaria parasites [45], but has a very short plasma half-life [46]. To combat this, artemisinin (or derivatives) combined with drugs that has a longer half-life such as chloroquine or lumefantrine. This is known as artemisinin combination therapy (ACT) and is currently the WHO recommended first line standard of treatment for malaria infections [47]. Antifolates target enzymes involved in the folate pathway, such as DHFR or dihydropteroate synthase [11]. Resistance toward chloroquine [48], ACTs [49, 50], and antifolates [51] have been reported. The WHO also recommends intermittent preventative treatment in pregnancy (IPTp) to treat pregnant women, regardless of malaria infection status [52]. Typically, sulfadoxine-pyrimethamine are used for IPTp from the second trimester onwards. This drug works by blocking the ability of the parasite to use folic acid and preventing the synthesis of tetrafolate [53].

Transmission-blocking chemotherapies target late stage (stage V) sexual parasites (gametocytes) to prevent infection. The biology of gametocytes is currently not fully understood, which aids in the challenge of developing gametocyte-blocking compounds. Compounds active against asexual parasites are typically inactive against late stage gametocytes [54]. Hence, the parasite can still be transmitted to the mosquito vector [55]. Of the currently used antimalarial chemotherapies, primaquine (PQ) is highly effective against gametocytes and a single dose of 0.25 mg/kg reduces transmission of the gametocytes and has been recommended by the WHO in areas approaching elimination [56]. However, PQ may cause haemolytic anaemia [56] or be toxic to individuals with a glucose-6-phosphate-dehydrogenase (G6PD) deficiency.

Artesunate and artemether reduce gametocyte transmission, but are unable to eliminate late stage sexual parasites, questioning their use in clinical settings [57-59]. Methylene blue is another drug that interferes with gametocyte development [60], but may be toxic and cause haemolysis in G6DP deficient patients. Side effects include green urine or blue sclera [61]. Therefore, parasites have shown resistance to currently available chemotherapies for malaria, while chemotherapies that block transmission either target early sexual stage parasites or have safety concerns. Novel compounds that target both asexual and sexual stage parasites are required to prevent disease, and block transmission from human to mosquito. Studying the biology of the *P. falciparum* could help identify new biological targets. One such biological target is ion homeostasis.

1.4 Ion homeostasis in intra-erythrocytic *P. falciparum* parasites

Concentrations of inorganic cations and anions differ across the plasma membrane of eukaryotic cells. In healthy mammalian cells extracellular concentration of Na^+, Ca^{2+}, and Cl^- is higher than in the cytoplasm, while K^+ has the opposite gradient. The ion concentration gradients across the plasma membrane are maintained by ATP-powered pumps that transport ions across the membrane against the ion concentration gradient, and channels that mediate the flow of ions down the electrochemical gradient [62].

In uninfected erythrocytes, the Na^+/K^+ ATPase maintain the intracellular Na^+ and K^+ at concentrations of 15 and 130 mM, respectively [63]. In *P. falciparum* infected erythrocytes the cytoplasmic pH is 7.1, but 6.9 around the parasite. [64]. By contrast, the cytosolic pH of *P. falciparum* parasites is 7.3. The difference between pH 6.9 and 7.3 is maintained by the vacuolar (V-type) H^+ ATPase (PfvapA) that pumps H^+ ions out of the parasite, creating a significant inward negative membrane potential (E_m) of -100 mV (Figure 3) [65].

However, approximately 18 hours post-invasion, new permeation pathways (NPPs) are established. NPPs are channels of broad-specificity that mediate increased uptake of various low molecular solutes by infected erythrocytes [62]. Due to increased diffusion of Na^+ and K^+ into and out of the erythrocyte, the ion concentration gradient across the erythrocyte membrane dissipate, generating a high Na^+ and low K^+ environment for the *Plasmodium* parasite inside the host cell (Figure 3) [66]. The *Plasmodium* parasite maintains a low $[Na^+]_{cys}$ of ~10 mM through the action of P-type Na^+-ATPase (PfATP4) responsible for pumping Na^+ from intra-erythrocytic parasites. PfATP4 has been proposed to be a counter transporter of H^+

[67], importing H^+ as Na^+ is exported [68]. While the combined action PfvapA [69] and PfATP4 creates a large inward negative electrical and chemical gradient for Na^+ influx, the mechanism by which this occurs is unknown [62]. High cytosolic [K^+] is maintained in the parasite [65, 70]. In *P. berghei* parasites described that the uptake of a K^+-like ion ($^{86}Rb^+$) was reduced when the K^+ channel was inhibited [71]. This finding is consistent with K^+ channels playing a primary role in K^+ uptake.

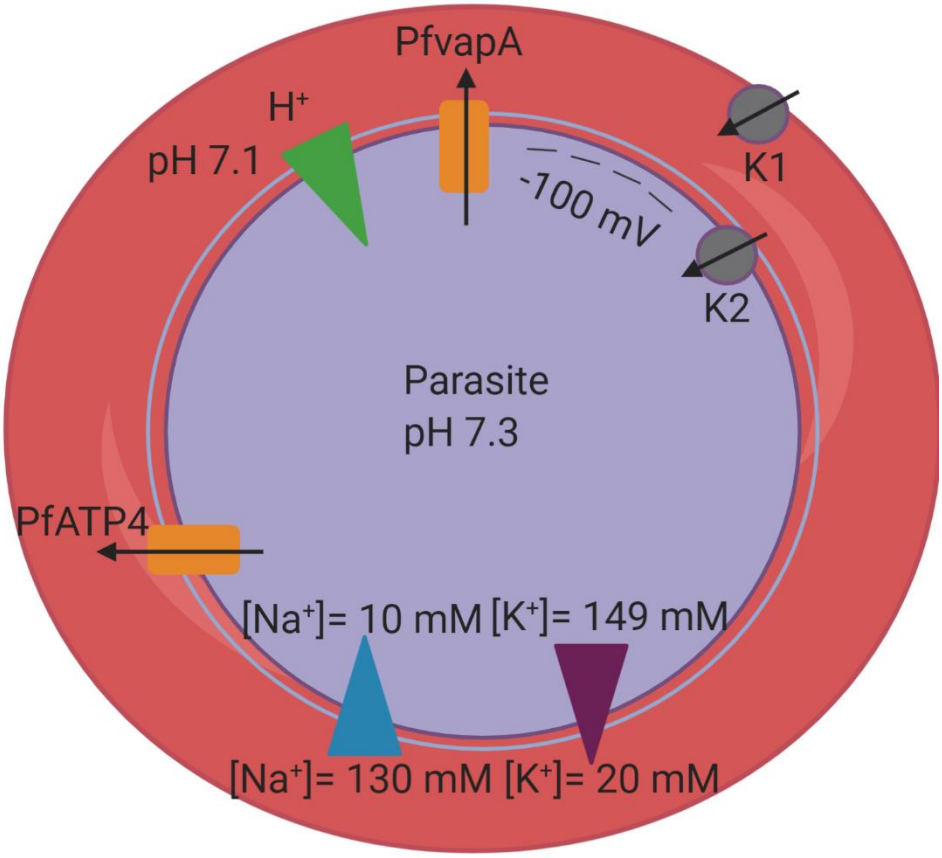

Figure 3: Maintenance of ion homeostasis in *P. falciparum* infected erythrocytes. The pH in the infected erythrocyte cytosol is 7.1, whereas the pH in the parasite cytosol is 7.3. A V-type H^+ ATPase (PfvapA) pumps H^+ out of the parasite, creating an inward negative membrane potential. Sodium ions diffuse from a high concentration in the erythrocyte to a low concentration in the parasite, and exported through a Na^+ ATPase (PfATP4). Potassium ions move into the parasite against the K^+ gradient due to the large inward negative membrane potential. Two K^+ channels (K1 & K2) are present to aid in maintaining the K^+ gradient. K1 is located in the erythrocyte membrane, and K2 is in parasite membrane Compiled using graphic components from BioRender. (https://app.biorender.com/).

1.5 Ion homeostasis as biological target in *Plasmodium* parasites

Phenotypic screening of large chemical libraries for compounds that kill the parasite a strategy to identify new antiplasmodial compounds [72, 73]. However, determining the target of these antiplasmodials often proves challenging. One approach involves the generation of resistant parasites through prolonged exposure to the compound of interest [73]. Once the genome is sequenced the encoding gene may be identified due to resistance associated mutations. Phenotypic screening resulted in the successful identification of spiroindolones [68, 74, 75], pyrazoleamides [76], dihydroisoquinolones [77] and aminopyrazoles [74] as possible antiplasmodial compounds. Subsequent mutation analyses identified PfATP4 as the target of these compounds [73]. PfATP4 pumps Na^+ from the intra-erythrocytic parasite as the primary Na^+ efflux pump, with associated H^+ import. It is hypothesized that inhibiting this ATPase results in an uncontrolled increase in cytosolic [Na^+] and cytosolic pH, causing the cell to swell due to the influx of Na^+ ions [76, 77] and increase in cell rigidity and sphericity [78], all of which could be fatal to the parasite. Spiroindolone (CIPARGAMIN, KAE609) has progressed through Phase I and Phase IIa clinical trials [68, 73] with rapid clearing of parasitaemia in adults with uncomplicated *P. vivax* or *P. falciparum* malaria [79].

It is clear that the protein(s) involved in Na^+ homeostasis is important for *Plasmodium* parasite survival. This raises the question whether K^+ channels similarly can be a biological target in *Plasmodium* parasites.

1.6 Potassium channels as a biological target in *Plasmodium* parasites

While there are no known antimalarial compounds that specifically target K^+ channels, it is known that the maintenance of the K^+ gradient is critically important for parasite survival. A study by D'Allesandro *et al.,* (2015) [80] revealed that if the K^+ gradient is disrupted by a K^+ ionophore such as salinomycin, both asexual and sexual stage parasites die. Additionally, known K^+ channel inhibitors prevent parasite proliferation of *P. falciparum* parasites, providing more evidence that K^+ channels are effective drug targets [81].

K^+ channels contain a central ion conduction pore forming domain for K^+ to flow through the membrane (Figure 4) [82]. The pore is formed by four α-subunits (homotetrameric) and contain a conserved sequence, TXGYGD, known as a core selectivity motif [83]. This selectivity filter is a defining feature of K^+ channels [84] that will only allow K^+ to pass through. The GYG in the

sequence of each of the four subunits form the mouth of the pore. The side chains of these amino acids form hydrogen bonds with other parts of the protein and expose the carbonyl oxygens of the backbone, which can replace water oxygens of the hydrated K^+. The K^+ dehydrates as it enters the pore and the water molecules bind to the carbonyl oxygens. The dehydrated K^+ can then pass through the channel [85]. Without water Na^+ is too small to bind to the carbonyl oxygens and can, therefore, not pass through these channels.

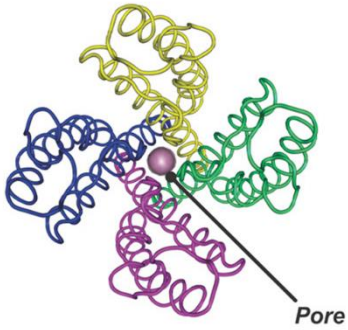

Figure 4: Schematic representation of a K^+ channel. K^+ channels are homotertamer structures with a pore. The selectivity filter is inside the pore and selects for K^+. Image from [86]

There are several types of K^+ channels including; two-pore, inward rectifier, calcium-gated and voltage-gated K^+ channels. Two-pore K^+ channels have four transmembrane domains, inward rectifying K^+ channels have two transmembrane domains, Ca^{2+} activated K^+ channels have six or seven transmembrane domains, which is divided in subfamilies of large conductance (BK), intermediate conductance (IK) and small conductance (SK) [87]. Voltage gated K^+ channels have six transmembrane segments [88]. Voltage gated K^+ channels are therapeutic drug targets for the treatment of heart disorders, epilepsy, ataxia and cognitive disorders in humans [88, 89] while protozoan K^+ channels have been identified as attractive drug targets in *Leishmania mexicana* [83].

The *P. falciparum* genome encodes for three putative voltage gated K^+ channels: K1 (Pf3D7_1227200), K2 (Pf3D7_1465500) and K3 (Pf3D7_1436100). K1 and K2 have readily recognizable K^+ channel selectivity sequences. By contrast, K3 has a highly unusual selectivity sequence region, raising questions regarding the physiological role of the protein [90]. K3 has also been discredited by Waller *et al.,* (2008) [91] as “unlikely to encode a K^+ channel due to its lack of several key features that are common to many K^+ channels”. K3 lacks appropriate flanking transmembrane domains, and the selectivity filter does not include the typical GYG motif, but instead has a GKG motif, which can be factors for discrediting this channels as a potassium channel. The genes encoding the K1 and K2 channels contain a single exon and

the sequences indicate that these genes would likely encode proteins that are highly charged [91]. The *k1* and *k2* genes have a degree of sequence similarity to other identified K^+ channels from other protozoan parasites, bacteria and yeasts [92].

The *k1* gene is located on chromosome 12 (position 1098129-1104223) and is approximately 6.1 kb in length [91]. The protein is expressed throughout the 48 h intra-erythrocytic asexual life cycle, increasing in expression as the parasite matures [91]. Waller *et al., (*2008) [91] hypothesised that a parasite-induced ion channel encoded by *k1* facilitates intracellular survival and maturation of the parasite by regulating K^+ flux. K1 is localised to the erythrocyte membrane and has been shown to be essential in asexual parasites with two different strategies in *P. falciparum*: i) targeted gene disruption, where the gene is knocked-out [91] and ii) transposon mutagenesis using the *piggyBac* transposon, which inserts a TTAA tetranucleotide target sequence in the gene to disrupt the gene and results in the loss of function of the gene [93]. However, *P. berghei* K1 homologue is not critical for asexual replication as shown with targeted gene disruption but is required for sexual replication in mosquitos [71].

The *k2* gene is located on chromosome 14 (position 2650755-2655140) and is approximately 4.4 kb in length. This channel is localised to the parasite membrane, with expression in merozoites and late schizonts in *P. falciparum* [91]. There are conflicting reports on whether K2 is essential in the asexual stages, with targeted gene disruption indicated that K2 is essential [91], while other reports using a *piggyBac* transposon indicated a non-essential role in *P. falciparum* [93].

K^+ channels are thus essential for the survival of asexual stage *P. falciparum* parasites. However, the essentiality of these channels remain unexplored in the transmissible gametocyte stages of the life cycle. K^+ gradient has been shown to be a biological target, and if disrupted, both asexual stage-parasites as well as gametocytes die [80]. This may suggest the K^+ gradient is essential in gametocytes. Furthermore, the localisation of K^+ channels in gametocytes is yet to be determined. These biological questions can be answered by producing conditional knockdown *P. falciparum* parasites lines with genetically modified K^+ channels. As described above, previous studies determined essentiality of K^+ channels with targeted gene disruption methods [91], however, these are not suitable for gametocytes. Gene disruption mechanisms determine gene essentiality, and if the gene is essential in the asexual stage and is then disrupted, the parasite will die before gametocytes are produced. Thus, to study gene functions and localisation in gametocytes, an inducible gene manipulation system is needed.

1.7 Genetic modification in *P. falciparum* parasites

Understanding *P. falciparum* membrane transport proteins would facilitate the characterisation and identification of novel drug targets that may aid in the elimination of malaria [94]. Reverse genetics is used to modify *P. falciparum* genes to study gene function, localisation and essentiality. Essential genes may be used as potential drug targets and the most direct way to study essentiality is to inactivate the gene of interest (GOI) and study the resulting phenotype.

Plasmodium is amendable to genetic manipulation by electroporation during the IDC, when the parasite genome is haploid. As a general strategy, a recombinant plasmid matching a part of the GOI is transfected into the *P. falciparum* parasite. The recombinant plasmid contains mechanisms (see below) that may be integrated into the genome to determine essentiality, or the ability for the gene to be disrupted without any phenotypical changes and/or localisation. This allows the generation of knockout, knockdown and knockin parasite lines. During gene knockout, a gene is deleted from the genome, whereas a conditional knockout is the deletion of a gene from the genome following a specific intervention such as the addition of a ligand. A knockdown is where the gene expression is attenuated by manipulating mRNA or proteins, and a knockin is where a mechanism (such as a riboswitch) or tag is inserted into the genome.

1.7.1 Knockout strategies used in *P. falciparum* for gene deletion

Gene deletion is the most radical and irreversible method to disrupt gene function by removing the whole gene or only partially removing parts of a gene from the genome [95]. Gene deletions are knockouts that disrupt the gene in the genome before it is expressed. This can provide mutant lines completely lacking expression of the GOI, but these can only be obtained if the GOI is not essential during the IDC [96]. To overcome these challenges, several systems have been adjusted to allow for conditional control of the system ensuring a gene is knocked out following a specific intervention. This includes DiCre, FLP-*FRT,* CRISPR-Cas9, and zinc-finger nucleases. A dimerisable Cre (DiCre) system [97] has been used to successfully study gene functions that are essential for host cell invasion. Here, loxP (Cre recombinase recognition sites) are inserted flanking the GOI. Recombinases are enzymes that catalyse recombination of DNA at specific catalytic sites, in this case loxP. Cre recombinase is controlled by splicing it into two moieties. One of these moieties is fused to FKBP12 (FK506 binding protein), and the other to FRB (binding domain of the FKBP12–rapamycin-associated protein) [98, 99]. In the presence of rapamycin, the two components form a heterodimer

FKBP1-FRB through cross-linking the protein fragments, which reconstitutes the original Cre recombinase [100], which then binds to the flanking loxP sites and knocks out the gene. The FLP-*FRT* system is similar to the DiCre system as the parasite is modified to carry the FLP recombinase whilst the GOI is modified with flanking flippase recognition target (*frt)* sites. The FLP recombinase cleaves the DNA at the flanking *frt* cites and catalyse a recombination between two target sequences, excising the gene, and thus creating a knockout [101]. The CRISPR-cas9 system uses a guide RNA to guide an endonuclease to a specific target site to cleave the DNA at this site. A knockout plasmid can then be inserted with homologous recombination [102]. Zinc-finger nucleases, ZFNL and ZFNR with unique specificity to adjacent sequences on both sides of the DNA helix are co-expressed under a single promotor, and recognise user-defined DNA sequences that are linked to an endonuclease (*Fok*I) to induce a double-strand break, thereby, triggering homologous recombination in the parasite. Another knockout plasmid carries the transgene as a desired cDNA version [103].

1.7.2 Knockdown strategies used in *P. falciparum*

1.7.2.1 Targeting mRNA transcription, translation or mRNA levels

As an alternative to targeting a gene on the genome level, several tools have been developed to knockdown gene expression by either targeting the mRNA or protein produced from a gene. To do this, an element is typically knocked in first to control gene expression [96]. The same recombinant plasmid can simultaneously insert the coding sequence of a protein tag, such as GFP or heamaggluttin (HA) to monitor the target protein levels and determine localisation.

On a mRNA level, the initial transcription of the gene, can be controlled for example using tetracycline-controlled transcriptional activation, or the tet-OFF tool [104]. A transactivator is produced by fusing a bacterial tetracycline transcription repressor (TetR) to an activating domain. The transactivator binds via the TetR to *tet* operator sequences (*TetO*) which is placed in front of a promotor and activates transcription. In the presence of tetracycline or anhydrotetracycline (ATc), the affinity of the TetR for the *TetO* is radically reduced and transcription is turned off [94, 95]. Tetracycline or ATc change the conformation of TetR so that it can no longer bind to the *TetO*. Tetracycline or ATc is added to the parasite culture when parasites are in a life-cycle stage where expression is studied. Thus, if the expression of a gene in the ring-stage is to be studied, tetracycline or ATc will added to the parasite culture medium in when it is majority ring-stage parasites.

Although transcription control is desirable, it is challenging to implement in *P. falciparum* because of the limited information of promotor regulatory elements [96]. However, there are studies showing this tool is successful in *P. berghei* [105]. Alternatively, a *glmS* riboswitch or tetR aptamer tool have been developed for post transcriptional control in *Plasmodium.*

As an alternative to preventing transcription, mRNA translation can be prevented using RNA binding proteins, which sequester the transcripts away from the active translation machinery [106]. The TetR-binding aptamer is inserted into 5' untranslated region of a reporter gene, and the TetR binding protein binds to the aptamer and inhibits translation. This can then be reversed by treating parasites with ATc. This results in a conformation change of the TetR binding protein, prohibiting binding to the TetR-binding aptamer [107]. Advantages of this system is robustness and reversibility [96].

Lastly, the mRNA levels of the GOI can be targeted. The *glmS* riboswitch is a 5' cis-regulatory element in the glucosamine-6-phosphate synthase gene in bacteria [108]. A riboswitch is a regulatory element that responds directly to small molecules [109]. The *glmS* riboswitch is a distinctive riboswitch in that it controls gene expression through self-cleavage following activation by glucosamine-6-phosphate (GlcN6P) (Figure 5). A ribozyme is an RNA molecule which can catalyse a biochemical reaction such as cleaving mRNA. This method is used to control gene expression by inserting the ribozyme sequence downstream of the GOI at the 3' UTR, resulting in mRNA transcripts of the GOI containing the riboswitch. The riboswitch will modulate the levels of GOI-riboswitch mRNA in response to GlcN6P. Activation of the *glmS* ribozyme is done by adding GlcN6P which releases short leader sequences that bears a triphosphate and exposes a 5'OH group in the ribozyme domain [110]. This results in the *glmS* ribozyme that self-cleaves mRNA and results in degradation of mRNA, knocking down protein expression [111]. This causes reduction in protein expression [96].

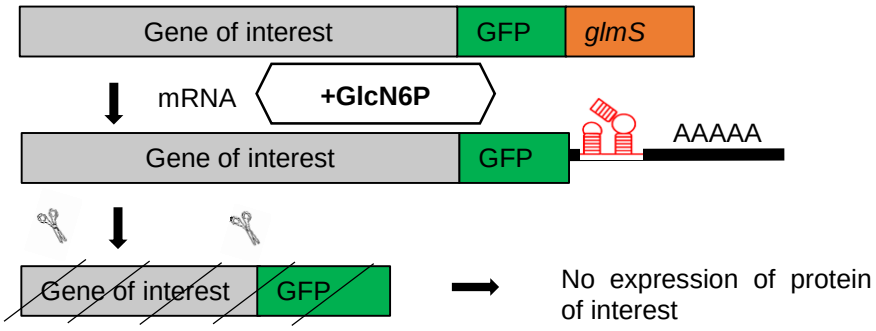

Figure 5: Schematic representation of the *glmS* ribozyme system as a conditional knockdown gene modification tool. The ribozyme is inserted at the 3' untranslated region of the gene of interest. The addition of glucosamine, which binds and activate the ribozyme, results in self-cleavage of the

mRNA and subsequently knocking down protein expression. *glmS*: glucosamine-6-phosphate riboswitch ribozyme, also indicated in red. GlcN6P: glucosamine-6-phosphate.

1.7.2.2 Targeting protein stability

Genetic tools that work on a protein level are desirable, because it is considered the fastest responding system [95]. Therefore, phenotypic effects will result faster than using disruption on a RNA level [96]. Two tools that can be used to destabilize proteins are destabilisation domains (DDs) and the auxin-inducible degron system.

The DD is an unstructured protein domain that targets proteins associated with the domain for degradation in the proteasome. A DD is inserted at the 3' untranslated region by single homologous crossover integration. Once the DD is expressed, fused to the C-terminus of the protein and targets the whole protein for degradation [99]. This can be regulated by adding Shld-1, a cell permeable ligand, which stabilizes the unstructured protein domain, preventing it from degradation. When Shld-1 is removed, the protein is degraded.

Instead of using a ligand to directly control protein stability via a DD, another tool to use for rapidly depleting protein levels is using the cell's own ubiquitination system to target proteins for degradation [112]. An auxin-inducible degron (AID) that originated in rice plants (*Oryzae sativa*) is used. The plant hormone mediates interaction of auxin specific E3 ubiquitin ligase SCF^{Tir} and auxin responsive plant transcription repressors (AUX/IAA's) leading to degradation of the protein by the proteasome of the cell [112]. A study in mammalian cells has found that this system can introduce a 20-fold reduction of the target protein levels [113]. It has also been established in *P. falciparum* [112] and *P. berghei* [114].

1.8 Genetic manipulation of *P. falciparum* K^+ channels

The aim of this study was to create genetically modified parasite lines for future localisation and functional studies of K1 and K2 in both asexual and sexual stages of *P. falciparum* parasites. Given that previous studies [91, 115] indicate that K1 and possibly K2 are essential during asexual development a conditional gene knockdown system will be used to ensure that gametocytes can be obtained for study. Specifically, a 3' green fluorescent protein (GFP) and *glmS* riboswitch will be added to the GOI to allow localisation of the protein as well as conditional knockdown of the mRNA product, in gametocytes of *P. falciparum*. Even though K2 has shown to be essential during asexual development [91], these already established

piggyBac transposon lines cannot be used to induce gametocytogenesis since viable parasites cannot be obtained. Gametocytes are produced from a minor fraction (<1 %) of asexual parasites and therefore it is important to have a viable asexual parasite culture from which gametocytes can be produced. Additionally, gametocytes are terminally differentiated, so once produced, these gametocytes per induction can only be used once. Only once gametocytogenesis is initiated, can one use genetic manipulation to test gene function. This implies that an inducible gene manipulation system has to be used to control manipulation of the GOI.

To ensure that the modified parasite lines can produce full length K^+ channels, the *glmS* riboswitch and GFP tag were added to the 3' end of the gene. If the 5' end was used, the gene expression will be interjected, resulting in a knockout. The general strategy is as follows: the DNA sequence of *k1* and *k2* encoding for a C-terminal fragment of the protein, hereafter referred to as "C-terminal fragment" are amplified and cloned into a specific plasmid system with an ampicillin resistance gene to allow for selection in *Escherichia coli*. The recombinant plasmids produced are transfected into *P. falciparum* parasites, and maintained under drug pressure to select for parasites that contain the recombinant plasmid episomally. Homologous integration of the recombinant plasmid into the gene locus are tested using PCR (Figure 6 and Figure 7).

There are two different plasmid systems currently in use in *P. falciparum* parasites to add a 3' GFP and *glmS* to the GOI: pGFP_*glmS* [111] and pSLI_*glmS* [116]. Both *k1* and *k2* C-terminal fragments were cloned into the pGFP_*glmS* plasmid. The pGFP_*glmS* plasmid contain blasticidin resistance to use blasticidin drug pressure for selection of integrated parasites (Figure 6).

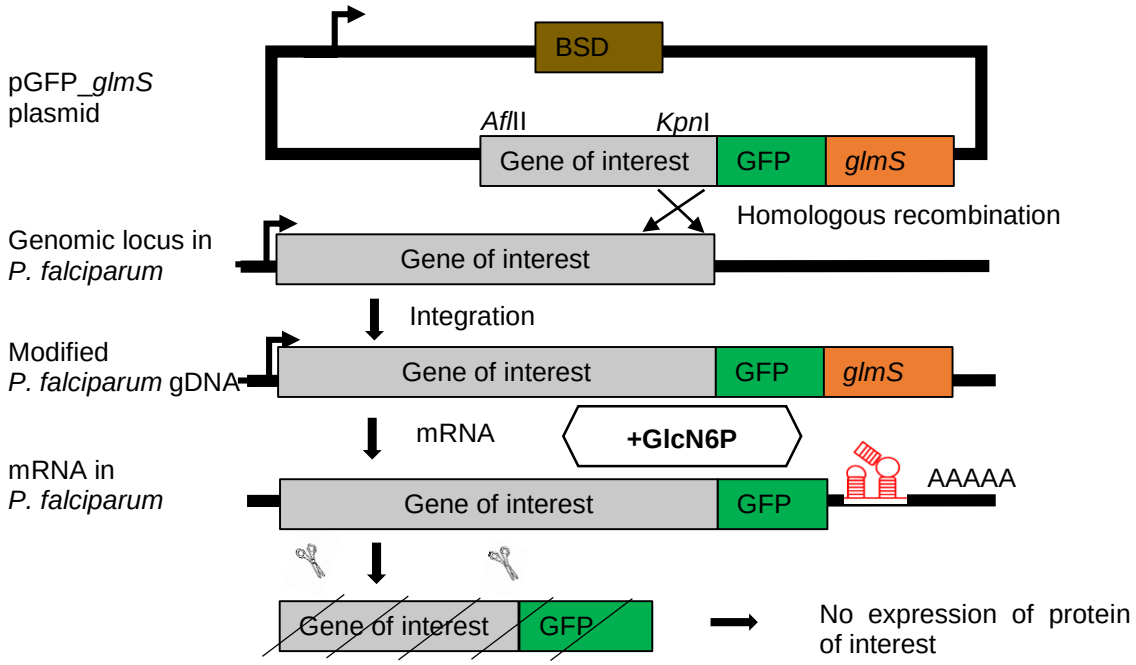

Figure 6: Schematic representation of genomic modification and subsequent conditional knockdown of the GOI using pGFP_*glmS*. Homologous recombination of the gene of interest at the 3' nucleic sequence will result in integration of the plasmid into the genome. *Afl*I and *Kpn*I are restriction enzymes used to insert a C-terminal fragment into the plasmid. GFP: Green fluorescent protein. *glmS*: glucosamine-6-phosphate riboswitch ribozyme, also indicated in red. GlcN6P: glucosamine-6-phosphate. BSD: blasticidin resistance marker.

Two different systems are available for conditional knockdown; the original *glmS* and the selection-linked integration (SLI) *glmS* system. The SLI system uses a double selection approach to select for episomal uptake of the plasmid using and claims to ensure successful and rapid genomic integration by using a two drug approach to select for parasites that have episomal uptake of the recombinant plasmid by using human dihydrofolate reductase (hDHFR), and then using a promotor-less Neo-R marker for final integration into the genome by [106]. Both the original *glmS* system and SLI *glmS* system have been published and used to determine gene essentiality [100, 105]. The SLI system also "forces" integration by using a skip peptide between the GOI and the Neo-R marker, whereas the original *glmS* system only integrates by chance. Therefore, theoretically the SLI *glmS* system is more advantageous.

Following the completion of the cloning of C-terminal fragments of *k1* and *k2* in pGFP_*glmS* constructs, a modified plasmid with a double selection system was generated that may lead to faster genomic integration compared to the original *glmS* system (Figure 7) [117]. Both *k1 and k2* fragments were also cloned into this plasmid. The pSLI_*glmS* plasmid containing a hDHFR resistance marker to initially select for parasites containing episomal plasmid following transfection using WR99210. Additionally, a T2 skip peptide and a promotor-less second

selection marker for neomycin resistance is added on the 3' end of the *glmS* riboswitch. Following successful integration, polycistronic mRNA is produced under the control of the GOI promoter. This results in the expression of two individual proteins, namely the GFP-tagged GOI and Neo-R. Additionally, a control plasmid with an inactive riboswitch due to a mutation on the *glmS* riboswitch, was also used.

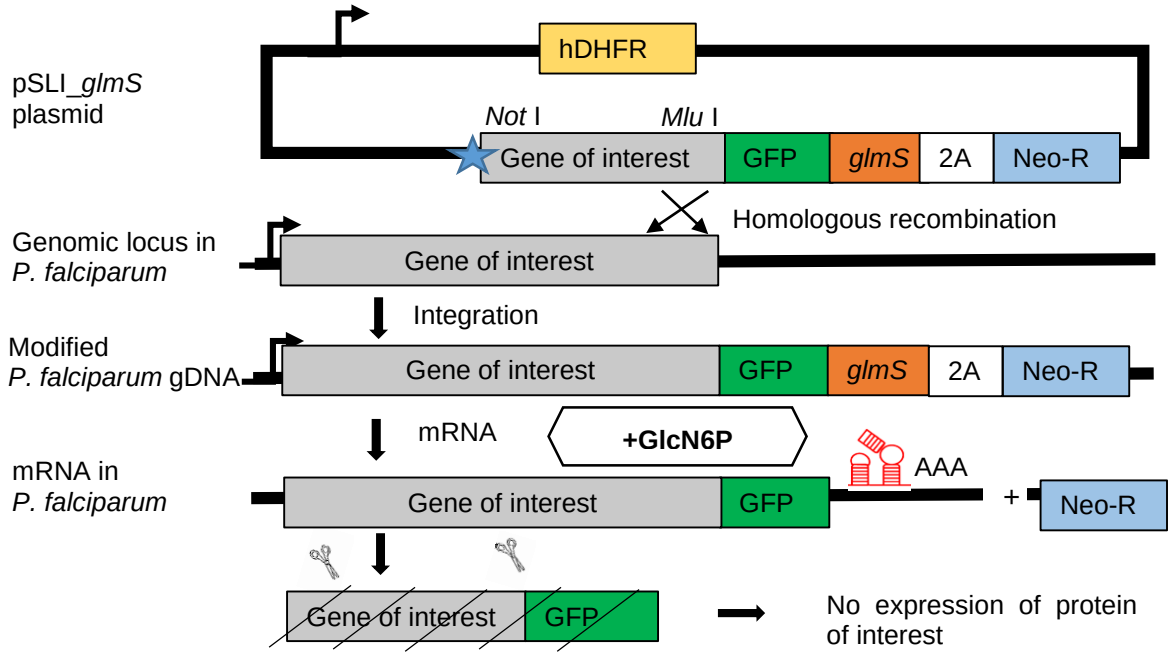

Figure 7: Schematic representation of the double section system in pSLI_*glmS* for genomic modification and subsequent conditional knockdown of the GOI. Homologous recombination of the gene of interest at the 3' nucleic sequence will result in integration of the plasmid into the genome. *Not*I and *Mlu*I are restriction enzymes used to insert a C-terminal fragment into the plasmid. Star: Stop codon TAA. GFP: Green fluorescent protein. *glmS*: glucosamine-6-phosphate riboswitch ribozyme, also indicated in red. GlcN6P: glucosamine-6-phosphate. 2A: Skip peptide. Neo-R: Neomycin resistance selection marker. hDHFR: human dihydrofolate reductase resistance marker.

1.9 Hypothesis, aims and objectives

Hypothesis:

P. falciparum parasites with genetically modified *k1* or *k2* can be generated with the pGFP*_glmS* and pSLI*_glmS* plasmid systems.

Aim:

To generate parasite lines for future conditional knockdown and localisation studies of K^+ channels.

Objectives:

1. *In silico* characterisation of *k1* and *k2* to determine transmembrane domains, conserved regions and expression of these genes during the IDC
2. Generate recombinant plasmids of pGFP*_glmS* and pSLI*_glmS* with *k1* and *k2* gene fragments
3. Generate 4 genetically modified *P. falciparum* (NF54_Δ*k1*_GFP*_glmS*, NF54_Δ*k2*_GFP*_glmS,* NF54_*k1*_SLI*_glmS* and NF54_Δ*k2*_SLI*_glmS*) parasite lines

Research outputs:

Els F., Mugo E., Stutzer C., and Niemand J. Investigating the essentiality of potassium channels during *Plasmodium falciparum* gametocytogenesis. 5th South African Malaria Research Conference. Poster presentation. Pretoria, South Africa, July 2019.

2 Chapter 2: Materials and Methods

2.1 *In silico* analysis of putative *P. falciparum* K^+ channels Pf3D7_1227200 (K1) and Pf3D7_1465500 (K2)

2.1.1 Transmembrane domain and membrane topology analysis

Amino acid sequences were obtained from PlasmoDB version 47 (https://plasmodb.org/plasmo/app, accessed August 2020). Transmembrane domains (TMDs) were predicted using three TMD prediction servers for an accurate estimate based on the characteristics of amino acids. TMDs can belong in three states i) inside loops, ii) transmembrane regions or iii) outside loops [118]. The three servers used to predict TMDs were TMHMM (http://www.cbs.dtu.dk/services/TMHMM-2.0/, accessed August 2020), Phobius (http://phobius.sbc.su.se/, accessed August 2020) [119], and TMPred (https://embnet.vital-it.ch/software/TMPRED_form.htmL, accessed August 2020) [120]. All three these use Hidden Markov Model (HMM) which predicts a sequence of TMDs from amino acid sequences. TMHMM uses a cyclic HMM model, whereas Phobius uses a combination of the HMM and a SignalP prediction model [121] and TMPred uses a combination of weight-matrices for scoring [122]. The consensus between all three TMD predictions based on the amino acid sequence were subsequently used to assign the TMDs in the proteins.

Hydropathy plots were used to investigate the number and approximate locations of hydrophobic regions and thus possible membrane spanning regions. These were generated with the Kyte-Doolittle hydrophobicity scale [123] of the ProtScale server (window size of 9) (https://web.expasy.org/protscale/, accessed August 2020) [124]. A Kyte-Doolittle hydrophobicity scale defines hydropathicity of amino acids based on the free energy change when an amino acid side chain (R group) moves from a hydrophobic solvent into water (ΔGtrans°). Negative ΔGtrans° are associated with hydrophilic regions, while positive ΔGtrans° value are associated with hydrophobic regions [125].

2.1.2 Analysis of K1 and K2 protein domains

The NCBI Conserved Domain Database was used to predict conserved domains to provide information of the type of transporter and superfamily the protein belongs to. The amino acid sequence of K1 and K2 proteins were analysed using a NCBI search (https://www.ncbi.nlm.nih.gov/Structure/cdd/wrpsb.cgi, accessed August 2020) and identified regions in the protein that are highly conserved in K^+ channels [126-129]. A multiple sequence alignment for domains conserved by K^+channels among *Plasmodium* and other species was performed using a multiple alignment tool, ClustalOmega (https://www.ebi.ac.uk/Tools/msa/clustalo/, accessed August 2020). Conserved sequence TVGYG (K^+ selectivity filter motif) were investigated in the alignments.

A protein model was built for K1 and K2 using SWISS Model (https://swissmodel.expasy.org/repository/, accessed August 2020) to visualise the quaternary structures of the proteins using a previously defined protein structure identified by the server to match the protein [130-133]. In addition, a Ramachandran plot was constructed to evaluate the statistical distribution based on acceptable angles of the peptide backbone angles. When phi(ϕ) (x-axis) and psi (ψ) (y-axis) angels are plotted against each other, a prediction of beta sheets and helixes can be made [134], and represented on a Ramachandran plot.

2.1.3 Expression of *k1* and *k2* in intra-erythrocytic *P. falciparum* stages

The expression profiles of mRNA transcripts identified during previous DNA microarray analyses were used to determine the expression of *k1* and *k2* during both the asexual intra-erythrocytic and gametocyte stages. DNA microarray data for the asexual stage parasites were obtained from Painter *et al.,* (2017) [135] for a complete 48 h life cycle (expression value at each hour). Data for a complete global transcriptome of *P. falciparum* gametocytogenesis over 13 days including gametocyte commitment and development were obtained from van Biljon *et al.,* (2018) [136]. Transcript expression profiles were provided as $\log_2$(Cy5/Cy3) expression values ($\log_2$ of the ratio between sample and reference, in a reference pool microarray design) at each time point. Expression values greater than zero indicate increased transcript expression, whereas values smaller than zero indicate decreased transcript expression.

2.2 Preparation of pGFP_*glmS* and pSLI_*glmS* plasmids with C-terminus coding fragments of *k1* and *k2*

2.2.1 *In vitro* cultivation of asexual stage *P. falciparum* parasites

Intra-erythrocytic *P. falciparum* parasite (strain NF54) cultures were maintained *in vitro* at 37 °C in human erythrocytes (any available blood type) at a 5 % haematocrit (ethics approval: University of Pretoria 180000094). Complete culture medium [(Roswell Park Memorial Institute (RPMI) 1640 supplemented with 1.25 mM 4-(2-hydroxymethyl)-1-piperazineethanesulfonate, pH 7.5 (HEPES, Sigma Aldrich, USA), 80.4 mM hypoxanthine (Sigma Aldrich, USA), 0.2 % (w/v) D-glucose (Sigma Aldrich, USA), 0.2 % sodium bicarbonate (Sigma Aldrich, USA), 24 µg/mL gentamicin (Fresenius, Germany) and 0.5 % AlbuMAX II (Life technologies, USA)] was replaced daily to support parasite proliferation. The parasite cultures were maintained in a 5 % O_2, 5 % CO_2 and 90 % N_2 (AFROX, South Africa) atmosphere [137, 138]. The cultures were agitated at 60 rpm to keep erythrocytes in suspension increasing merozoite invasion and avoiding multiple merozoites invading one erythrocyte [139]. Parasite morphology and proliferation were monitored daily with Giemsa-stained slides (Merck, Germany) as per the manufacturers instruction and were viewed under a light microscope at 1000x magnification (Nikon, Japan).

Although *P. falciparum* parasites remain synchronised throughout development *in vivo*, synchronisation of *in vitro* parasites tend to decrease over several life cycles [138]. It is therefore essential to synchronise *in vitro P. falciparum* parasites for stage-specific studies of the parasite. Ring-stage parasites were synchronised via isosmotic lysis of trophozoite-stage parasites and schizont-stage parasites with D-sorbitol (Sigma-Aldrich, USA) [140], resulting in a predominantly ring-stage parasite culture. Intra-erythrocytic *P. falciparum* parasite cultures (5 % haematocrit, 3 - 5 % parasitaemia) were centrifuged with a Heraeus Megacentrifuge 40 (ThermoFisher Scientiic, USA) (3500 x*g*, 5 min), the supernatant aspirated and the pellet resuspended in 3 x pellet volume of 5 % (w/v) sorbitol/H_20 solution and incubated for 15 min at 37 °C. The lysed parasites and sorbitol were subsequently removed by 3 washes with 5 mL incomplete (medium without AlbuMAX II) medium. The remaining ring-stage parasites were placed back into culture and maintained as described above. Mature parasites increase membrane fluidity in erythrocytes, permitting sorbitol uptake into the erythrocytes. Osmolysis eliminates mature parasites, retaining a culture enriched in mainly ring-stage infected erythrocytes and uninfected erythrocytes.

2.2.2 Genomic DNA isolation from *P. falciparum* parasites

Genomic DNA (gDNA) from intra-erythrocytic *P. falciparum* parasites (>5 % parasitaemia, >95 % trophozoite-stage parasites,) was isolated using a Quick-gDNA Blood Miniprep kit (Zymo research, USA) as per the manufacturer's recommendations. Proprietary genomic lysis buffer (800 µL, containing guanidinium thiocyanate with added β-mercaptoethanol (0.5 % v/v)) to lyse cells and inactivate RNases) was added to a 200 µL parasite pellet that was subsequently vortexed and incubated for 10 min at room temperature. The cell lysate was loaded onto a Zymo-Spin IIC Column (Zymo research, USA) and centrifuged using a MiniSpin plus centrifuge (10 000 x*g*, 1 min) (Eppendorf, Germany), after which columns were washed with DNA Pre-Wash Buffer (200 µL containing propan-2-ol and guanidinium chloride to remove excess salt and debris and destabilize proteins). Thereafter, the column was washed with gDNA Wash Buffer (500 µL containing ethanol and propan-2-ol). DNA was eluted in TE buffer, pH 9.0 (10 mM Tris, 1 mM EDTA) or triple distilled water (dddH_2O). DNA concentration and purity were measured spectroscopically using a NanoDrop ND-1000 spectrophotometer (ThermoFisher Scientific, USA). DNA absorbance is measured at 260 nm, as the heterocyclic rings of the nucleotides in the DNA absorb ultraviolet light. Proteins and organic substances absorb wavelengths of 280 nm and 230 nm, respectively and absorbance was measured to determine purity of the DNA. The optimal range a DNA sample for the A_{260}/A_{280} is 1.7 – 1.9 and A_{260}/A_{230} is 2.0 – 2.2.

2.2.3 Primer design of the oligonucleotides used in the study

Primers were designed using Benchling software, (www.benchling.com, accessed between May 2019 and June 2020) to amplify fragments of various sizes as described in Table 1. Primers were manufactured by Integrated DNA technologies (USA) or Inqaba Biotechnical Industries (South Africa) and resuspended in TE buffer, pH 9.0 (10 mM Tris and 1 mM EDTA) as per manufacturer's instructions. The first group of primers used for cloning of GOI fragments into the pGFP_*glmS* and pSLI_*glmS* plasmids were designed to produce a C-terminal fragment of the GOI of approximately 1000 bp. Furthermore, these primers were designed to produce fragments in frame relative to the GFP protein encoded in the plasmid. For the pGFP_*glmS* plasmid, forward and reverse primers that amplify the C-terminal fragments were designed with *Afl*II and *Kpn*I restriction sites, respectively. By contrast, the forward primers for the pSLI_*glmS* plasmids contained a *Not*I restriction site as well as a stop codon to prevent expression of the fragment before it is integrated into the genome, while the reverse primers contained *Mlu*I restriction sites.

The second group of primers include plasmid backbone-specific primers used in sequencing reactions to validate that the C-terminal GOI fragments were correctly inserted into the plasmids The sequencing reactions produced fragments of approximately 1050 bp.

Table 1: Oligonucleotides used in the study for cloning of C-terminal fragments into pGFP_*glmS* and pSLI_*glmS* plasmids, sequence validation of produced plasmids and testing for successful gDNA integration following transfection into the *P. falciparum* parasite. Green: Restriction enzyme (RE) recognition sites. Red: stop codon. Blue: gene annealing region. Purple: Plasmid backbone region

Purpose	Gene	Primer name		Primer sequence	(bp)
Amplification of C-terminal fragment for cloning into pGFP_*glmS* plasmids	*k1*	*glmS*_PF1227200_aflII_fw	F	gcgcCTTAAGCAGTCCAAATATAAATGAAATGATAAAGGG	1030
	k1	*glmS*_PF1227200_kpnI_rv	R	tgtGGTACCCATTCTGTGTGCAATAACATAAGC	
	k2	*glmS*_PF1465500_aflII_fw	F	gcatCTTAAGACATAAACACATGCTACAGCG	1026
	k2	*glmS*_PF1465500_kpnI_rv	R	ataGGTACCCAATATATAAACTATATCATCGAATCG	
Amplification of C-terminal fragment for cloning into pSLI_*glmS* plasmids	*k1*	GD_PF1227200_notI_fw	F	gcatGCGGCCGCtaaCCAAATATAAATGAAATGATAAAGGG	1029
	k1	GD_PF1227200_mluI_rv	R	gccACGCGTTTCTGTGTGCAATAACATAAGC	
	k2	GD_PF1465500_notI_fw	F	gcatGCGGCCGCtaaGCCATTTACTTTTGAATTATAAAAAGC	1075
	k2	GD_PF1465500_mluI_rv	R	ggtACGCGTCAATATATAAACTATATCATCGAATCG	
Backbone primers to validate the produced plasmids via colony PCR, sequencing and test for integration		*glmS*_backbone_fw	F	GGTCTTAACTTAACTAACTTAG	
		SLI_backbone_fw	F	AGCGGATAACAATTTCACACAGGA	
		GFP_rv	R	ACAAGAATTGGGACAACTCCAGTGA	
Test 5' integration and wild type locus	*k1*	K1_F1int	F	GATAAAGATGCATATAGAATAGATAACG	1353
Test 3' integration and wild type locus	*k1*	K1_R3int	R	CATTTATATATTCATAATTCTTTCCTTTATACCCC	
Test 5' integration and wild type locus	*k2*	K2_F1int	F	GGTGAATTTAATGAAACAAAATTATATCATC	1416
Test 3' integration and wild type locus	*k2*	K2_R3int	R	CAAAATATTTAATGTAACCATTTGGATG	

Lastly, three primer sets were designed to check the successful integration of the recombinant gene fragment into the parasite genome (Table 3). These primers bind upstream or downstream of the cloning site. For 5' integration, a forward primer that binds to the gene (K1_F1int or K2_F1int) and a reverse primer that binds to the GFP tag (GFP_rv) was used. For 3' integration, a forward primer that binds to the backbone of the pGFP_*glmS* plasmid (*glmS*_backbone_fw or SLI_backbone_fw) and a reverse primer (K1_R3int or K2_R3int) that binds to the neighbor gene were used. To identify potential wild type parasites in the culture, a forward primer that binds to the gene (K1_F1int or K2_F1int) and a reverse primer (K1_R3int or K2_R3int) that binds to the neighbor gene were used. In the presence of wild types parasites, an approximately 1400 bp fragment would be amplified, while successful integration, would amplify an 8400 bp fragment (Table 2).

Table 2: Fragment sizes of amplified regions within the integrated clonal line

Primer combination	Size of fragment *k1*	Size of fragment of *k2*	Wild type
F1/R1- 5' integration	1272	1368	
F4/R3- 3' integration	1245	1259	
F1/R3- integration on right locus	1353	1416	>8000
F4/R1- Episomal uptake	1089	1138	

A multistep cloning strategy was followed to produce final plasmids for transfection (Figure 8). C-terminal GOI fragments were amplified with cloning primers as shown in Table 2. The C-terminal gene fragment was inserted into pGFP_*glmS* and pSLI_*glmS* by cleaving the plasmids with restriction enzymes and inserting the C-terminal GOI fragment into the linear plasmid. K1 was subjected to an intermediate cloning step, by first cloning into a pGEM®-T-Easy plasmid and then subcloning into pGFP_*glmS* and pSLI_*glmS*. Final plasmids were used for transfection into *P. falciparum* parasites.

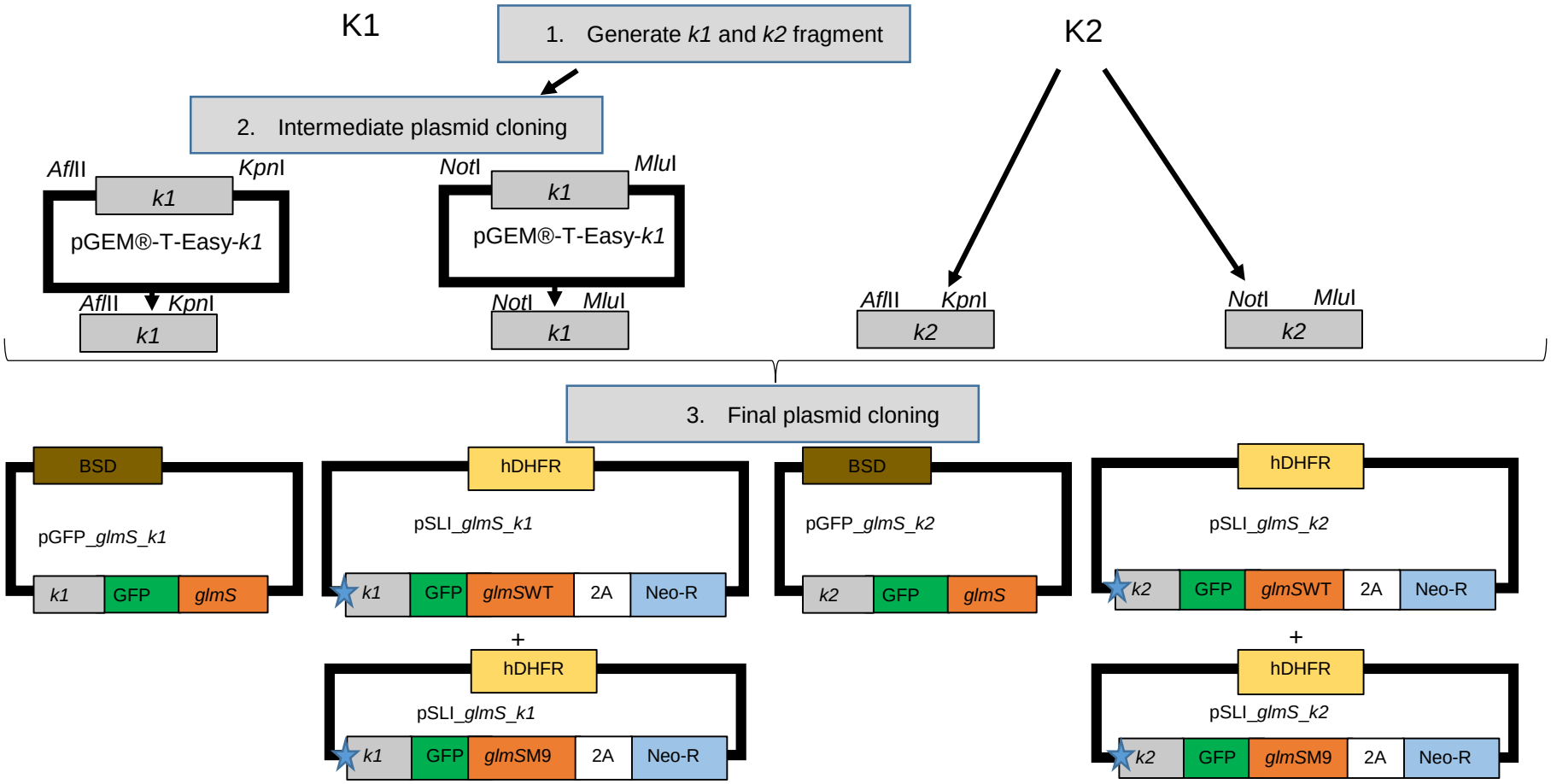

Figure 8: Cloning strategy to generate the pGFP_*glmS* and pSLI_*glmS* plasmids with C-terminus fragments of *k1* and *k2*. A C-terminal gene fragment will be amplified via PCR and ligated into a plasmid using restriction enzymes. *k1* fragment cloned into a pGEM®-T-Easy plasmid, and subsequently subcloned into pGFP_*glmS* and pSLI_*glmS* plasmids. *k2* fragment will be cloned into pGFP_*glmS* and pSLI_*glmS* plasmids for transfection into the parasite. *Afl*II, *Kpn*I, *Not*I, *Mlu*I are restriction enzymes used to insert a C-terminal fragment into the plasmid. **Star:** Stop codon TAA (only present in pSLI_*glmS* plasmids). **GFP:** Green fluorescent protein. ***glmS*:** glucosamine-6-phosphate riboswitch ribozyme. **GlcN6P:** glucosamine-6-phosphate. **2A:** Skip peptide. **Neo-R:** Neomycin resistance selection marker. **hDHFR:** human dihydrofolate reductase resistance marker. **BSD:** Blasticidin resistance marker

2.2.4 PCR amplification of *k1* and *k2* C-terminus fragments

C-terminus regions of *k1* and *k2* were amplified using a 1x KAPA Taq polymerase master mix (0.4 U KAPA Taq polymerase, 1.5 mM $MgCl_2$, 0.2 mM of each ddNTPs, KAPA Biosystems, USA) together with 10 ng of parasite gDNA, 10 pmol forward primer and 10 pmol reverse primer. PCR reactions were run in either a 2720 Thermal cycler (Applied Biosystems, USA) or GeneAmp PCR system 2400 (Perkin Elmer, USA) with the cycling conditions listed below.

To amplify the *k1* and *k2* gene fragments for pGFP*_glmS* cloning, initial denaturation was 94 °C for 5 min, followed by denaturation at 94 °C for 1 min, annealing at 51 °C for 30 s and extension at 68 °C for 2 min for 25 cycles. A final extension step at 68 °C for 5 min was also included. The optimal temperature for Taq is 72 °C, however, extension was done at 68 °C because of the AT rich genome in *P. falciparum.*

To amplify the *k1* and *k2* gene fragments that were used for pSLI*_glmS* cloning, initial denaturation was 94 °C for 3 min, followed with denaturation at 94 °C for 2 min, annealing at 51 °C for 30 s and extension at 68 °C for 2 min for 25 cycles. A final extension step at 68 °C for 5 min was also included.

2.2.5 Gel electrophoresis analysis of DNA fragments

Agarose gel electrophoresis was used to visualise the amplified PCR products and digested plasmids to confirm that only the expected fragment sizes were present. DNA samples (between 5 ng and 500 ng) were loaded with 1x loading dye (0.4 % orange G, 0.03 % bromophenol blue, 0.03 % xylene cyanol FF, 50 mM EDTA (pH 8.0), 10 mM Tris-HCl (pH 7.5) and 15 % Ficoll 400) (Promega, USA) on 1.5 % (w/v) agarose (Lonza, Switzerland) /TAE (20 mM Tris, 20 mM Acetic acid and 1 mM EDTA, pH 8.0) gel containing ethidium bromide (1.2 mg/mL) and separated with electrophoresis using an electric current 6 - 8 V/cm in a electrophoresis chamber (BioRad Sub-Cell® GT Cell, USA) for 1 h to facilitate the migration of DNA, from the cathode to the anode. A volume of 2 µL 1 kb or 100 bp (Promega, USA) ladder was loaded as a molecular marker. DNA was observed under UV light using a GelDoc™XR+ gel visualisation system (Bio-Rad, USA) and analysed using Image Lab ™ Software (Bio-Rad, USA) version 3.0.

2.2.6 Purification of amplified PCR products

PCR products were purified using the NucleoSpin Gel and PCR clean-up kit (Machery-Nagel, Germany). To allow binding or retaining of the DNA to the silica column via hydrogen binding interaction, binding buffer NTI (containing guanidium thiocyanate) was mixed with the PCR product in a 2:1 ratio. Guanidium thiocyanate acts as a chaotrope allowing positively charged ions to form a salt bridge between the negatively charged DNA backbone and negatively charged silica. The mixture was loaded on a NucleoSpin Gel and PCR clean-up column by centrifugal force (11 000 x*g*, 30 s) in a MiniSpin plus centrifuge (Eppendorf, Germany), washed with 700 µL Buffer NT3, and dried by centrifugal force (11 000 x*g*, 30 s). The purified gene fragments were eluted from the silica membrane with Buffer NE and quantified spectroscopically. Purified DNA was stored at 4 °C until further use.

2.2.7 Preparation of competent *E. coli* cells

E. coli (DH5α*,* ThermoFisher Scientific, USA) cells were made chemically competent to allow for the uptake of foreign DNA. *E. coli* cells were inoculated in Luria-Bertani (LB) broth and incubated at 37 °C for 16 h, with agitation (200 rpm). After overnight incubation, 1 mL of overnight bacterial culture was inoculated into 50 mL LB broth, and incubated at 37 °C, with agitation (200 rpm), until mid-logarithmic growth phase was reached (OD_{600} of ~ 0.4) determined by GeneQuant (GE Healthcare, USA). Cells were then incubated on ice for 10 - 20 min and centrifuged (1865 x*g*, for 30 s) at 4 °C in a SL 8R Centrifuge (ThermoFisher Scientific, USA). The supernatant was aspirated and cells were resuspended in 25 mL ice cold 0.1 M $CaCl_2$ followed by centrifugation at 4 °C as above. Glycerol stocks were made by suspending the pellet in a suspension buffer (0.25 M ice cold $CaCl_2$ and 375 µL glycerol) and incubated on ice for 1 h. Aliquots of the stock were stored at - 80 °C.

2.2.8 Isolation of pGFP_*glmS* and pSLI_*glmS* plasmids from *E. coli*

pGFP_*glmS* and pSLI_*glmS* plasmids were isolated using a NucleoSpin Plasmid Transfection-grade kit (Machery-Nagel, Germany). Glycerol stocks of *E. coli* cells (ThermoFisher Scientific, USA) containing the pGFP_*glmS* and pSLI_*glmS* plasmids were used to inoculate LB-broth, pH 7.5 (1 % (w/v) NaCl, 1 % (w/v) tryptone and 0.5 % (w/v) yeast extract) containing 50 µg/mL ampicillin (LB-Amp). Cultures were incubated with agitation

(200 rpm), at 37 °C for 16 h. Saturated cultures (5 mL) were centrifuged in a MiniSpin plus centrifuge (Eppendorf, Germany) (11 000 x*g*, 30 s) and the supernatant aspirated. Buffer A1 (containing RNase A to degrade RNA present) was used to resuspend the pellet, after which Buffer A2 containing NaOH and sodium dodecyl sulphate (SDS) to denature genomic DNA and lyse cells was added. Lastly, buffer A3 (containing guanidine HCl used to facilitate a salt bridge between the negatively charged DNA backbone and negatively charged silica) was added. The mixture was centrifuged (11 000 x*g* 10 min) and the supernatant containing the plasmid were loaded on to NucleoSpin Plasmid TG Column. The column was washed with Buffer ERB (containing propan-2-ol) and then with Buffer AQ (containing ethanol), and dried with centrifugal force (11 000 x*g*, 1 min). The plasmid was eluted from the silica membrane with Buffer AE and the yields were quantified spectroscopically. pGFP*_glmS* and pSLI*_glmS* plasmids were stored at 4 °C until further use.

2.2.9 Restriction enzyme (RE) digestion of pGFP*_glmS* and pSLI*_glmS* plasmids

Restriction mapping was performed to confirm the identities of the pGFP*_glmS* and pSLI*_glmS* plasmids. pGFP*_glmS and* pSLI*_glmS* plasmids were digested with *Bam*HI and *Hind*III (Promega, USA) for 3 h at 37 °C. Each 50 µL reaction contained 5 µL 1x cutsmart buffer (Promega, Madison, USA), 3 µg of plasmid DNA and RE (10 Weiss units of each RE per mg of DNA). Digestion reactions were incubated at 37 °C for 3 h, after which the digested plasmids were separated using electrophoresis.

Plasmids and PCR products from the GOI were digested with restriction enzymes to create 5' or 3' overhangs required for sticky-end ligation. The pGFP*_glmS* plasmids and PCR products were digested with the restriction enzymes *Afl*II and *Kpn*I, while *Not*I and *Mlu*I (all New England Biolabs, USA) were used to digest the pSLI*_glmS* WT and pSLI*_glmS* M9 plasmids and corresponding PCR product. Each 50 µL reaction contained 5 µL 1x cutsmart buffer (New England Biolabs, USA), 3 µg of plasmid DNA (or 37.5 ng of insert) and 10 Weiss units of each RE per mg of DNA. Digestion reactions were incubated at 37 °C for 3 h, after which the digested PCR products of the GOI were purified using a NucleoSpin Gel and PCR clean-up kit (Machery-Nagel, Germany) as described in section 2.2.6 above. The digested plasmids were separated using electrophoresis (described above in section 2.2.5) to separate the plasmid backbone from the original insert. The plasmid backbone was excised from the gel and subsequently purified using a NucleoSpin Gel and PCR clean-up kit (Machery-Nagel,

Germany) as described in section 2.2.6. Both the PCR products and plasmids were quantified spectroscopically.

2.2.10 Ligation of *k1* and *k2* gene fragments into pGFP_*glmS* and pSLI_*glmS*

Purified PCR products and plasmids with sticky ends were ligated in a reaction containing an insert:plasmid molar ratio of 3:1. Each 10 µL reaction volume contained 1 Weiss unit of T4 ligation enzyme (New England Biolabs, USA), 1x T4 ligation buffer (New England Biolabs, USA), 100 ng digested plasmid, 37.5 ng insert DNA and $dddH_20$. The reaction mix was incubated at 4 °C overnight.

Since the initial ligation reaction did not produce recombinant plasmids for *k1*, the purified C-terminal fragment was first cloned into a pGEM®-T-easy plasmid (Promega, USA) using AT cloning, since Taq polymerase adds template independent 3' A overhangs to PCR products. Additionally, this system enables easy selection of positive colonies with blue-white selection. [141].

The ligation reaction was set up in a 3:1 insert: plasmid ratio as stated above. Each 10 µL reaction contained 2 Weiss units of T4 DNA ligase (Promega, USA), 50 ng pGEM®-T-easy plasmid, 37.5 ng insert DNA and 1x Rapid Ligation Buffer, pH 7.8 (60 mM Tric-HCl, 20 mM $MgCl_2$, 2 mM TP, 10 % polyethylene glycol and 20 mM DTT) (New England Biolabs, USA). The reaction mix was incubated at 4 °C overnight.

2.2.11 Transformation of ligation reactions into competent cells

The complete ligation reactions were subsequently added to thawed competent cells and incubated on ice for 30 min. The cells were heat shocked at 42 °C for 90 s and immediately incubated on ice for 2 min. To allow the cells to recover, 900 µL warm LB-glucose (LB broth and 20 mM glucose) was added to the mixture and incubated at 37 °C, with agitation (200 rpm), for 1 h. The recovered cells were plated onto LB-amp agar plates (1 % (w/v) agar in LB-broth supplemented with 100 µg/mL ampicillin) and, thereafter incubated overnight at 37 °C. Selected colonies were tested for successful ligation of the C-terminal fragments of the GOI into the plasmid of interest.

In conditions where blue white selection is possible, the LB-amp agar (1 % (w/v) plates supplemented with X-gal (80 µg/mL) and IPTG (0.5 mM) were used to plate recovered cells. White colonies were an indication of possible positive clones and were selected and tested for successful ligation of the C-terminal fragments of the GOI into the plasmid of interest.

2.2.12 Screening for positive clones: restriction enzyme mapping and colony - screening PCR

To select for positive clones, and to ensure the C-terminal fragment of the GOI were correctly ligated into the plasmid, a colony screening PCR and subsequent restriction enzyme mapping was carried out. Positive colonies on the LB-amp agar plate were selected, individually inoculated in LB-amp (5 mL) and incubated at 37 °C, with agitation (200 rpm), for 3 h. PCR reactions contained 1 x KAPA Master mix, 10 pmol forward primer, 10 pmol reverse primer, inoculated LB-amp overnight culture (1 µL). Primers that bind specifically to the backbone of the plasmid (Table 2) were used to amplify the C-terminal fragment of the GOI. PCR conditions used were as follows: initial denaturation at 94 °C for 3 min, followed by denaturation at 94 °C for 2 min, annealing at 51 °C for 30 s and extension at 68 °C for 2 min for 25 cycles. A final extension step at 68 °C for 5 min was also included. The PCR reaction was visualised using agarose gel electrophoresis as described in section 2.2.5.

Positive clones identified via colony PCR were inoculated into LB-amp broth and incubated overnight at 37 °C, with agitation (200 rpm). Plasmids were isolated from these clones as described in section 2.2.8.

Isolated plasmids were digested to confirm the length of the inserted fragment in the recombinant plasmid. pGFP_*glmS* recombinant plasmids were digested with *Afl*II and *Kpn*I and pSLI_*glmS* WT and M9 were digested with *Not*I and *Mlu*I as previously described in section 2.2.9. Plasmids were digested for 3 h at 37 °C and separated by agarose gel electrophoresis.

A miniprep alkaline lysis method described by Green and Sambrook (2016) [142] was used to isolate plasmids when inserts were cloned into the pGEM®-T-easy plasmid. A single white colony was inoculated in LB-amp broth (5 mL) and incubated overnight at 37 °C, with agitation (200 rpm). The culture was centrifuged at (11 000 x*g*, 60 s) in a MiniSpin plus centrifuge (Eppendorf, Germany), the supernatant aspirated, and the pellet suspended in Solution 1 (10 mM EDTA (pH 8.0), 25 mM Tris (pH 8.0), 50 mM glucose). Solution 2 (1 % (w/v) SDS and 0.2

M NaOH) was added and the suspension was incubated on ice for 5 min. Ice cold Solution 3 (5 M KCH_3COO^-, 11.5 % (v/v) glacial acetic acid) was added and the suspension incubated on ice for 10 min followed by centrifugation (11 300 x*g*, 5 min). The supernatant was removed and transferred to a new Eppendorf tube where 600 µL phenol was added and vortexed for 1 minute, followed by centrifuging (11 300 x*g*, 1 min). The upper aqueous layer was removed and transferred to a new Eppendorf tube. $CHCl_3$:isoamyl alcohol (24:1) was added, mixed and centrifuged (11 300 x*g*, rpm, 2 min). The top aqueous layer was removed again, and transferred to a new Eppendorf tube, where ice cold 100 % ethanol was added. The suspension was incubated at - 70 °C for 30 min and centrifuged (11 300 x*g*, 30 min). The supernatant was aspirated and the pellet resuspended in 70 % v/v ethanol followed by centrifugation (11 300 x*g*, 30 min). The supernatant was aspirated again, and the pellet dried *in vacuo* for 10 min. The dry pellet was then dissolved in TE-buffer containing 0.5 mg/mL RNAse. Samples were stored at 4 °C until further use.

Restriction enzyme digestion was performed for all the isolated pGEM®-T-easy plasmids by digesting with a restriction enzyme flanking the cloning site in the pGEM®-T-easy plasmid. *EcoRI* (Promega, USA) was used and incubated at 37 °C overnight. The sizes of the digested products were determined using agarose gel electrophoresis as described in section 2.2.5.

2.2.13 Sanger dideoxy nucleotide sequencing

To validate the identity of the insert in the recombinant plasmid, the exact sequence was determined with Sanger dideoxy sequencing. A 20 µL sequencing reaction containing 2 µL BigDye Mix, 4 µL 1x BigDye buffer, 5 pmol plasmid backbone primers (forward *glmS*_backbone_fw or SLI_backbone_fw or reverse GFP_rv) and 100 ng template DNA was set up with the following conditions for 25 cycles: Denaturation at 96 °C for 10 s, followed by annealing at 51 °C for 5 s and extension at 60 °C for 4 min using a 2720 Thermo Cycler (Applied Biosystems, USA). The reaction mix was kept at 4 °C until precipitation.

Ethanol precipitation was used to purify the dideoxynucleotide containing DNA before sequencing. NaOAc (3 M) was added to the PCR reaction in a 1:10 ratio in addition to 100 % ethanol (3x the reaction volume). The mixture was centrifuged in a 5415R Eppendorf centrifuge (Hamburg, Germany) at 4 °C (16 000 x*g,* 30 min). The supernatant was aspirated, and 250 µL ice cold 70 % ethanol was added to the pellet followed by centrifugation at 4 °C (16 000 x*g*, 10 min) to precipitate the DNA. The supernatant was aspirated, and DNA pellets

were air dried until all the ethanol had evaporated. The dried DNA pellets were stored at 4°C until further analysis.

Sanger dideoxy sequencing was performed at the University of Pretoria FABI AGCT Sequencing facility using an ABI PRISM® Genetic analyser (Applied Biosystems, USA). Sequence base-calling and alignment was performed using BioEdit (v7.2.5) and Benchling (https://www.benchling.com/).

2.3 Production of NF54_Δ*k1*_GFP_*glmS*, NF54_Δ*k2*_GFP_*glmS,* NF54_Δ*k1*_SLI_*glmS* and NF54_Δ*k2*_SLI_*glmS* parasite lines

2.3.1 Plasmid preparation for transfection into *P. falciparum* parasites

A large-scale plasmid isolation was performed using a NucleoBond Xtra Midi/Maxi (Machery-Nagel, Germany) plasmid DNA purification kit to obtain sufficient quantities (50 - 100 µg) of recombinant plasmid DNA for transfection. *E. coli* glycerol stocks containing the recombinant plasmids were inoculated into 5 mL LB-amp and incubated overnight at 37 °C, with agitation (200 rpm). A volume of 3 mL of the overnight culture was used to inoculate 200 mL LB-amp, which was subsequently incubated overnight at 37 °C with agitation (200 rpm). Bacterial cells were harvested by centrifugation at 4 °C (3260 x*g*, 30 min). The supernatant was discarded, and cells were resuspended in Buffer RES (containing RNase A). Cells were lysed by adding Buffer LYS. The suspension was incubated at room temperature for 5 min. The NucleoBond Xtra column was equilibrated with Buffer EQU. Buffer NEU was added and mixed by inversion followed by centrifugation at 4 °C (3260 x*g*, 10 min). Thereafter, the supernatant was loaded into the equilibrated column and allowed flow through the silica membrane by gravitational force. The column was washed with Buffer EQU to remove remaining cell lysate. The filter was removed, and the column washed a second time with Buffer WASH. Plasmid DNA was eluted with Buffer ELU (containing propan-2-ol to elute DNA) and quantified spectroscopically. Samples were stored at 4 °C until further use.

Plasmid DNA was precipitated by adding room temperature >99.5 % isopropanol (3.5 mL) (Sigma-Aldrich, USA) mixed thoroughly, and centrifuging at 4 °C (15 000 x*g*, 30 min). Ethanol (70 % v/v) was added followed by centrifugation (15 000 x*g*, 5 min) at room temperature. The ethanol was aspirated, and the pellet allowed to air dry at room temperature. The DNA pellets were dissolved in TE buffer, after which yields were quantified spectroscopically and stored at 4 °C until further use.

After isopropanol precipitation, ethanol precipitation was performed before transfection to remove any excess contaminants as described in section 2.2.13, with minor modifications. NaOAc (3 M) (1/10th of the reaction volume) and 100 % ethanol were added to the eluted plasmid DNA and centrifuged at 4 °C (13 000 x*g*, 30 min). The supernatant was aspirated and 1 mL 70 % (v/v) ethanol was added, and the samples were centrifuged at 4 °C (13 000 x*g*, 30 min). The supernatant was aspirated again, 1 mL of 100 % ethanol was added and centrifuged at 4 °C (13 000 x*g*, 10 min). The supernatant was aspirated, and the pellet was centrifuged at maximum speed for 1 - 2 min at 4 °C. The remaining ethanol was aspirated in a sterile laminar flow hood and the pellet was allowed to air dry at room temperature. DNA pellets were reconstituted in cytomix, pH 7.6 (120 mM KCl, 0.15 mM $CaCl_2$, 2 mM EGTA, 5 mM $MgCl_2$, 10 mM K_2HPO_4, 25 mM HEPES), and yields quantified spectroscopically. The DNA was stored at 4 °C until transfection.

2.3.2 Transfection of recombinant plasmids into NF54 *P. falciparum* cultures

A synchronised intra-erythrocytic *P. falciparum* (NF54) parasite culture (5 % haematocrit, >5 % parasitaemia, >95 % ring-stage parasites) was used for transfection. Parasitaemia was determined 3 h before transfection and parasites were harvested from a 20 mL culture by centrifugation (3500 x*g*, 5 min). The supernatant was aspirated leaving behind an infected erythrocyte pellet to which 46 µg - 115 µg purified plasmid DNA resuspended in cytomix (pGFP*_glmS_k1*, pGFP*_glmS_k2,* pSLI*_glmS*WT*_k1,* pSLI*_glmS*M9*_k1*, pSLI*_glmS*WT*_k2* or pSLI*_glmS*M9*_k2*) was added. *P. falciparum* parasites were electroporated using a Gene Pulser electroporator (Bio-Rad, USA) with a pulse administered with the exponential decay program, 0.31 kV and 950 uF, and maximum resistance for a 2 mm cuvette to ensure optimal time constants of 10 - 15 ms. After electroporation, the infected erythrocytes were combined with 5 mL of complete culture medium at 5 % haematocrit. The culture flasks were gassed with 5 % O_2, 5 % CO_2 and 90 % N_2 gas mixture and placed in a stationary incubator at 37 °C for 3 h to recover. After recovery, the cultures were centrifuged (3500 x*g*, 5 min) and supernatant and lysed erythrocytes removed. Pre-warmed complete culture medium was added to the culture and cultures were maintained at a 5 % haematocrit.

2.3.3 Drug cycling to select for genetically modified intra-erythrocytic *P. falciparum* parasites

Twenty-four hours after transfection of pGFP*_glmS_k1* or pGFP*_glmS_k2* into intra-erythrocytic *P. falciparum* parasites, selection for transgenic parasites started by adding 0.5 mg/mL blasticidin to the complete culture medium used to replace the spent medium. The parasites were maintained under drug pressure for 14 days by daily replacement of complete culture medium containing blasticidin in a final concentration of 0.5 mg/mL. Blasticidin inhibits protein synthesis by inhibiting peptide bond formation by the ribosome which results in the cell not being able to create new proteins through translation of mRNA [143]. Therefore, only parasites that contained the pGFP*_glmS* plasmid with the resistance marker for blasticidin survived. After the 14-day drug cycle, parasites were left to recover in drug-free complete culture medium.

The parasitaemia was monitored daily for the duration of drug cycling and recovery. Fresh erythrocytes were added every 7 days to replace lysed erythrocytes and maintain a 5 % haematocrit. Once parasitaemia was >2 %, PCR screening (described in section 2.3.4) was performed to determine if the plasmid was present episomally. When the plasmid was present episomally, another 14-day drug cycle commenced as explained above. After 14 days, parasites were left to recover in drug-free medium. Once parasitaemia was >2 %, PCR screening was performed to determine if the plasmid had integrated into the genome and if there were wild type parasites present.

Alternatively, 24 h after transfection of pSLI*_glmS*WT*_k1,* pSLI*_glmS*M9*_k1*, pSLI*_glmS*WT*_k2 and* pSLI*_glmS*M9*_k2* into intra-erythrocytic *P. falciparum* parasites, selection for transgenic parasites started by adding 4 nM WR99210 to the complete culture medium. The parasites were maintained under drug pressure for 10 days by daily replacement of complete culture medium containing WR99210 (4 nM). WR99210 is an antifolate drug used to select for the human dihydrofolate reductase (DHFR) resistance marker found in the pSLI*_glmS* plasmid. This drug stops nucleic acid synthesis by disabling the *Plasmodium* DHFR enzyme [144]. Therefore, only parasites that contained the pSLI*_glmS* plasmid containing the resistance marker for DHFR survived since malaria DHFR is replaced with the expression of human DHFR. After the 10-day drug cycle, parasites were left to recover in drug-free medium.

The process was repeated as above during drug cycling and recovery. When episomal presence was confirmed, another 14-day drug cycle commenced with G418 (neomycin). G418 blocks polypeptide synthesis, and ensures that only parasites with genomic integration will survive. The parasites were maintained under drug pressure for 10 days by daily replacement of complete culture medium containing G418 in a final concentration of 400 µg/mL, and then every second day for 2 days. Following selection using neomycin, the parasites were transferred to a shaking incubator for recovery in a drug-free complete culture medium. Once parasitaemia was >2 %, PCR screening was performed to determine integration of the plasmid into the genome and whether wild type parasites were present.

2.3.4 Selection of transgenic parasites via PCR screening

The new transgenic parasite lines (NF54_Δ*k1*_GFP_*glmS*, NF54_Δ*k2*_GFP_*glmS,* NF54_*k1*_SLI_*glmS* WT*,* NF54_*k1*_SLI_*glmS* M9*,* NF54_Δ*k2*_SLI_*glmS* WT *and* NF54_Δ*k2*_SLI_*glmS* M9) were screened by PCR amplification to determine episomal uptake and genomic integration of pGFP_*glmS*_*k1*, pGFP_*glmS*_*k2,* pSLI_*glmS*WT_*k1,* pSLI_*glmS*M9_*k1*, pSLI_*glmS*WT_*k2 and* pSLI_*glmS*M9_*k2*. Once the transfected parasites reached >2 % parasitaemia, samples were collected for screening and DNA isolated as described in section 2.2.2.

To determine episomal uptake for pGFP_*glmS* and pSLI_*glmS* plasmids, a PCR with primers that bind to the backbone of the plasmid was used (Table 2). The conditions were as follows: initial denaturation at 9 °C fo4r 5 min, followed by denaturation at 94 °C for 1 min, annealing at 51 °C for 30 s and extension at 68 °C for 2 min for 30 cycles. A final extension step at 68 °C for 5 min was also included. PCR products were visualised using gel electrophoresis as previously described.

Integration of the pGFP_*glmS* and pSLI_*glmS* into the genome was determined using template DNA obtained from the transgenic parasite lines (NF54_Δ*k1*_GFP_*glmS*, NF54_Δ*k2*_GFP_*glmS,* NF54_*k1*_SLI_*glmS* WT*,* NF54_*k1*_SLI_*glmS* M9*,* NF54_Δ*k2*_SLI_*glmS* WT *and* NF54_Δ*k2*_SLI_*glmS* M9) and NF54 parasites (wild type control) using primers in Table 1. PCR conditions were as follows: initial denaturation at 94 °C for 5 min, followed by denaturation at 94 °C for 1 min, annealing at 50 °C for 1 min and extension at 68 °C for 2 min for 35 cycles followed by a final extension step at 68 °C for 5 min. PCR products were visualised using gel electrophoresis as previously described.

3 Chapter 3: Results

3.1 *In silico* analysis of *P. falciparum* K^+ channels

3.1.1 Transmembrane domain and membrane topology analyses of the putative *P. falciparum* K^+ channels, K1 and K2 correspond with known K^+ channels

Integral membrane proteins including membrane transport proteins (MTPs) have typical hydropathy profiles, which include a single large extracellular domain and regular spacing of transmembrane domains [145]. All K^+ channels have several transmembrane α-helices that span the lipid bilayer. In addition, K^+ channels can be further classified based on function and structure. These include the two-pore/tandem pore domain (four transmembrane helices), inward rectifying (two transmembrane helices), ligand-gated K^+ channels (two or four transmembrane helices) such as cyclic nucleotide-gated, Ca^{2+}-gated and voltage-gated K^+ channels (six transmembrane helices) [146].

The *P. falciparum* genome contain two putative K^+ channel genes, namely PF3D7_1227200 (*k1*) and PF3D7_1465500 (*k2*). To confirm that the K1 and K2 proteins may indeed be K^+ channels, the presence of TMD were determined with three different TMD predictive tools, TMHMM [147], Phobius [121] and TMPred [122]. According to Cuthbertson *et al.,* (2005) [148], TMPred is the most accurate prediction tool of the three used in this study. The accuracy of the data can be validated against a Kyte-Doolittle plot which determines hydrophobicity regions of the proteins. When the TMD prediction and the Kyte-Doolittle plot correspond, data obtained are more reliable.

Table 3: TMD of K1 determined with TMHMM, Phobius and TMPred

	Amino acid location of prediction transmembrane domains										
TMHMM	44-67	73-96	569-592	611-634	643-666	706-729	743-762	768-786			
Phobius	44-65	77-102	570-593	613-635	642-666	706-729	741-760	766-786		1037-1058	
TMPred	49-67	69-101	575-593		642-667	706-726		766-784	833-851	1039-1063	1314-1333
Consensus	**49-65**	**77-96**	**575-592**		**642-666**	**706-726**		**766-784**			

K1 had 6 consensus predicted TMD present (Table 3). This correlates with the Kyte-Doolittle hydropathy plot (Figure 9) where the six peaks of the hydropathy plot indicate hydrophobicity correspond with the location of predicted TMDs. [91].

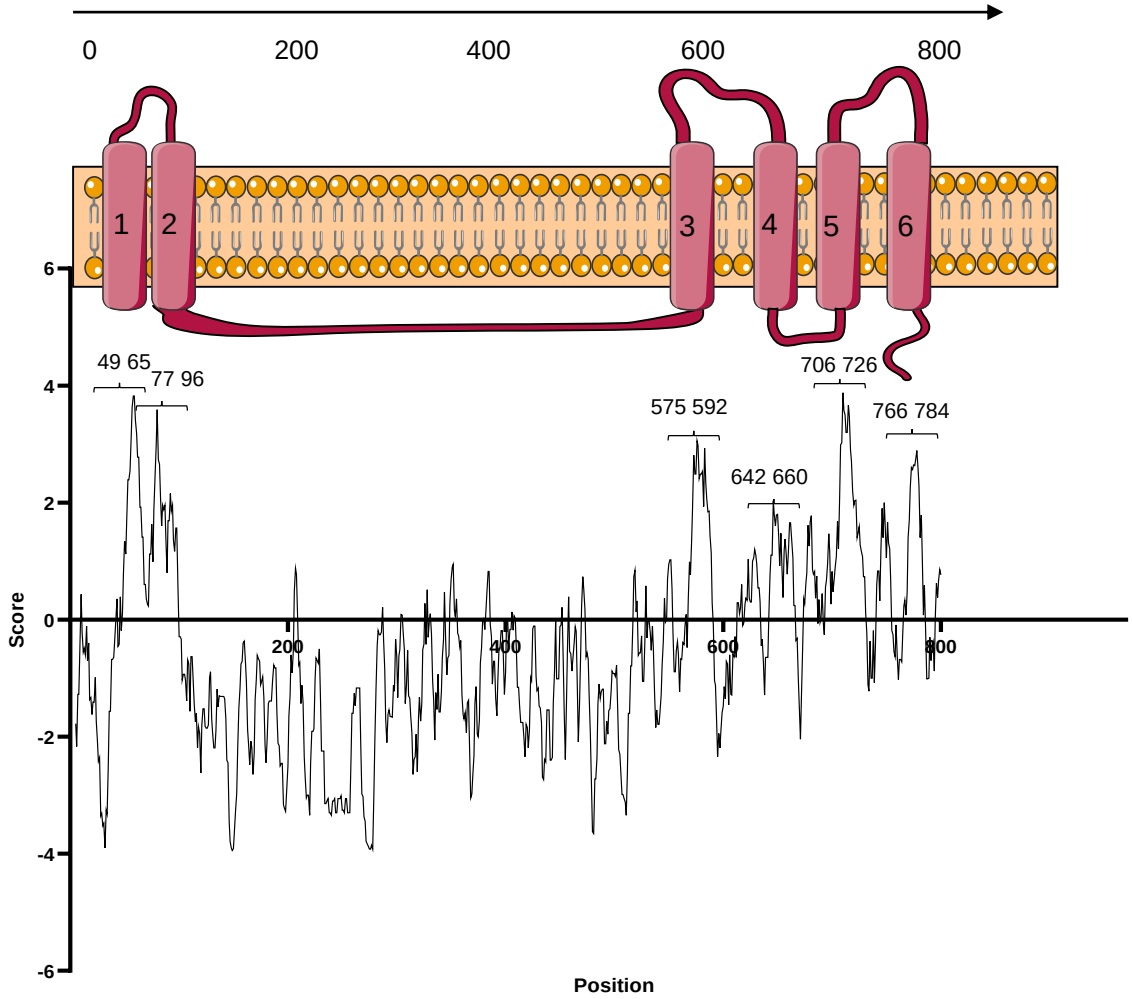

Figure 9: K1 contains 6 predicted TMDs. TMD consensus sequences were determined with TMHMM, Phobius and TMPred and correspond with the Kyte-Doolittle hydropathy plot. A positive score indicates hydrophobic regions and a negative score indicate hydrophilic regions. Lipid bilayer image components used from Servier Medical art licenced under a Creative Commons Attribution 3.0 Unported License.

By contrast, K2 had 7 consensus predicted TMDs (Table 4). These seven consensus TMDs do correlate with the peaks of the hydropathy plot (Figure 10). However, compared to the K1 hydropathy plot, the K2 hydropathy plot is less convincing, as the peaks are not well defined. This could be because the K2 protein has not been annotated before, or the algorithms used for this prediction were not accurate.

Table 4: TMD of K2 determined with TMHMM, Phobius and TMPred

	Amino acid location of prediction transmembrane domains										
TMHMM	11-34	43-66		181-204	218-238		280-303	317-340	346-369		
Phobius	12-32	44-70	142-164	182-205	217-238	244-265	277-302	322-340	347-369		
TMPred	11-38	47-75		179-205	217-328		278-297	316-336	346-362	540-559	603-628
Consensus	**12-32**	**47-66**		**182-204**	**218-238**		**280-297**	**322-336**	**347-362**		

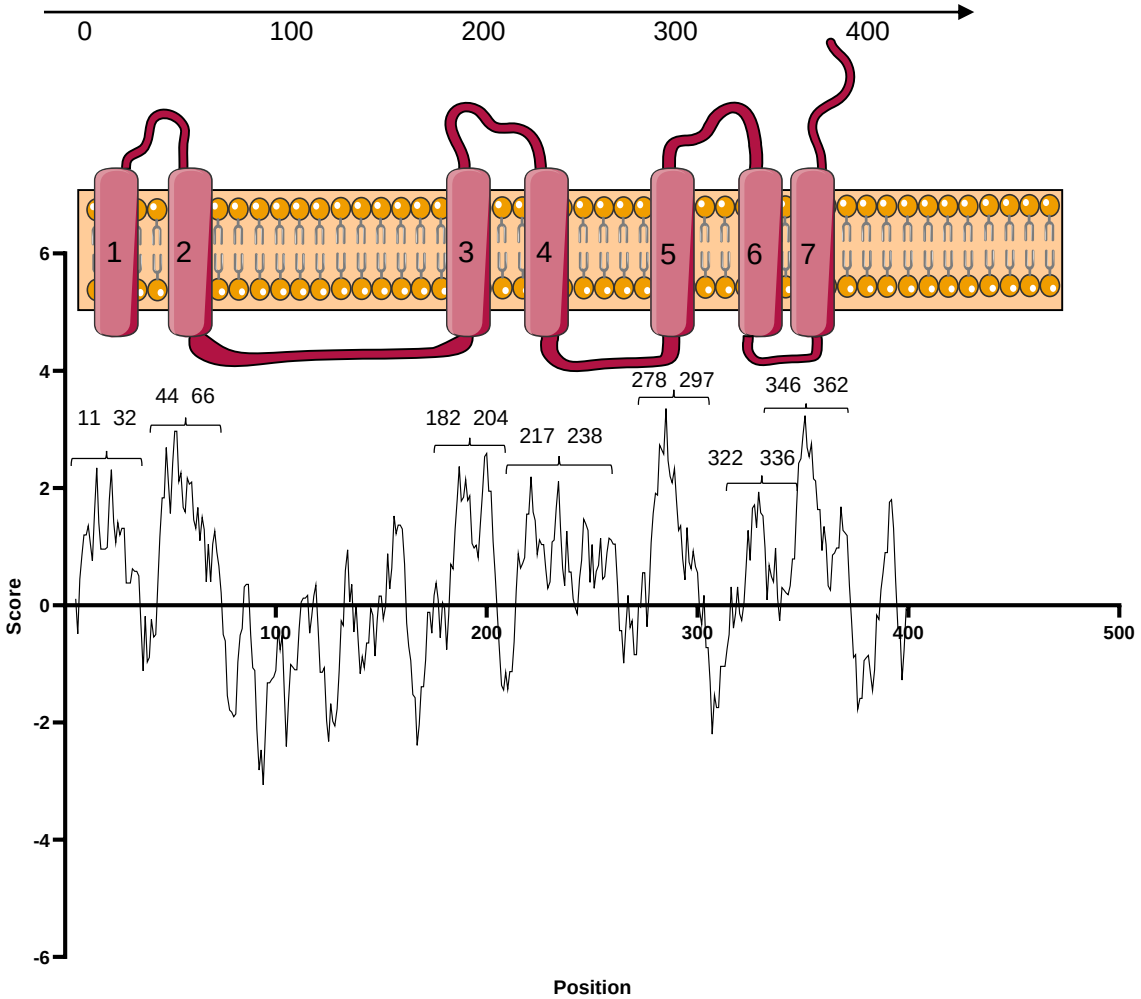

Figure 10: K2 contains 7 predicted TMDs. TMD consensus sequences were determined with TMHMM, Phobius and TMPred and correspond with the Kyte-Doolittle hydropathy plot. A positive score indicates hydrophobic regions and a negative score indicate hydrophilic regions. Lipid bilayer image components used from Servier Medical art. licenced under a Creative Commons Attribution 3.0 Unported License.

Therefore, both K1 and K2 are membrane proteins with the multiple TMDs expected in a K^+ channel.

3.1.2 K1 and K2 have the typical characteristics of K^+ channels

To determine whether K1 and K2 have the typical characteristics of K^+ channels, predicted protein domains were examined, and the presence of a typical selectivity filter in the pore region of a K^+ channel investigated. Proteins were characterised based on amino acid sequence alignments from ClustalO. Alignments of the pore region sequence from K1 and K2 with other well characterised K^+ channels confirm the presence of the selectivity filter (TVGYG) (Figure 11).

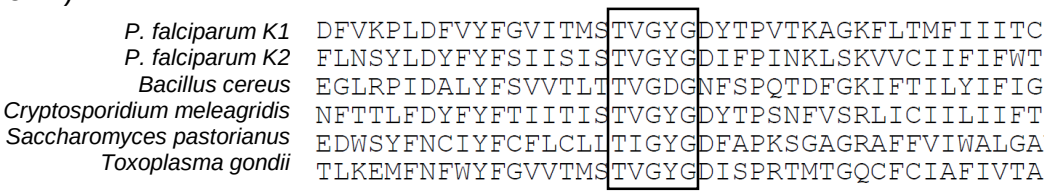

Figure 11: Multiple sequence alignment of known K^+ channels. K^+ channel sequences were obtained from PlasmoDB and aligned with ClustalO. GenBank assesion numbers are in parenthesis. *P. falciparum* K1 (Q8I5E6), *P. falciparum* K2 (Q8IKI3), *Bacillus cereus* (Q81HW2), *Cryptosporidium meleagridis* (A0A2P4Z2U8), *Saccharomyces pastorianus* (A0A6C1EA71) and *Toxoplasma gondii* (V4Z7H9) contain the conserved selectivity sequence TVGYG.

Apart from the selectivity pore region sequence, the proteins also contained domains conserved in the ion transporter superfamily, characterising the protein as an ion transporter as well as large conductance Ca-$^{2+}$-activated K^+ channel as a subfamily, whereas K1 also had a ring-infected erythrocyte surface antigen conserved region (Figure 12).

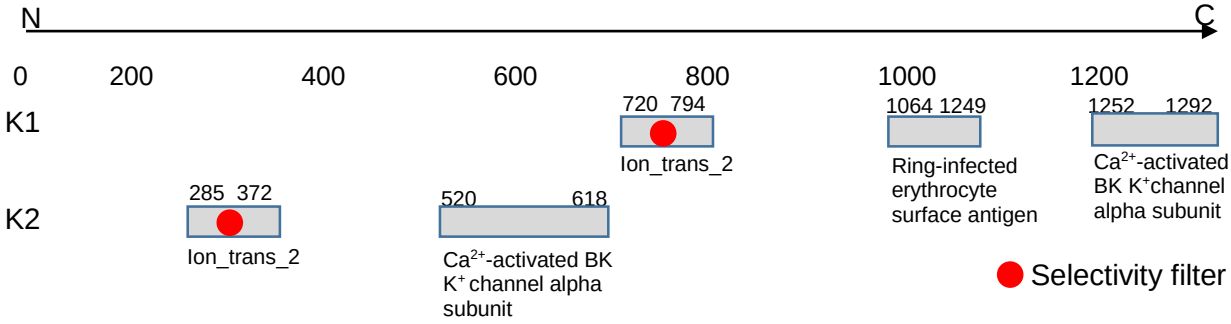

Figure 12: Characterisation of K^+ channels in *P. falciparum*. Multiple sequence alignment between K1, K2 and other known K^+ channels show the selectivity filter. Conserved regions and classifications have been determined by NCBI Conserved Regions. Ion trans: Ion transporter family domain. BK K^+ channel: Big conductance K^+ channel. Red dot: selectivity filter.

Lastly, a K1 protein model was built on a human Ca^{2+}-free Slo1 channel template (6v3g.1.A) identified by SWISS model and confirms a homotetramer state (Figure 13). The sequence similarity is 30 % to the template and there is 44 % coverage on the template. Furthermore,

SWISS model also classified K1 as a Ca^{2+}-activated K^+ channel. Figure 13 shows the model with pore selectivity filter region, Ca^{2+}-activated BK K^+ channel alpha subunit, ring infected erythrocyte surface antigen and ion transporter region. The Ramachandran plot shows torsional angles are permitted by grouping of β-sheets, right handed α-helix and left-handed α-helix.

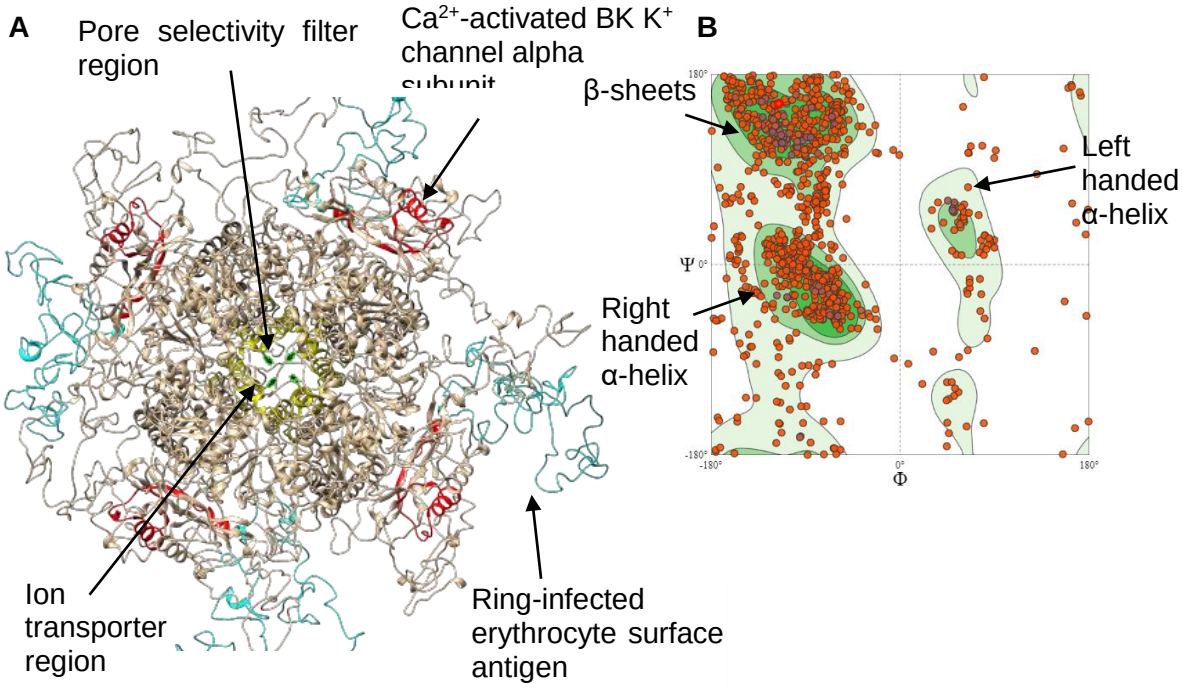

Figure 13: Structure of the *P. falciparum* K1. A) Modelling of the K1 protein in SWISS model revealed conserved regions using the human Ca^{2+}-free Slo1 channel template (6v3g.1.A). Pore selectivity filter region: green. Ca^{2+}-activated K^+ channel alpha subunit: red. Ion transporter region: yellow. Ring-infected erythrocyte surface antigen: cyan. **B)** Ramachandran plots show β-sheets grouped together and α-helixes grouped together. Model annotated with UCSF Chimera v 1.15.

As for K1, a protein model for K2 showed a homotetramer state when the model was built on a human Ca^{2+}-free Slo1 channel template (6v3g.1.A) identified by SWISS model (Figure 14). The sequence similarity to the template is 30 % and there is 28 % coverage on the template. Furthermore, SWISS model also classified K2 as a Ca^{2+}-activated K^+ channel. Figure 14 shows the model with pore selectivity filter region, Ca^{2+}-activated BK K^+ channel alpha subunit, and ion transporter region. The Ramachandran plot shows the grouping of β-sheets, right handed α-helix and left-handed α-helix, which indicates which torsional angles are permitted.

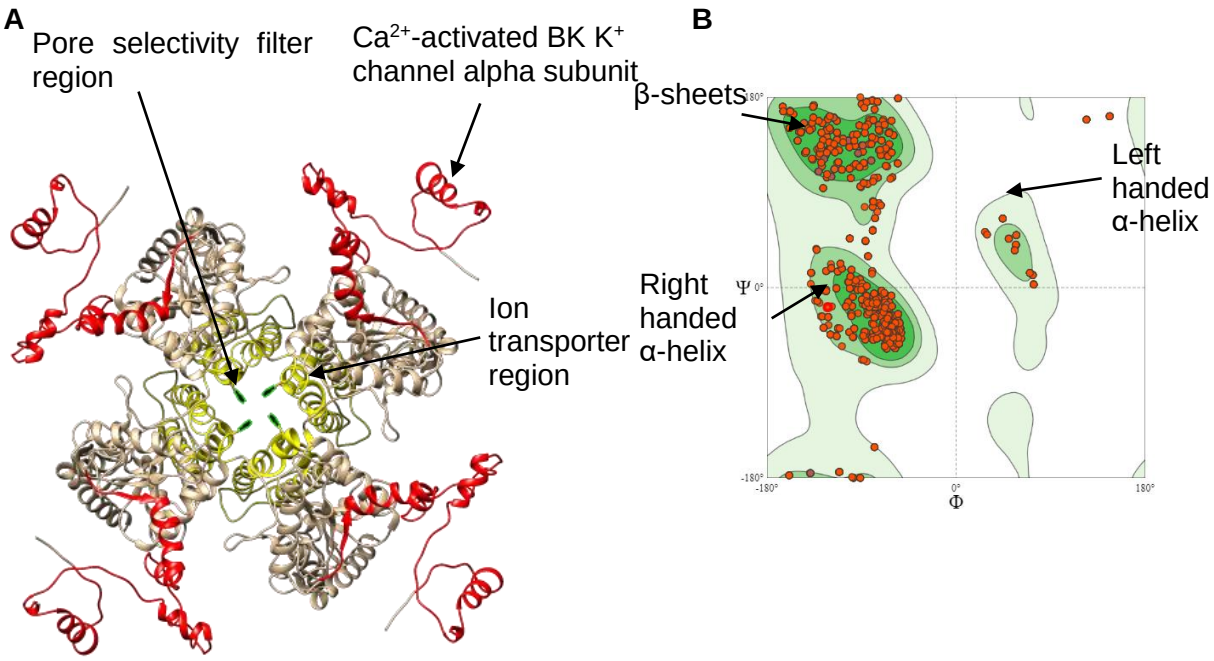

Figure 14: Structure of the *P. falciparum* K1. Modelling of the K2 protein in SWISS model revealed conserved regions using the human Ca^{2+}-free Slo1 channel template (6v3g.1.A). Pore selectivity filter region: green. Ca^{2+}-activated BK K^+ channel alpha subunit: red. Ion transporter region: yellow. **B)** Ramachandran plots show β-sheets grouped together and α-helixes grouped together. Model annotated with UCSF Chimera v 1.15.

Ca^{2+}-activated and voltage gated K^+ channels contain six (or seven in the case of large conductance K^+) TMDs. Six and seven TMDs have been predicted in K1 and K2 respectively, and the predicted pore selectivity filter region most resembles those of Ca^{2+}-activated K^+ channels [91]. Therefore, based on the presence of the selectivity filter and the conserved regions classified as ion transporter and Ca^{2+}-activating big conductance superfamily, it can be concluded that K1 and K2 are K^+ ion channels. This is also supported with the protein models as the ion transporter region, Ca^{2+}-activated BK K^+ channel alpha subunit and pore selectivity filter can be annotated on the models.

3.1.3 Expression of *k1* and *k2* in intra-erythrocytic *P. falciparum* stages

To determine when *k1* and *k2* are expressed during the *P. falciparum* life cycle, the stage-specific mRNA expression profiles of both *k1* and *k2* were investigated in both asexual intra-erythrocytic parasites [135] and gametocytes [136] (Figure 15) using published data. Expression profile for asexual parasites are measure hours post invasion (hpi), and *k1* shows increased abundance during merozoites (0 - 10 hpi), rings (10 - 16 hpi) and trophozoite stages (17 - 32 hpi), and decreased abundance in schizont stages (33 - 47 hpi), as well as during the gametocyte stages. By contrast, expression profiles for *k2* shows increased abundance during

merozoite, early ring and schizont parasite stages as well as during gametocytogenesis (Figure 15).

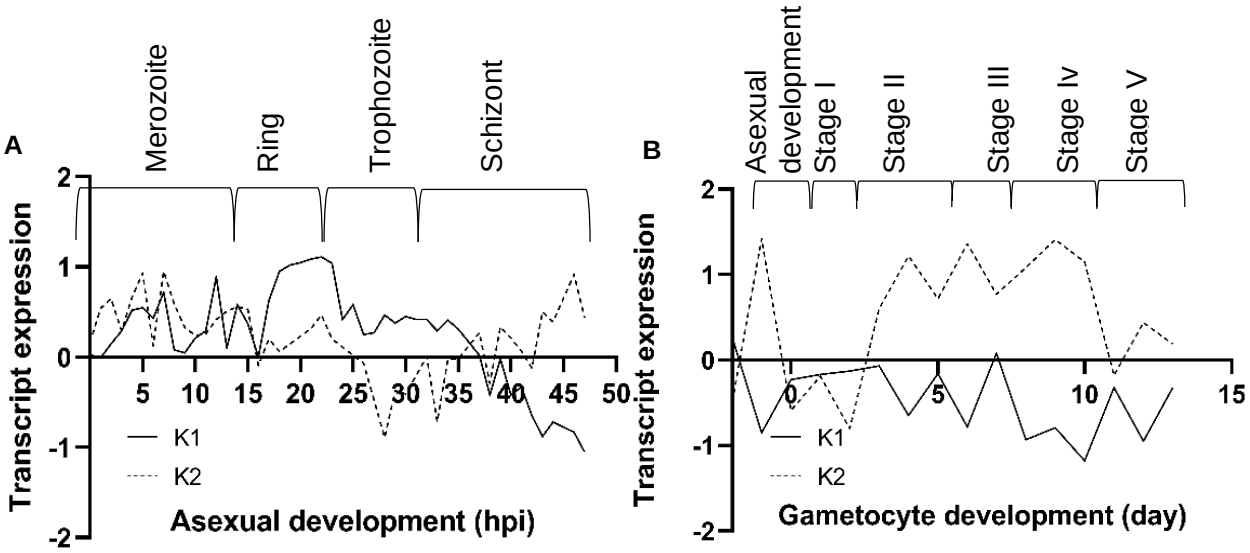

Figure 15: Stage-specific transcript expression profiles of *k1* (solid line) and *k2* (dotted line) genes throughout both A) asexual and B) gametocyte stages. The transcript expression profiles of the genes are given as log2(Cy5/Cy3) expression values on the y-axis at each time point on the x-axis. Data used from Painter et al., 2017 [135] and van Biljon *et al*., 2019 [136]. **hpi:** hours post invasion.

In conclusion, K1 and K2 have TMDs, indicating that it is located in a membrane. Furthermore, these proteins also contain the selectivity filter specific to potassium ions and conserved regions specific to ion transporters and big conductance channels, indicating that both K1 and K2 are potassium ion channels. Lastly, while both *k1* and *k2* are expressed during asexual development, *k2* is the only predicted K^+ channel expressed during gametocytogenesis.

To confirm the expression of these K^+ channels during asexual and sexual development, as well as the functional importance therefore, genetically modified parasites that allow for localization and knockdown studies must be generated.

3.2 Generate recombinant plasmids of pGFP_*glmS* and pSLI_*glmS* with *k1* and *k2* gene fragments

To investigate the functional importance of a gene, a conditional knockdown recombinant line can be generated. This is done by creating a plasmid with a *glmS* riboswitch, and inserting it into the genome of the parasite though transfection and drug cycling.

3.2.1 *In vitro* cultivation of asexual stage *P. falciparum* parasites

Asexual *P. falciparum* parasites were cultivated *in vitro* throughout the study to source gDNA for PCR amplification and for the transfection and establishment of genetically modified lines. The parasites were visible as thin discoidal ring shapes after 10 -16 hpi, whereas the early trophozoite stages, observed from ~17 hpi were characterised by haemozoin crystal development. Development from the early to late trophozoite stage was associated with an increase in the size of parasites. The schizonts stage parasites, containing multiple nuclei, were visible from ~ 33 - 44 hpi (Figure 16).

Stage	Ring	Early trophozoite	Late trophozoite	Schizont
Morphology		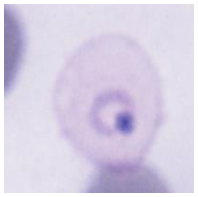	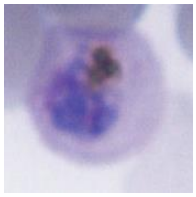	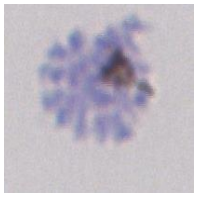
~ hpi	10-16	17-24	25-32	33-44

Figure 16: Evaluation of *P. falciparum* asexual parasites morphology following *in vitro* cultivation. The ring, early trophozoite, late trophozoite and schizont stages are shown with their respective hours post invasion (hpi). Parasite cultures were used to make thin blood smears, fixed with methanol, and stained with Giemsa-stain. The parasites were viewed and photographed at 1000x magnification.

3.2.2 Isolation of genomic DNA from asexual *P. falciparum* parasites

Genomic DNA was isolated from NF54 *P. falciparum* parasites (>95 % trophozoite stage parasites, 5 % haematocrit) and used as a template to amplify fragments of the GOI for cloning. The quantity and quality of the isolated gDNA was determined using a spectrophotometer with concentrations ranging from 11 ng/µL – 146 ng/µL and A_{260}/A_{280} and A_{260}/A_{230} purity ratios ranging from 1.49 – 2.57 obtained. This quantity was sufficient for PCR amplification, however, the purity ranges were out of recommended purity ratios. This could be as a result of salt or protein contamination.

3.2.3 Amplification of C-terminus fragments of *k1* and *k2* using PCR

C-terminal fragments from the GOI were amplified from gDNA using the gene specific primers in Table 1. All PCR products obtained were the expected size relative to the primers designed

(Figure 17). A non-specific band of ~ 900 bp was observed in amplification of the *k1* fragment which can be attributed to non-specific binding of primers to the GOI. Since several attempts to optimise PCR conditions to obtain a single *k1* product were unsuccessful, the band with the correct expected size (1030 bp and 1029 bp) was excised from the gel and purified (Figure 17 A), whereas *k2* (1026 bp and 1075 bp) (Figure 17 B) was purified using a kit as per manufacturers instruction for downstream experiments, yielding concentrations ranging from 69 - 85 ng/µL and purity ratios for A_{260}/A_{280} and A_{260}/A_{230} ranging from 0.41 – 1.96 for both *k1* and *k2.* Even though this ratio does not fall in the optimal range as stated in section 2.2.6 (purification of amplified PCR products), the manufacturer stated in the guide [149] that this is most likely because of chaoptropic salt contamination, but will not affect downstream experiments because of the low yields of purified PCR product.

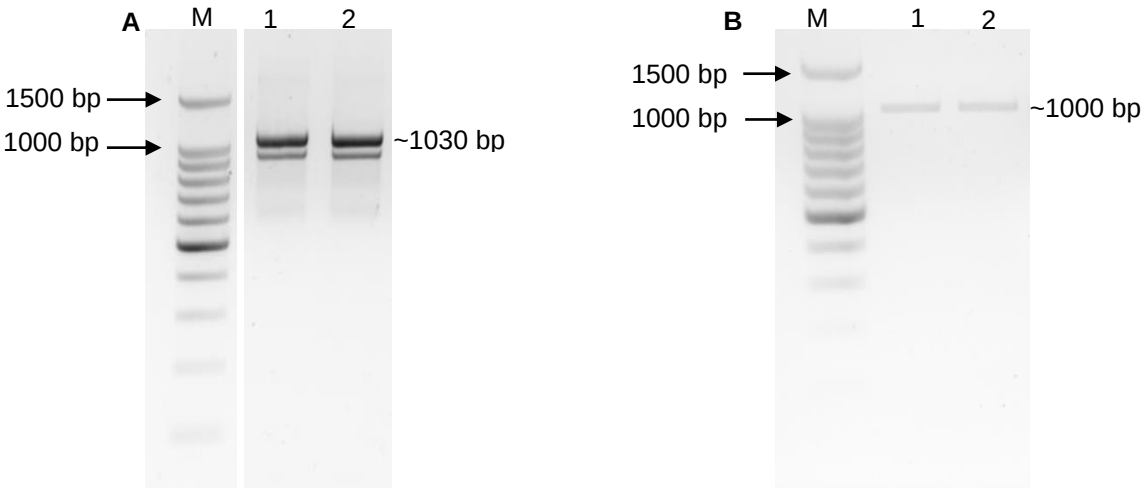

Figure 17: PCR amplification of gene specific fragments. A) PCR amplification of *k1* expected size 1030 bp and 1029 bp. M: 100 bp ladder (Promega™, Madison, USA). Lane 1: fragment used for pGFP_*glmS* plasmid. Lane 2: Fragment used for pSLI_*glmS* plasmid. **B)** PCR amplification of *k2 expected size*1026 bp and 1075 bp. M: 100 bp ladder (Promega™, Madison, USA). Lane 1: Fragment used for pGFP_*glmS*. Lane 2: Fragment used for pSLI_*glmS*. PCR products were separated with 1.5 % (w/v) agarose/TAE gel and visualised with EtBr (1.2 mg/mL) under UV light.

3.2.4 Preparation of pGFP_*glmS* and pSLI_*glmS* plasmids for cloning procedures

To validate the identity of pGFP_*glmS* and pSLI_*glmS* plasmids and thus ensure the correct plasmids were used, restriction enzyme mapping was performed using *Bam*HI and *Hind*III. Digestion produced two fragments of the expected sizes: 7742 bp and 399 bp for pGFP_*glmS* and 7238 bp and 568 bp for pSLI_*glmS* (Figure 18).

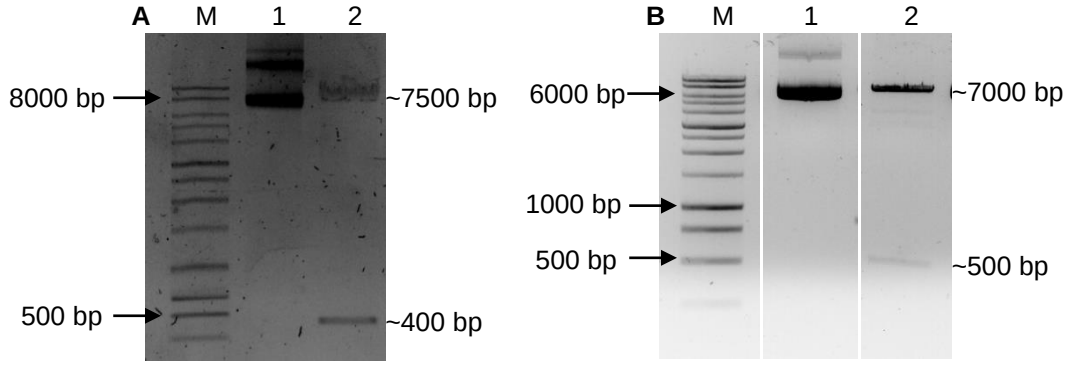

Figure 18: Restriction enzyme maps of pGFP_*glmS* and pSLI_*glmS* plasmids. A) pGFP_*glmS* plasmid expected sizes 7742 bp and 399 bp. M: 1 kb ladder (Promega™, Madison, USA). Lane 1: Uncut pGFP_*glmS* plasmid. Lane 2: Plasmid digested with *Bam*HI and *Hind*III **B)** pSLI_*glmS* WT plasmid 7238 bp and 568 bp. M: 1 kb ladder (Promega™, Madison, USA). Lane 1: Uncut pSLI_*glmS* WT plasmid. Lane 2: pSLI_*glmS* WT plasmid digested with *Bam*HI and *Hind*III. The DNA was separated with 1 % (w/v) agarose/TAE gel and visualised with EtBr (1.2 mg/mL) under UV light. Complete gel can be seen in Supplementary Figure 1.

Subsequently, both the pGFP_*glmS* and pSLI_*glmS* plasmids were digested with the relevant restriction enzymes to obtain the plasmid backbone needed for ligation. Two fragments were produced for each digestion (Figure 19). The backbone of approximately 6500 - 7000 bp (6490 bp for pGFP_*glmS* and 6932 bp for pSLI_*glmS*) of each plasmid was excised and purified for a ligation reaction, yielding a 52 - 57 ng/µL DNA with purity values for A_{260}/A_{280} and A_{260}/A_{230} values ranged from 0.28 – 1.93. As above, according to the manufacturers guide, these rtatios will affect downstream experiments [149].

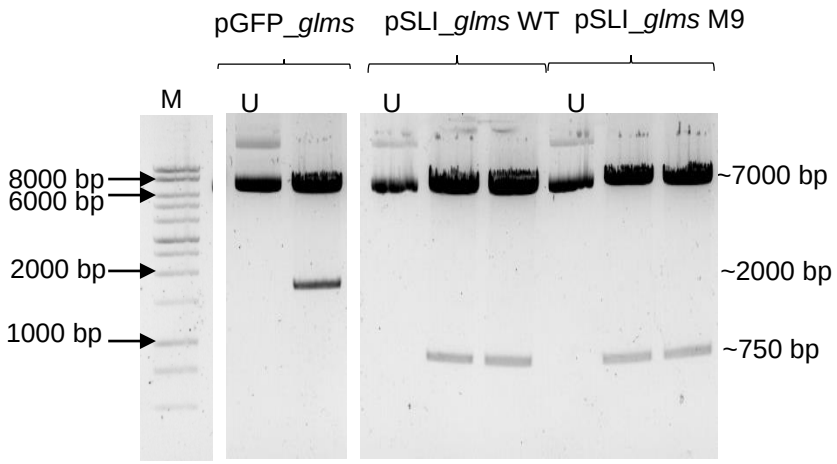

Figure 19: Preparation of pGFP_*glmS*, pSLI_*glmS* WT & pSLI_*glmS* M9 restriction enzyme digested plasmids for ligation. M: 1 kb ladder (Promega™, Madison, USA). U: Uncut plasmid. pSLI_*glmS* WT & pSLI_*glmS* M9 plasmid was digested with *Not*I and *Mlu*I. pGFP_*glmS* plasmid was digested with *Afl*II and *Kpn*I. The DNA was separated with 1 % (w/v) agarose/TAE gel and visualised with EtBr (1.2 mg/mL) under UV light. Complete gel can be seen in Supplementary Figure 2.

3.2.5 Cloning of *k1* gene fragment into pGFP_*glmS*, pSLI_*glmS* WT and pSLI_*glmS* M9 to generate pGFP_*glmS*_*k1,* pSLI_*glmS* WT_*k1* and pSLI_*glmS* M9_*k1*

The purified *k1* fragments were digested with the required restriction enzymes and combined with the plasmids in standard ligation reactions. After ligation, the recombinant plasmids were transformed into chemically competent DH5α *E. coli* cells. After multiple attempts, no positive colonies could be obtained for the pGFP_*glmS*, pSLI_*glmS* WT and pSLI_*glmS* M9 with a *k1* fragment, therefore, the *k1* fragment was subcloned into pGEM®-T Easy plasmid using AT-cloning. Subcloning ensures the *k1* fragments are fully digested when cut out of the pGEM®-T Easy plasmid, and allows for sequencing. Plasmids from 22 putative *k1* (to be cloned into pGFP_*glmS*) positive colonies based on blue-white screening was analysed by digestion with *Eco*RI (Figure 20 A). From these, 2 clones contained the correct fragment size intended for cloning into pGFP_*glmS.* Plasmids from 28 putative *k1* (to be cloned into pSLI_*glmS*) positive colonies based on blue-white screening was analysed by digestion with *Eco*RI (Figure 20 B). From these, 13 clones contained the correct fragment size intended for cloning into pSLI_*glmS.* The presence of the correct insert for each plasmid system was confirmed using the respective restriction enzymes for cloning (either *Afl*II or *Kpn*I for pGFP_*glmS* and *Not*I or *Mlu*I for pSLI_*glmS*) resulting in the correct sized fragment excised from the pGEM®-T Easy backbone (Figure 20 C). The identity of the inserts was verified with Sanger dideoxy sequencing. Primers specific to the backbone of the pGEM®-T Easy plasmid were used in the sequencing reaction to confirm the sequence of the C-terminal gene fragment. The

sequencing alignment results for *k1* in pGEM®-T Easy are shown in Figure 20 D, and validate that the gene fragments were successfully cloned into pGEM®-T Easy plasmid in the correct orientation and without mutations. Next, fragments were excised from pGEM®-T Easy plasmid and ligated into pGFP_*glmS* and pSLI_*glmS* plasmids.

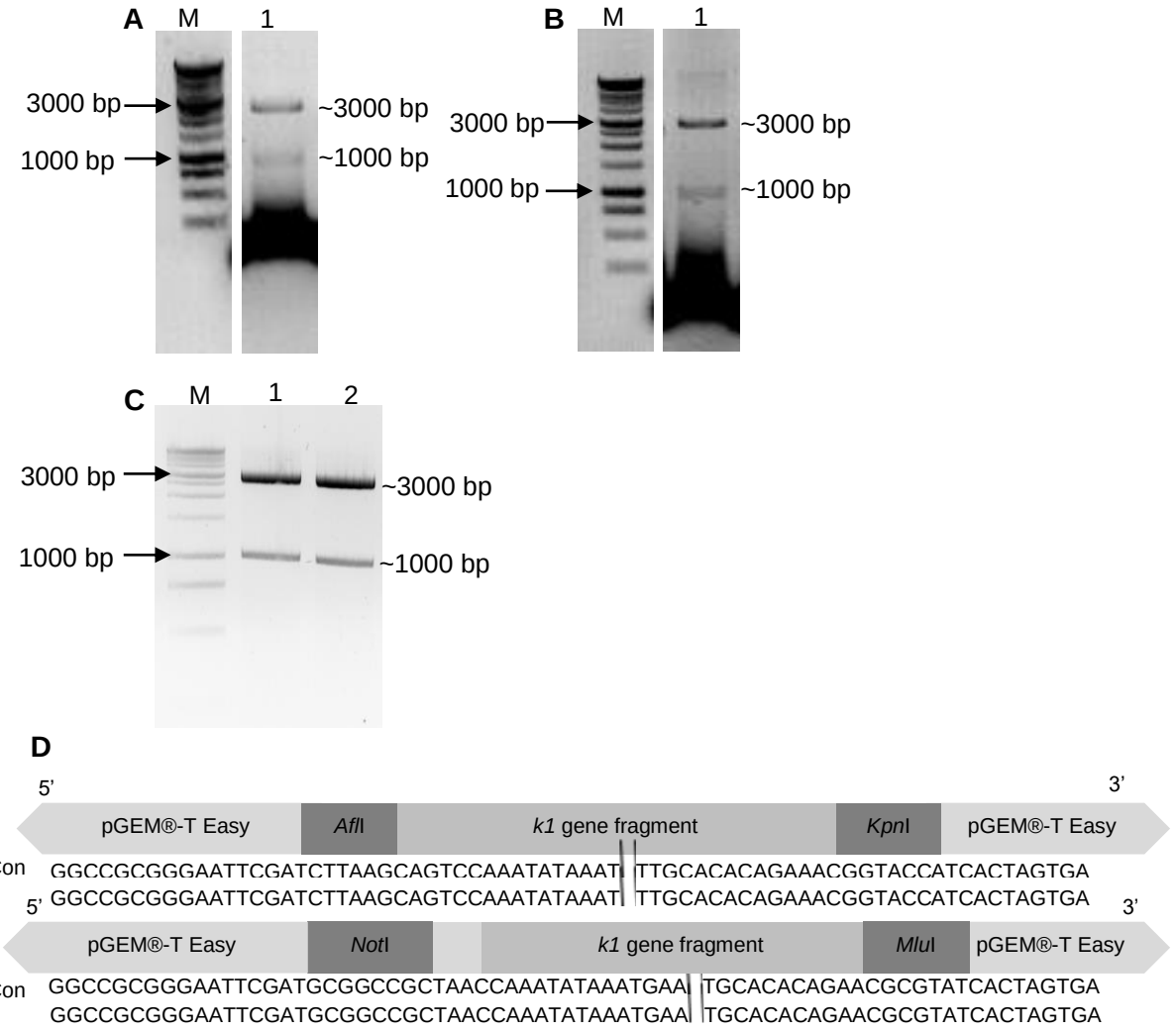

Figure 20: *k1* fragments for both plasmid systems were cloned into pGEM®-T Easy plasmids. A) and **B)** are representative examples of the plasmid screening, with complete gels in Supplementary Figure 3 and 4**. A) RED positive recombinant plasmids of *k1* in pGEM®-T Easy plasmids for pGFP_*glmS.*** M: 1 kb ladder (Promega™, Madison, USA). Lane 1: pGEM T-Easy plasmid containing *k1* insert for pGFP_*glmS* digested with *Eco*RI. **B) RED positive recombinant plasmids of *k1* in pGEM®-T Easy plasmids for pSLI_*glmS*** M: 1 kb ladder (Promega™, Madison, USA). Lane 1: pGEM®-T Easy plasmid containing *k1* insert for pSLI_*glmS* digested with *Eco*RI. **C) RED positive recombinant plasmids of *k1* in pGEM®-T Easy plasmids for pGFP_*glmS* and pSLI_*glmS*** M: 1 kb ladder (Promega™, Madison, USA). Lane 1. pGEM®-T Easy plasmid with *k1* insert for pGFP_*glmS* digested with *Afl*II and *Kpn*I. Lane 2: pGEM®-T Easy plasmid with *k1* insert for pSLI_*glmS* digested with *Not*I and *Mlu*I. The products of digestion were separated on a 1 % (w/v) agarose/TAE gel and visualised with EtBr staining (1.2 mg/mL) under UV light. **D**) **Sequence alignments confirming the identity of the *k1* gene inserts**. DNA fragments in schemes not drawn to scale. **Con:** consensus sequence.

The gene fragments cut from pGEM®-T Easy (Figure 20 C) as well as pGFP*_glmS* and pSLI*_glmS* plasmids were digested with their respective restriction enzymes in preparation for directional, in-frame cloning of the gene fragments. Colony PCR was used to test 5 positive colonies of each recombinant plasmid after ligation. Primer pairs for the initial PCR amplification of C-terminal gene fragments were used. For pGFP*_glmS_k1*, pSLI*_glmS_k1* WT and pSLI*_glmS_k1* M9, 1 positive colony each was identified with colony PCR (Figure 21 A), after subcloning. Recombinant plasmid DNA from positive clones were digested with the relevant restriction enzymes to validate the presence of the *k1* gene fragment. The digested recombinant plasmids were analysed with gel electrophoresis (Figure 21 B). Bands of approximately ~1030 bp were obtained (expected size 1030 bp for pGFP*_glmS_k1* and 1029 bp for pSLI*_glmS_k1*) confirming that each of the fragments were successfully cloned into the pGFP*_glmS*, pSLI*_glmS* WT and pSLI*_glmS* M9 plasmids. Each positive recombinant plasmid was sequenced with Sanger dideoxy sequencing.

Sanger sequencing was performed with primers specific to the backbone of the plasmids were used to confirm the presence of the C-terminal gene fragment sequence. The sequencing alignment results for *k1* fragments in each plasmid are shown in Figure 21 C and confirm all gene fragments were successfully cloned into each plasmid in the correct orientation, without mutations and were thus appropriate for use in transfection.

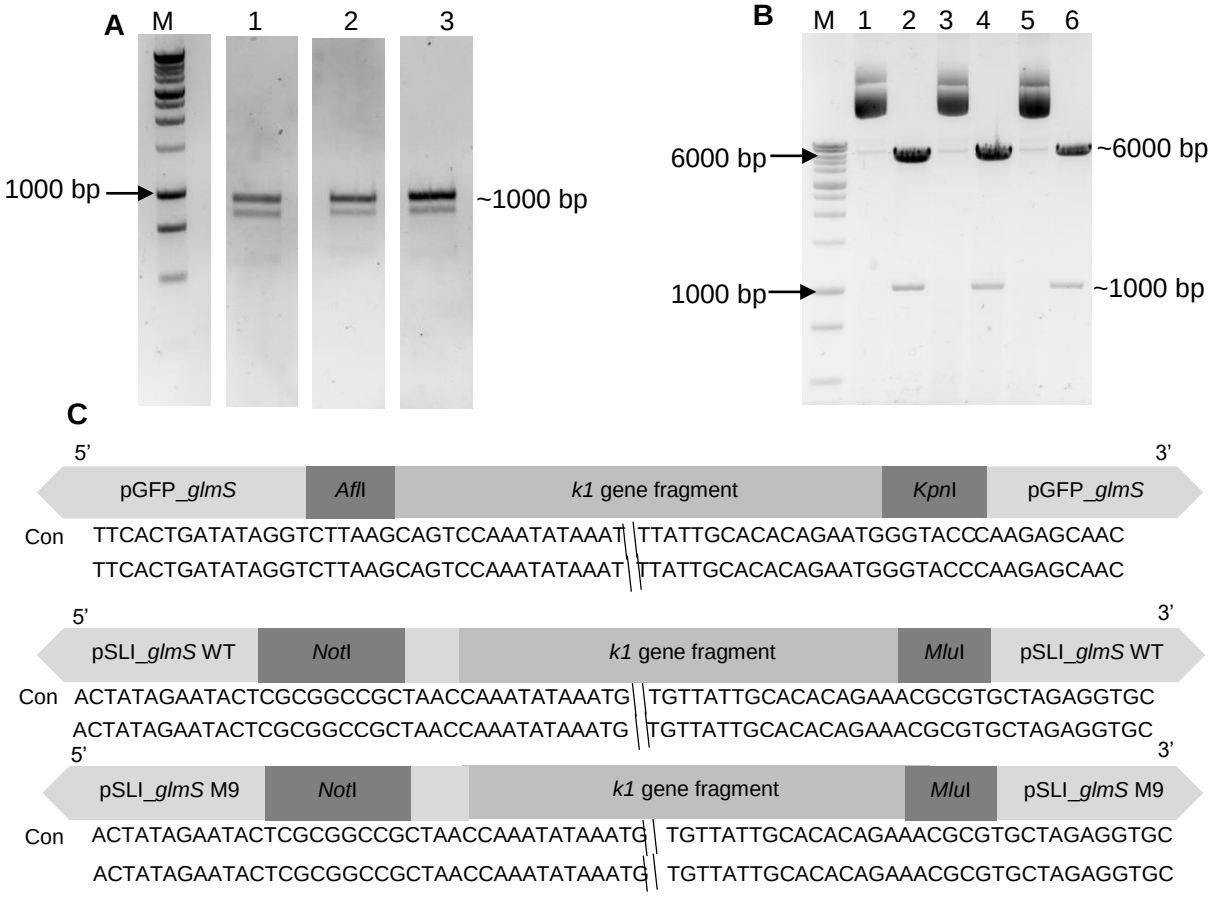

Figure 21: Validation of *k1* in pGFP_*glmS*, pSLI_*glmS* WT and pSLI_*glmS* M9 plasmidsare representative examples of the plasmid screening, with complete gels in Supplementary Figure 5. A) Colony PCR screening for colonies with *k1* inserts M: 1 kb ladder (Promega™, Madison, USA). Lane 1: Screening for positive clones containing pGFP_*glmS*, with C-terminal fragment. Lane 2: Screening for positive clones containing pSLI_*glmS* WT, with C-terminal fragment. Lane 3: Screening for positive clones containing pSLI_*glmS* M9, with C-terminal fragment. **B) RED positive recombinant plasmids of *k1* in pGFP_*glmS*, pSLI_*glmS* WT and pSLI_*glmS* M9.** M: 1 kb ladder (Promega™, Madison, USA). Lane 1: Uncut *k1* fragment in pGFP_*glmS*. Lane 2: *k1* fragment in pGFP_*glmS* digested with *Afl*II and *Kpn*I. Lane 3: Uncut *k1* fragment in pSLI_*glmS* WT. Lane 4: *k1* fragment in pSLI_*glmS* WT digested with *Not*I and *Mlu*I. Lane 5: Uncut *k1* fragment in pSLI_*glmS* M9. Lane 6: *k1* fragment in pSLI_*glmS* M9 digested with *Not*I and *Mlu*I.The DNA was separated with 1 % (w/v) agarose/TAE gel and visualised with EtBr (1.2 mg/mL) under UV light. **C) Sequence alignments validating the successful recombination of pGFP_*glmS*, pSLI_*glmS* WT and pSLI_*glmS* M9 and *k1* gene inserts.** DNA fragments in schemes not drawn to scale. **Con:** consensus sequence.

3.2.6 Cloning of *k2* gene fragment into pGFP_*glmS* and pSLI_*glmS* WT and pSLI_*glmS* M9 to generate pGFP_*glmS*_*k2,* pSLI_*glmS* WT_*k2* and pSLI_*glmS* M9_*k2*

The *k2* gene fragments as well as pGFP_*glmS* and pSLI_*glmS* plasmids were digested with their respective restriction enzymes in preparation for directional, in-frame cloning of the gene fragments. After ligation, the recombinant plasmids were transformed into chemically competent DH5α *E. coli* cells. Colony screening PCR was performed on colonies resulting from the ligation and transformation reactions, using the primer pairs used during the initial PCR amplification of gene fragments. For pGFP_*glmS*, only 1 colony was screened and found positive (Figure 22 A). All colonies (13 screened) were positive for the pSLI_*glmS* WT and pSLI_*glmS* M9 *k2* gene fragments after ligation (Figure 22 B & C). Recombinant plasmid DNA from positive clones were digested with the relevant restriction enzymes to validate the presence of the gene fragment. The digested recombinant plasmids were analysed with gel electrophoresis (Figure 22 C). Bands of approximately ~1030 and 1070 bp were obtained (expected size 1026 bp for pGFP_*glmS*_*k2* and 1075 bp for pSLI_*glmS*_*k2*) confirming that each of the fragments were successfully cloned into the pGFP_*glmS*, pSLI_*glmS* WT and pSLI_*glmS* M9 plasmids. One of each positive recombinant plasmid was randomly chosen for Sanger dideoxy sequencing.

Sanger dideoxy sequencing was performed to confirm the inserts cloned into the plasmids contained no mutations and that the gene of interest was cloned into the respective plasmids in the correct reading frame by using primers specific to the backbone of the plasmids to confirm the presence of the C-terminal gene fragment sequence. The sequencing alignment results for *k2* fragments in each plasmid are shown in Figure 22 D and confirm all gene

fragments were successfully cloned into each plasmid in the correct orientation, without mutations and were thus appropriate for use in transfection.

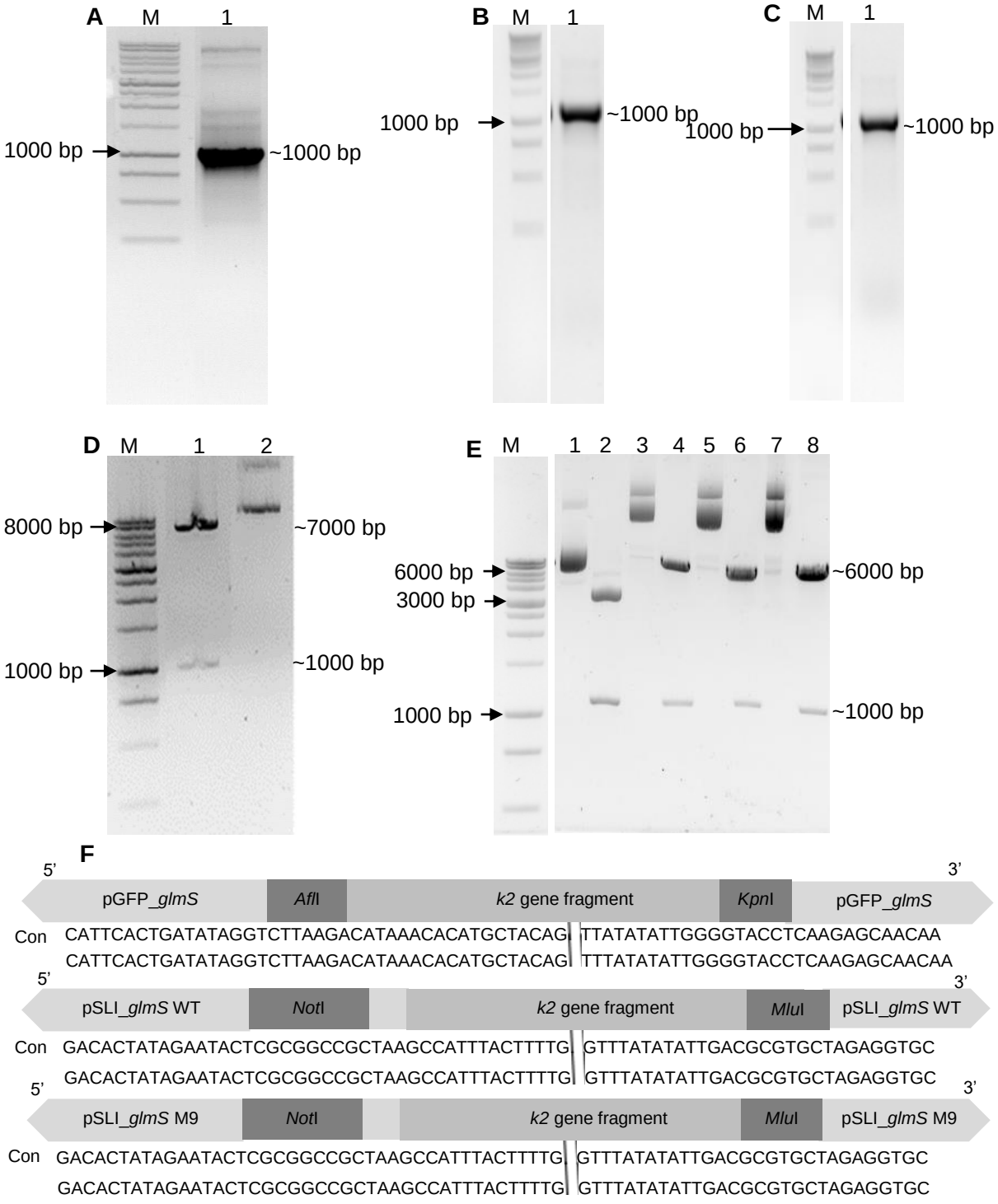

Figure 22: Validation of *k2* in pGFP*_glmS*, pSLI*_glmS* WT and pSLI*_glmS* M9 plasmids. A) Colony screening PCR for positive clones containing the *k2* gene fragment in pGFP*_glmS* plasmid. M: 1 kb ladder (Promega™, Madison, USA). Lane 1: Screening for a positive clone containing pGFP*_glmS*, with C-terminal fragment. **B) Colony screening PCR for positive clones containing the *k2* gene fragment in pSLI*_glmS* WT plasmid. B) are representative examples of the plasmid screening, with complete gels in Supplementary Figure 6.** M: 1 kb ladder (Promega™, Madison, USA). Lane 1: Screening for positive clone containing pSLI*_glmS* WT, with C-terminal fragment. **C) Colony screening PCR for positive clones containing the *k2* gene fragment in pSLI*_glmS* M9**

plasmid. C) are representative examples of the plasmid screening, with complete gels in Supplementary Figure 7. M: 1 kb ladder (Promega™, Madison, USA). Lane 1: Screening for positive clone containing pSLI_*glmS* M9, with C-terminal fragment. **D) RED of positive recombinant plasmid of *k2* in pGFP_*glmS*.** M: 1 kb ladder (Promega™, Madison, USA). Lane 1: *k2* in pGFP_*glmS* digested with *Afl*II and *Kpn*I. Lane 2: Uncut *k2* in pGFP_*glmS*. **E) RED of positive recombinant plasmids of *k2* in pSLI_*glmS* WT and M9.** M: 1 kb ladder (Promega™, Madison, USA). Lane 1: Uncut *k2* in pSLI_*glmS* WT colony 1. Lane 2: *k2* in pSLI_*glmS* WT digested with *Not*I and *Mlu*I colony 1. Lane 3: Uncut *k2* in pSLI_*glmS* WT colony 2. Lane 4: *k2* in pSLI_*glmS* WT digested with *Not*I and *Mlu*I colony 2. Lane 5: Uncut *k2* in pSLI_*glmS* M9 colony 1. Lane 6: *k2* in pSLI_*glmS* M9 digested with *Not*I and *Mlu*I colony 1. Lane 7: Uncut *k2* in pSLI_*glmS* WT colony 2. Lane 8: *k2* in pSLI_*glmS* WT digested with *Not*I and *Mlu*I colony 2. The DNA was separated with 1 % (w/v) agarose/TAE gel and visualised with EtBr (1.2 mg/mL) under UV light. **F) Sequence alignments validating the successful recombination of pGFP_*glmS*, pSLI_*glmS* WT and pSLI_*glmS* M9 and *k2* gene inserts.** DNA fragments in schemes not drawn to scale. **Con:** consensus sequence.

In conclusion, C-terminal fragments of *k1* and *k2* were successfully cloned into pGFP_*glmS*, pSLI_*glmS* WT and pSLI_*glmS* M9 to generate pGFP_*glmS*_*k1,* pSLI_*glmS*WT_*k1,* pSLI_*glmS*M9_*k1*, pGFP_*glmS*_*k2,* pSLI_*glmS*WT_*k2,* pSLI_*glmS*M9_*k2.* These plasmids were subsequently transfected into *P. falciparum* NF54 parasites.

3.3 Production of NF54_Δ*k1*_GFP_*glmS*, NF54_Δ*k2*_GFP_*glmS,* NF54_*k1*_SLI_*glmS* and NF54_Δ*k2*_SLI_*glmS* parasite lines.

3.3.1 Transfection and confirmation of episomal uptake of recombinant lines

After plasmids were successfully cloned, pGFP_*glmS*_*k1,* pSLI_*glmS*WT_*k1,* pSLI_*glmS*M9_*k1*, pGFP_*glmS*_*k2,* pSLI_*glmS*WT_*k2,* pSLI_*glmS*M9_*k2* were transfected into *P. falciparum* NF54 parasites to produce parasite lines.

For transfection of *P. falciparum* parasites, generally 50 - 100 mg DNA was used [111, 117]. This was accomplished as described in section 2.2.3 with the concentration obtained for each recombinant plasmid after each precipitation step shown in Table 5. There was on average a 73 % loss of DNA in the clean-up process and the total DNA amount of each recombinant plasmid after ethanol precipitation was transfected into *P. falciparum* NF54 parasites.

Table 5: Quantity of recombinant plasmids isolated and transfected into *P. falciparum* NF54 parasites

Recombinant plasmid	[ ]Before isopropanol	[ ] After isopropanol	Ethanol precipitation
pGFP_*glmS*_k1	875 µg	625 µg	110.5 µg
pSLI_*glmS* WT_k1	115 µg	53 µg	46 µg
pSLI_*glmS* M9_k1	650 µg	630 µg	95 µg
pGFP_*glmS*_k2	365 µg	347 µg	85 µg
pSLI_*glmS* WT_k2	490 µg	128.5 µg	87.5 µg
pSLI_*glmS* M9_k2	865 µg	400 µg	115 µg

Following transfection, parasites were subjected to drug cycling, to select for parasites with episomal uptake of the plasmid in the cytosol. Parasites that recovered after 14 days of blasticidin treatment for pGFP_*glmS* or 10 days of WR22910 treatment for pSLI_*glmS*, were confirmed to have episomal uptake using PCR amplification with primers specific for the backbone of the recombinant plasmid (Figure 23). All six of the transfected constructs were present episomally after the first drug treatment. Parasites that were confirmed to have successful episomal uptake of plasmids were subjected to a second drug cycle to allow integration of the plasmids into the parasite genome.

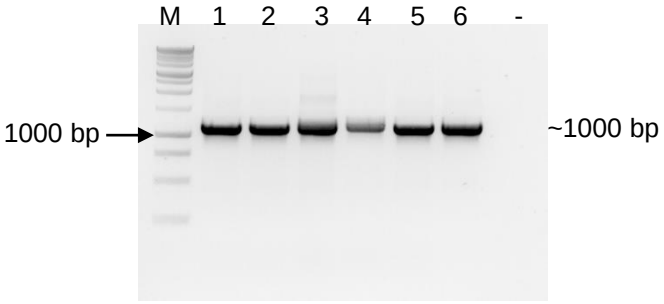

Figure 23: Confirmation of episomal uptake of recombinant plasmids transfected into parasites. PCR amplification was performed using primer pairs that bind to the backbone of the plasmid. M: 1 kb ladder (Promega™, Madison, USA). Lane 1: *k1* in pGFP_*glmS*. Lane 2: *k1* pSLI_*glmS* WT: Lane 3: *k1* pSLI_*glmS* M9. Lane 4: *k2* pGFP_*glmS*. Lane 5: *k2* pSLI_*glmS* WT. Lane 6: *k2* pSLI_*glmS* M9. Lane -: Negative control contains no DNA. The DNA was separated with 1 % (w/v) agarose/TAE gel and visualised with EtBr (1.2 mg/mL) under UV light.

3.3.2 Genome modification of *k1* and *k2* using pGFP_*glmS*

After parasites were subject to a second drug cycle of blasticidin for pGFP_*glmS_k1* and pGFP_*glmS_k2* they were allowed to recover (without drug pressure). To test if the plasmid had integrated into the genome of the parasites after drug cycling, an PCR to test for genomic integration was done.

For pGFP_*glmS_k1* a 5' integration will result in a fragment of 1368 bp using a forward primer that binds to the gene (F1) and a reverse primer that binds to the GFP tag (R1). If there is 3' integration, a fragment of 1259 bp would be present using a forward primer that binds to the plasmid backbone (F4) and a reverse primer that binds to the next gene (R3). To test if there are any wild type parasites present in the culture line, a forward primer that binds to the gene (F1) and a reverse primer that binds to the next gene (R3) is used and will produce a 2041 bp fragment, as shown in Figure 24 A. Figure 24 B shows that there is no 5' or 3' integration, and only wild type parasites present in the culture line. However, the episomal band had increased in size indicating that the plasmid might have formed concatamers with itself [150-152] and

could not find a homologous region to recombine with. The presence of a band in the wild type locus lane indicates that there are only wild type parasites present in the culture.

Similarly, for pGFP_*glmS_k2* a 1368 bp fragment should be present using a forward primer that binds to the gene (F1) and a reverse primer that binds to the GFP tag (R1) if there is 5' integration. A 1259 bp fragment would be present using a forward primer that binds to the plasmid backbone (F4) and a reverse primer that binds to the next gene (R3). A forward primer that binds to the gene (F1) and a reverse primer that binds to the next gene (R3) is used to test if there are any wild type parasites present in the culture line and will produce a 1416 bp fragment as shown in Figure 24 C. Figure 24 D shows that pGFP_*glmS*_k2 was tested for integration and shown there is 5' and 3' integration. However, there are still wild type parasites present in the culture as an approximately 1400 bp band was amplified at the wild type allele locus.

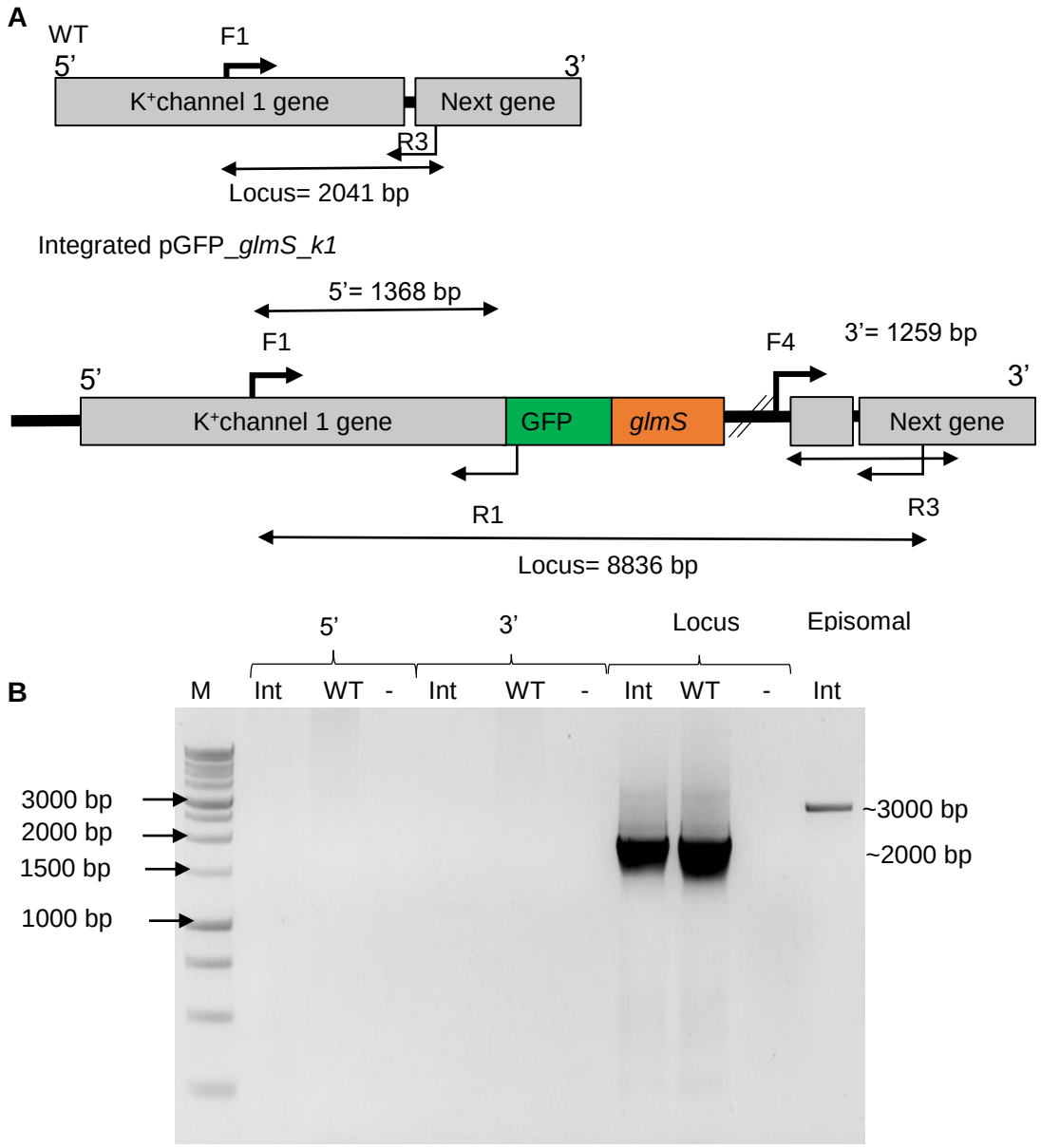

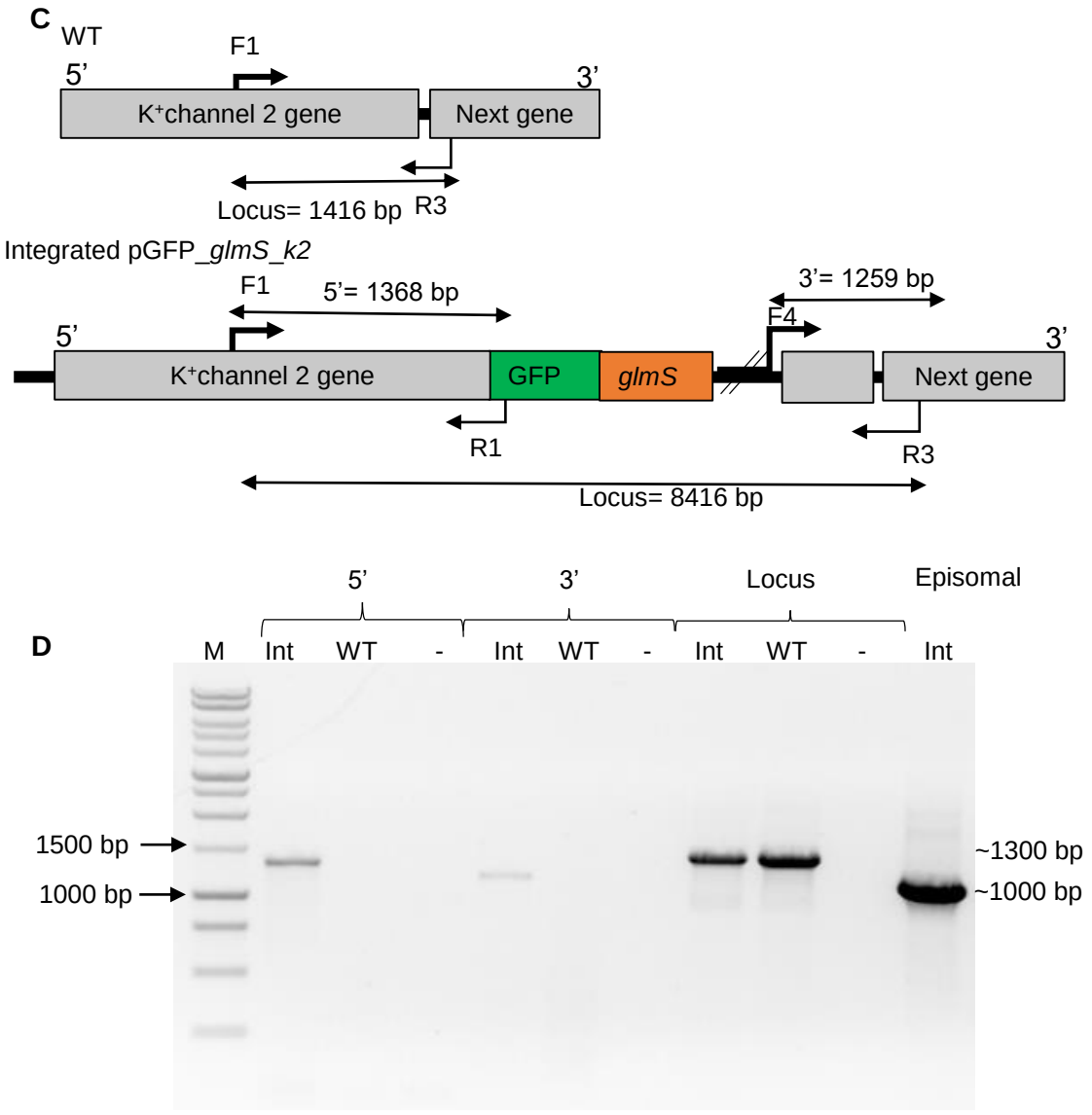

Figure 24: Integration of pGFP_*glmS* plasmids into the genome to create NF54_Δ*k1*_GFP_*glmS* and NF54_Δ*k2*_GFP_*glmS.* A) Schematic representation of PCR to test for integration of pGFP_*glmS*_*k1.* B) Schematic representation of integration PCR for pGFP_*glmS*_*k2.* Primers used for 5' integration are F1 and R1. Primers used for 3' integration are F4 and R3. Primers used for locus are F1 and R3. **C) Schematic representation of PCR to test for integration of pGFP_*glmS*_*k2.* D) Schematic representation of integration PCR for pGFP_*glmS*_*k2.*** Primers used for 5' integration are F1 and R1. Primers used for 3' integration are F4 and R3. Primers used for locus are F1 and R3. Episomal presence was confirmed using plasmid backbone primers. The DNA was separated with 1 % (w/v) agarose/TAE gel and visualised with EtBr (1.2 mg/mL) under UV light.

3.3.3 Genome modification of *k1* and *k2* using pSLI_*glmS*

For both pSLI_*glmS*_*k1* WT and pSLI_*glmS*_*k1* M9 plasmids, drug pressure with neomycin (400 µg/mL) was started for 10 consecutive days, and then every second day for 4 days. Parasitaemia remained below 1.5 % and parasites were visibly stressed. After drug pressure was released, parasitaemia remained below 1.5 % and the parasites never recovered.

After parasites were subject to a second drug cycle of neomycin for pSLI_*glmS_k2* WT and pSLI_*glmS_k2* M9 parasites were allowed to recover (without drug pressure) and a PCR was performed to test genomic integration. If there is 5' integration a fragment of 1368 bp would be present using a forward primer (F1) and a reverse primer (R1). A fragment of 1259 bp would be present if there is 3' integration, using a forward primer (F4) and a reverse primer (R3). To test if there are any wild type parasites in the culture line, a 1416 bp fragment would be produced with a forward primer (F1) and a reverse primer (R3) is used. Figure 25 A and Figure 25 B, shows that pSLI_*glmS_k2* WT and pSLI_*glmS_k1* M9 was tested for integration and showed 5' and 3' integration. However, the 1400 bp band present at the wild type alleles locus indicates that there are still wild type parasites present in the culture.

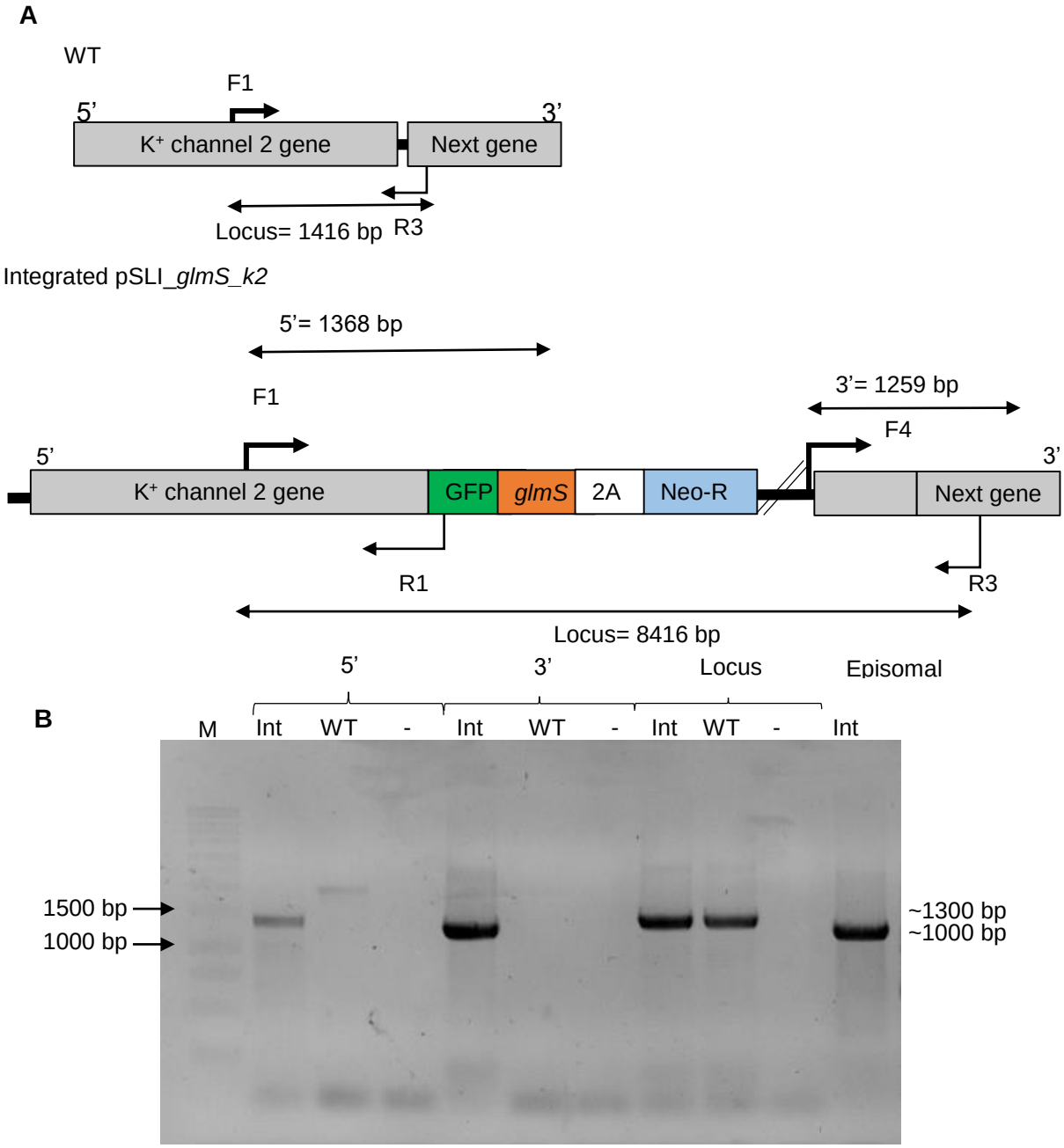

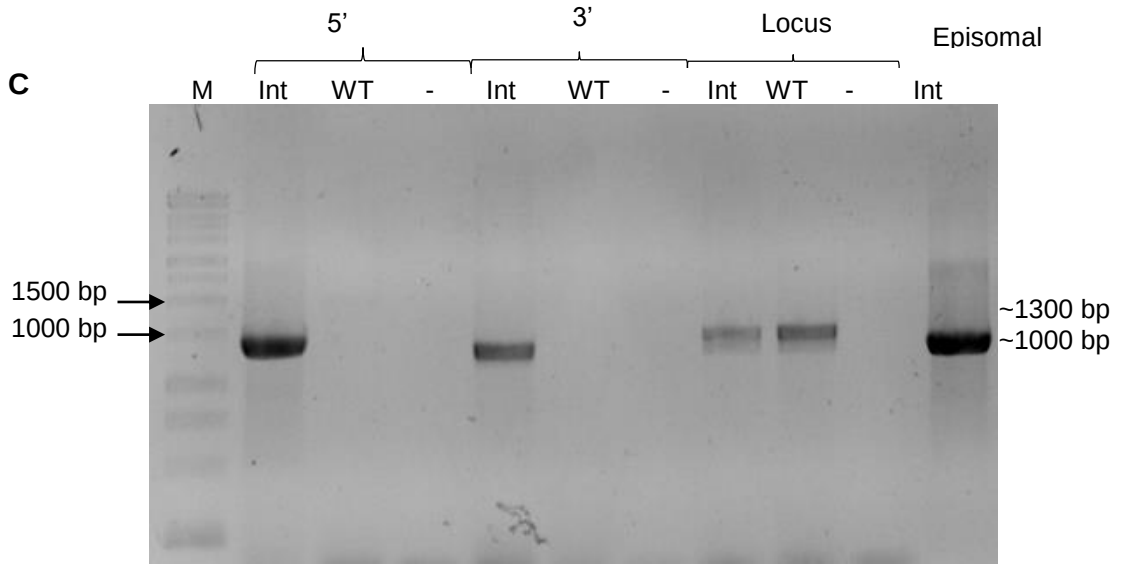

Figure 25: Integration of pSLI_*glmS*_k2 WT and pSLI_*glmS*_k2 M9 plasmids into the genome to create NF54_Δk2_SLI_*glmS* WT and NF54_Δk2_SLI_*glmS.* A) Schematic representation of integration PCR for pSLI_*glmS*_*k2* WT. B) Schematic representation of integration PCR for pSLI_*glmS*_*k2* M9. Primers used for 5' integration are F1 and R1. Primers used for 3' integration are F4 and R3. Primers used for locus are F1 and R3. **C) Schematic representation of integration PCR for pSLI_*glmS*_*k2* WT.** Primers used were same as above (M9). Episomal presence was confirmed using plasmid backbone primers The DNA was separated with 1 % (w/v) agarose/TAE gel and visualised with EtBr (1.2 mg/mL) under UV light.

3.3.4 Comparison of the pGFP_*glmS*_and pSLI_*glms* plasmid systems for genetic modification of K^+ channels

After transfection, drug pressure was administered in cycles and parasites were allowed to recover. Parasites were cultured without drug pressure and were tested once parasites re-emerged and were healthy. Figure 26 shows drug cycling and recovery of integrated parasite lines.

NF54_Δ*k1*_GFP_*glmS,* NF54_Δ*k1*_SLI_*glmS* WT and NF54_Δ*k1*_SLI_*glmS* M9 did not re-emerge after the second drug treatment, whereas NF54_Δ*k2*_GFP_*glmS,* NF54_Δ*k2*_SLI_*glmS* WT and NF54_Δ*k2*_SLI_*glmS* M9 showed integration after the second drug treatment. NF54_Δ*k2*_GFP_*glmS* was the fastest line to recover after drug treatment, and showed integration 31 days faster than NF54_Δ*k2*_SLI_*glmS* WT and 34 days faster than NF54_Δ*k2*_SLI_*glmS* M9. Thus, the original pGFP_*glmS* plasmid integrated faster than the modified pSLI_*glmS* plasmid.

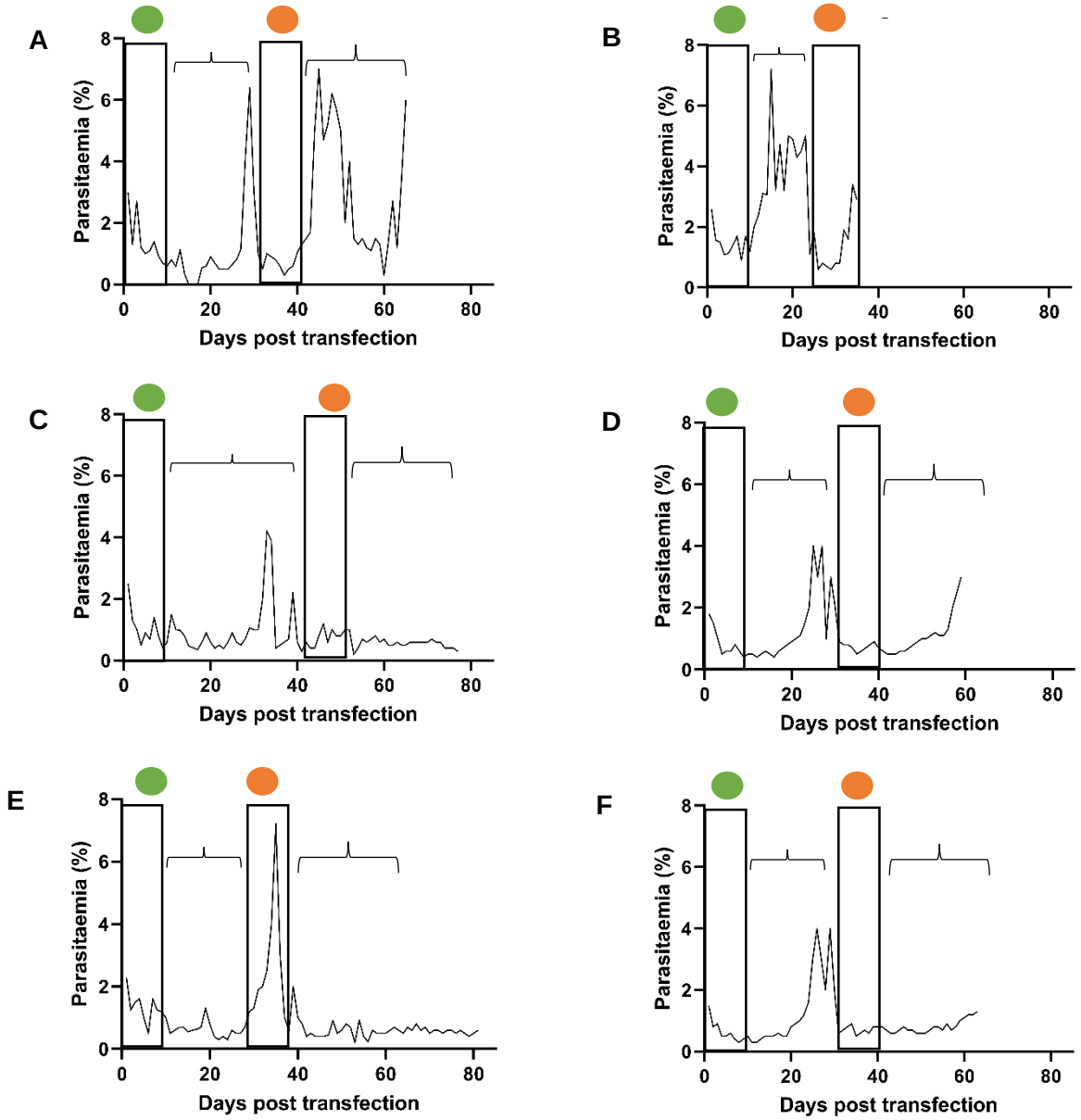

Figure 26: Recovery and selection of *P. falciparum* parasites after transfection. A: NF54_Δ*k1*_GFP_*glmS* was subject to a 14-day drug cycle with blasticidin, and recovered after 14 days. It was then subjected to another 14-day drug cycle and recovered after 14 days and tested for integration into the genome **B: NF54_*Δk2*_GFP_*glmS*** was subject to a 14-day drug cycle with blasticidin, and recovered directly after. It was then subjected to another 14-day drug cycle and recovered directly after and tested for integration into the genome **C: NF54_Δ*k1*_SLI_*glmS* WT** was subject to a 10-day drug cycle with WR99210, and recovered after 22 days and tested for episomal uptake of the plasmid. It was then subjected to another 14-day drug cycle and never recovered. **D: NF54_Δ*k2*_SLI_*glmS* WT** was subject to a 10-day drug cycle with WR99210, and recovered after 14 days and tested for episomal uptake of the plasmid. It was then subjected to another 14-day drug cycle and recovered after 16 days **E: NF54_Δ*k1*_SLI_*glmS* M9** was subject to a 10-day drug cycle with WR99210, and recovered after 22 days and tested for episomal uptake of the plasmid. It was then subjected to another 14-day drug cycle and never recovered. **F: NF54_Δ*k2*_SLI_*glmS* M9** was subject to a 10-day drug cycle with WR99210, and recovered after 15 days and tested for episomal uptake of the plasmid. It was then subjected to another 14-day drug cycle and recovered after 21 days Recovery refers to parasites that are healthy and can be seen under the 100x magnification. Green dot: first drug-cycle. Orange dot: Second drug cycle. Bracket: Recovery

Both systems failed to generate *P. falciparum* parasite lines with *k1* modified for localization and knockdown studies. By contrast, both systems were successful in modifying *k2*, although a mixed parasite population containing wild-type parasites were obtained in each case. Somewhat surprisingly, the original pGFP*_glmS* system generated recombinant parasites faster than the pSLI*_glmS* system that was designed to increase genetic modification efficacy [117].

4 Chapter 4: Discussion

Malaria is an infectious disease and the most significant parasitic infection worldwide. This disease is hard to combat, largely because of the complex life cycle that occurs both in the human host and the *Anopheles* mosquito vector. The *Plasmodium* parasite is able to take on at least 17 different life cycle stages as it changes between blood stage asexual proliferation and sexual differentiation. Asexual parasite proliferation is associated with a dramatic increase in parasite numbers in infected humans, causing characteristic symptoms such as cyclical fever. Sexual differentiation (or gametocytogenesis) only occurs in a small portion (<10 %) of the parasite population and ensures continued transmission of the parasite from the human host to the mosquito vector. The implementation of global malaria elimination programmes has resulted in a substantial decrease in malaria incidence and mortality rates since 1995, with chemotherapeutic interventions a key contributor to this success [153]. However, given the increasing spread of parasite resistance toward conventional malaria chemotherapies, the identification of novel drug targets and development of new antimalarial medications are crucial.

P. falciparum parasites are exposed to multiple changes in their environment, and must be adaptable to respond to variable ionic conditions. In order to adapt to these ever-changing conditions, membrane transporters are used. Membrane transport proteins have been shown to be valuable drug targets. A hexose transporter in *P. falciparum* has been validated as a novel drug target [154]. CIPARGAMIN, a drug that has shown activity against PfATP4 (a Na^+ transporter), is a spiroindolone that has progressed through Phase I and Phase IIa clinical trials with positive results suggesting that transporters have the potential to be used as drug targets [73]. Salinomycin is an ionophore that has also shown to disrupt the potassium ion gradient, resulting in parasite death [80]. In *Toxoplasma gondii*, an L-lactate transporter has been identified as a drug target, and compounds blocking the FNTs in this parasite inhibits its growth [155].This suggests that membrane transporters an ion homeostasis make good drug targets, and leads to the question of whether K^+ channels are essential for gametocytogenesis, and thus present druggable targets.

An interesting observation in this study is the stage-specific expression of the K^+ channels. Ion regulation has been studied extensively in asexual stages, but information on ion regulation during the gametocyte stages is limited [156]. The analysis of expression data, indicated that K1 is expressed throughout the asexual blood stages but not throughout the gametocyte

stages, whereas K2 is expressed during both the asexual and gametocyte stages, and may be considered as a novel drug target [28]. At any given point, a K^+ channel is expressed during the asexual stage, which aids in maintaining the high K^+ concentration. This suggests that K^+ transport begins in the ring stage to maintain the ion concentration. Expression of both K^+ channels indicate that both K^+ channels are required during the various life cycle stages and their localisation might give some insight as to why two K^+ channels are expressed.

Knowing where a transporter is located within a cell is important in understanding its physiological role. Until recently, only a small subset of *Plasmodium* transporters had been described as localised to specific membranes (Reviewed in Kirk & Lehane (2014), and Martin (2019) [156, 157]). With new transfection methods that allow expression of proteins with a fluorescent tag, this number has increased substantially [96]. Most of these studies have focussed on the asexual blood stages, and little is still known about other life stages [156]. In order to perform localisation studies, the K^+ channel was tagged with a fluorescent GFP tag. Previous studies showed that K1 is located on the host erythrocyte surface in *P. falciparum* [91] to facilitate the maturation and intracellular survival of the parasite by regulating K^+ influx across the infected erythrocyte membrane. This maintains the electrochemical gradient and membrane potential across the infected erythrocyte plasma membrane. In contrast, knockout of K1 in *P. berghei* resulted in a reduction of K^+ channel activity in the parasite plasma membrane [71]. These data for *P. berghei* suggests that the K1 channel is rather localised to the parasite plasma membrane, while a study in *Saccromyces cerevisiae* also found that a K1 fragment tagged with GFP mainly localised to the plasma membrane [158]. In contrast to K1, K2 is directly associated with the parasite membrane [91], and in *S. cerevisiae*, a K2 N-terminal fragment tagged with GFP showed that K2 associated with internal structures [158].

Gene manipulation in *Plasmodium* is no easy task, partially attributable to the lack of tools to successfully determine essential gene functions, inefficiency of these tools and lack of robust selectable markers used to select for positive parasites [94]. The inability to knockout genes has often been associated with essentiality of the gene in parasite survival; however, this could also result from poor integration efficiency of the knockout plasmids and/or growth of the mutant parasite, as these restrictions would reduce the potential for generating and cloning the mutant parasite [156]. However, improved gene disruption approaches (such as CRISPR-cas9, DiCre, destabilisation domains and *glmS* ribozyme) have paved the road for several knockout and knockdown studies. K2 for example has been shown to be dispensable in three studies, but essential in one [91, 93, 115, 159]. The misidentification of genes as dispensable is a result of three events: 1) off-target integration of the plasmid 2) replication and retention of the plasmid as an episome and 3) a pre-existing duplication of a region encompassing the

target gene and the mutant parasite possessing both disrupted and intact versions of the gene [160].

The *glmS* system used in this study has proven effective in *P. falciparum* parasites [111]. Two different systems are available; the original *glmS* and the selection-linked integration (SLI) *glmS* system. The SLI system claims to ensure successful and rapid genomic integration by using a two drug approach to select for parasites that have episomal uptake of the recombinant plasmid by using hDHFR, and final integration into the genome by using a promotor-less Neo-R marker [117]. Both the original *glmS* system and SLI *glmS* system has been used to determine gene essentiality [111, 116]. However, the modified SLI *glmS* system has only been published recently in 2020 [116], whereas the original *glmS* system has been used in more studies [111, 161, 162]. The modified SLI *glmS* system is based on a SLI knockout system that has been established in determining essentiality in eight other genes and is a rapid method to disrupt nonessential genes to determine whether the gene is important for parasite development [117]. The SLI system also contains a skip peptide which "forces" integration, whereas the original *glmS* system only integrates by chance. Therefore, theoretically the SLI *glmS* system has more advantages. In previous studies integration (mixed population) of the original *glmS* system occurred 49 - 56 days after transfection [111, 161], whereas in this study integration (mixed population) occurred 28 days after transfection. There is currently no data on integration time on the modified SLI *glmS* system published in 2020, however, integration (pure integrated population) of selected genes occurred 5 - 23 days after transfection in the original SLI knockout system [117]. Somewhat unsuspectedly, in this study, integration with the modified SLI *glmS* system took 54 – 66 days, much longer than indicated by the original SLI system paper [116, 117]. In this case, integration of the original *glmS* system occurred more rapidly than the modified SLI *glmS* system. Although the reason for this is unclear, it may be an indicator that hDHFR is a better selectable marker for faster integration.

Transfection into *P. falciparum* is used for gene knockout, transgene expression, and allelic replacement. Plasmids are transfected in the form of undigested circular DNA and will initially replicate episomally. These will eventually integrate into the genome by single–crossover homologous recombination [163]. In this study, transfection was successful for K2, but not for K1, contradictory to other studies [91]. pGFP*_glmS_k1* showed that the gene fragment in the recombinant plasmid was twice as large as the fragment originally transfected. This may have arisen from the gene fragment forming concatamers during episomal replication, preventing integration using single homologous crossover [151, 152, 163]. The other pSLI*_glmS_k1* parasites did not emerge after a second drug cycle which could be as a result from harsh drug treatments and slow integration.

The main aim of this study was to generate genetically modified *P. falciparum* NF54 parasite lines using a riboswitch and GFP tag to investigate the gene essentiality and localisation of K1 and K2. This was achieved with lines NF54_Δ*k2*_GFP_*glmS,* NF54_Δ*k2*_SLI_*glmS* WT and NF54_Δ*k2*_GFP_*glmS* M9. These lines can be used in subsequent studies to determine gene essentiality and localisation of K^+ channels. Furthermore, the lines may serve as a tool to assess the functional importance of K^+ channels by investigating changes in K^+ uptake or phenotypical changes in the parasite following successful knockdown. Together, these results indicate that the aim of the study was achieved.

5 Chapter 5: Conclusion

The *P. falciparum* parasite is the main cause of malaria and is responsible for 409 000 deaths globally, mostly affecting children under the age of five [1]. Malaria is a treatable disease, but there have been reports on rising resistance towards current antimalarial drugs, which threatens the effective treatment of malaria. Therefore, there is an urgent need for new drug targets for both the disease causing asexual stage, as well as the transmissible sexual stage.

Parasitic protozoa, such as *P. falciparum* parasites, are complex and evolved features for survival in host environments. Ion maintenance is strictly controlled to ensure viability, and there is a need of in depth characterisation of the transporters.

In this study, K^+ channels have been characterised *in silico*, C-terminal fragments cloned into various plasmids and genetically modified in *P. falciparum* parasites. Both K^+ channels were subject to genetic modification by inserting a GFP tag and a *glmS* ribozyme on the C-terminus. This was done with transfection of recombinant plasmids into *P. falciparum* parasites, and adding drug pressure to ensure the plasmid is taken up episomally, and eventually integrated into the genome. Parasites transfected with plasmids containing gene fragments of *k1* plasmids never fully recovered, whereas plasmids containing gene fragments of *k2* integrated into the genome resulting in a mixed population with wild type parasites present. By cloning out these lines to obtain a single clonal line, these lines can be used for future to determine essentiality and localisation.

Future work in this study will include isolating integrated parasites to obtain a pure culture, after which subsequent experiments will be done. Subsequent experiments include confocal microscopy to determine localisation of K2. After localisation has been determined, *k2* will be knocked down by adding Glc6P to the culture. Parasite viability, morphology and ability to form gametocytes will be investigated. The viability and morphology of gametocytes after the knock down will help investigate functional importance of this channel. In addition, the K^+ concentration will be measured before and after knock down to investigate the function of *k2* in *P. falciparum*.

6 References

1 World Health Organization. (2020) World malaria report 2020. World Health Organization, Geneva, Switzerland

2 Phillips, M. A.*, et al.* (2017) Malaria. Nature Reviews Disease Primers. **3**, 17050

3 Bertschi, N. L.*, et al.* (2018) Transcriptomic analysis reveals reduced transcriptional activity in the malaria parasite *Plasmodium cynomolgi* during progression into dormancy. Elife. **7**

4 Bourgard, C.*, et al.* (2018) *Plasmodium vivax* biology: Insights provided by genomics, transcriptomics and proteomics. Frontiers in Cellular and Infection Microbiology. **8**, 34

5 Richter, J.*, et al.* (2010) What is the evidence for the existence of *Plasmodium ovale* hypnozoites? Parasitology Research. **107**, 1285-1290

6 Chavatte, J. M.*, et al.* (2015) Molecular characterization of misidentified *Plasmodium ovale* imported cases in Singapore. Malaria Journal. **14**, 454

7 Collins, W. E. and Jeffery, G. M. (2007) *Plasmodium malariae:* parasite and disease. Clinical Microbiology Reviews. **20**, 579-592

8 World Health Organization. (2015) Global technical strategy for malaria 2016 to 2030. ed.)^eds.), World Health Organization, Generva, Switzerland

9 Sherman, I. W. (1979) Biochemistry of *Plasmodium* (Malarial Parasites). Microbiological Reviews. **43**, 453-495

10 Soulard, V.*, et al.* (2015) *Plasmodium falciparum* full life cycle and *Plasmodium ovale* liver stages in humanized mice. Nature Communications. **6**, 7690

11 White, N. J.*, et al.* (2014) Malaria. The Lancet. **383**, 723-735

12 Coronado, L. M.*, et al.* (2014) Malarial hemozoin: from target to tool. Biochimica et Biophysica Acta. **1840**, 2032-2041

13 Baker, D. A. (2010) Malaria gametocytogenesis. Molecular & Biochemical Parasitology. **172**, 57-65

14 Lui, Z.*, et al.* (2011) Gametocytogenesis in malaria parasite: commitment, development and regulation. Future Microbiology. **6**, 1351-1369

15 Dixon, M. W. A.*, et al.* (2012) Shape-shifting gametocytes: how and why does *P. falciparum* go banana-shaped? Trends in Parasitology. **28**, 471-478

16 Meibalan, E. and Marti, M. (2017) Biology of malaria transmission. Cold Spring Harbor Perspectives in Medicine. **7**

17 Farid, R.*, et al.* (2017) Initiation of gametocytogenesis at very low parasite density in *Plasmodium falciparum* infection. The Journal of Infectious Diseases. **215**, 1167-1174

18 Sinden, R. E.*, et al.* (2010) The flagellum in malarial parasites. Current Opinion in Microbiology. **13**, 491-500

19 Wagman, J.*, et al.* (2020) Combining next-generation indoor residual spraying and drug-based malaria control strategies: observational evidence of a combined effect in Mali. Malaria Journal. **19**, 293

20 Nasir, S. M. I.*, et al.* (2020) Prevention of re-establishment of malaria: historical perspective and future prospects. Malaria Journal. **19**, 452

21 Kelly-Hope, L.*, et al.* (2008) Lessons from the past: managing insecticide resistance in malaria control and eradication programmes. Lancet Infectious Disease

22 Lobo, N. F.*, et al.* (2018) Modern vector control. Cold Spring Harbor Perspectives in Medicine. **8**

23 Spitzen, J.*, et al.* (2017) Effect of insecticide-treated bed nets on house-entry by malaria mosquitoes: The flight response recorded in a semi-field study in Kenya. Acta Tropica. **172**, 180-185

24 Ranson, H. (2017) Current and future prospects for preventing malaria transmission via the use of insecticides. Cold Spring Harbor Perspectives in Medicine. **7**

25 Burke, A.*, et al.* (2019) *Anopheles parensis* contributes to residual malaria transmission in South Africa. Malaria Journal. **18**, 257

26 Medjigbodo, A. A.*, et al.* (2020) Phenotypic insecticide resistance in *Anopheles gambiae* (Diptera: Culicidae): specific characterization of underlying resistance mechanisms still matters. Journal of Medical Entomology
27 Tangena, J. A.*, et al.* (2020) Indoor residual spraying for malaria control in sub-Saharan Africa 1997 to 2017: an adjusted retrospective analysis. Malaria Journal. **19**, 150
28 Burrows, J. N.*, et al.* (2017) New developments in anti-malarial target candidate and product profiles. Malaria Journal. **16**, 26
29 Draper, S. J.*, et al.* (2018) Malaria vaccines: recent advances and new horizons. Cell Host Microbe. **24**, 43-56
30 Crompton, P. D.*, et al.* (2010) Advances and challenges in malaria vaccine development. The Journal of Clinical Investigation. **120**, 4168-4178
31 Laurens, M. B. (2020) RTS,S/AS01 vaccine (Mosquirix): an overview. Human Vaccines Immunotherapeutics. **16**, 480-489
32 Rts, S. C. T. P.*, et al.* (2012) A phase 3 trial of RTS,S/AS01 malaria vaccine in African infants. The New England Journal of Medicine. **367**, 2284-2295
33 Sissoko, M. S.*, et al.* (2017) Safety and efficacy of PfSPZ vaccine against *Plasmodium falciparum* via direct venous inoculation in healthy malaria-exposed adults in Mali: a randomised, double-blind phase 1 trial. The Lancet Infectious Diseases. **17**, 498-509
34 Ewer, K. J.*, et al.* (2015) Progress with viral vectored malaria vaccines: A multi-stage approach involving "unnatural immunity". Vaccine. **33**, 7444-7451
35 Douglas, A. D.*, et al.* (2011) The blood-stage malaria antigen PfRH5 is susceptible to vaccine-inducible cross-strain neutralizing antibody. Nature Communications. **2**, 601
36 Datoo, M. S.*, et al.* (2021) Efficacy of a low-dose candidate malaria vaccine, R21 in adjuvant Matrix-M, with seasonal administration to children in Burkina Faso: a randomised controlled trial. The Lancet. **397**, 1809-1818
37 Kapulu, M. C.*, et al.* (2015) Comparative assessment of transmission-blocking vaccine candidates against *Plasmodium falciparum*. Scientific Reports. **5**, 11193
38 Wong, W.*, et al.* (2017) Mefloquine targets the *Plasmodium falciparum* 80S ribosome to inhibit protein synthesis. Nature Microbiology. **2**, 17031
39 NDoH. (2017) South African Guidelines for the prevention of malaria. ed.)^eds.)
40 Raval, J. P.*, et al.* (2018) Development of injectable in situ gelling systems of doxycycline hyclate for controlled drug delivery system. In Applications of Nanocomposite Materials in Drug Delivery (Inamuddin, Asiri, A. M. and Mohammad, A., eds.). pp. 149-162, Woodhead Publishing
41 Gaillard, T.*, et al.* (2017) The end of a dogma: the safety of doxycycline use in young children for malaria treatment. Malaria Journal. **16**, 148
42 Savelkoel, J.*, et al.* (2018) Abbreviated atovaquone-proguanil prophylaxis regimens in travellers after leaving malaria-endemic areas: A systematic review. Travel Medicine and Infectious Disease. **21**, 3-20
43 Rout, S. and Mahapatra, R. K. (2019) *Plasmodium falciparum*: Multidrug resistance. Chemical Biology & Drug Design. **93**, 737-759
44 Moore, L. R.*, et al.* (2006) Hemoglobin degradation in malaria-infected erythrocytes determined from live cell magnetophoresis. FASEB Journal. **20**, 747-749
45 Meshnick, S. R. (1998) Artemisinin antimalarials: mechanisms of action and resistance. Med Trop (Mars). **58:13-7**
46 Klayman, D. L. (1985) Qinghaosu (artemisinin): an antimalarial drug from China. Science. **228**, 1049
47 Olliaro, P. L. and Taylor, W. R. (2003) Antimalarial compounds: from bench to bedside. Journal of Experimental Biology. **206**, 3753-3759
48 Krogstad, D. J.*, et al.* Efflux of chloroquine from *Plasmodium falciparum*: mechanism of chloroquine resistance. Science. **238**, 1283-1285
49 Lu, F., Culleton, R., Zhang, M., Ramaprasad, A., von Seidlein, L., Zhou, H., Zhu, G., Tang, J., Liu, Y. and Wang, W. (2017) Emergence of indigenous artemisinin-resistant *Plasmodium falciparum* in Africa. New England Journal of Medicine. **376**, 991-993

50 Tilley, L.*, et al.* (2016) Artemisinin action and resistance in *Plasmodium falciparum*. Trends in Parasitology. **32**, 682-696
51 Gatton, M. L.*, et al.* (2004) Evolution of resistance to sulfadoxine-pyrimethamine in *Plasmodium falciparum*. Antimicrobial Agents and Chemotherapy. **48**, 2116-2123
52 World Health Organization. (2019) Intermittent preventive treatment in pregnancy (IPTp). ed.)^eds.), World Health Organization
53 Fried, M. and Duffy, P. E. (2017) Malaria during pregnancy. Cold Spring Harbor Perspectives in Medicine. **7**
54 White, N. J. (2013) Pharmacokinetic and pharmacodynamic considerations in antimalarial dose optimization. Antimicrobial Agents and Chemotherapy. **57**, 5792-5807
55 Price, R. N.*, et al.* (2004) Mefloquine resistance in *Plasmodium falciparum* and increased *pfmdr1* gene copy number. The Lancet. **364**, 438-447
56 Raman, J.*, et al.* (2019) Safety and tolerability of single low-dose primaquine in a low-intensity transmission area in South Africa: an open-label, randomized controlled trial. Malaria Journal. **18**, 209
57 Ippolito, M. M.*, et al.* (2017) The relative effects of artemether-lumefantrine and non-artemisinin antimalarials on gametocyte carriage and transmission of *Plasmodium falciparum*: A systematic review and meta-analysis. Clinical Infectious Diseases. **65**, 486-494
58 Targett G, D. C., Jawara M, von Seidlein L, Coleman R, Deen J, Pinder M, Doherty T, Sutherland C, Walraven G. (2001) Artesunate reduces but does not prevent posttreatment transmission of *Plasmodium falciparum* to *Anopheles gambiae*. The Journal of Infectious Diseases. **183**, 1254-1259
59 Price RN, N. F., Luxemburger C, Ter Kuile FO, Paiphun L, Chongsuphajaisiddhi T, White NJ. (1996) Effects of artemisinin derivatives on malaria transmissibility. The Lancet. **347**, 1654-1658
60 Adjalley, S. H.*, et al.* (2011) Quantitative assessment of *Plasmodium falciparum* sexual development reveals potent transmission-blocking activity by methylene blue. Proceedings of the National Academy of Sciences of the United States of America. **108**, E1214-1223
61 Avula, B.*, et al.* (2013) Profiling primaquine metabolites in primary human hepatocytes using UHPLC-QTOF-MS with 13C stable isotope labeling. Journal of Mass Spectrometry. **48**, 276-285
62 Kirk, K. (2015) Ion regulation in the malaria parasite. Annual Review of Microbiology. **69**, 341-359
63 Mauritz, J. M.*, et al.* (2011) X-ray microanalysis investigation of the changes in Na^+, K^+, and hemoglobin concentration in *Plasmodium falciparum*-infected red blood cells. Biophysical Journal. **100**, 1438-1445
64 Hayashi, M.*, et al.* (2000) Vacuolar H^+-ATPase localized in plasma membranes of malaria parasite cells, *Plasmodium falciparum*, is involved in regional acidification of parasitized erythrocytes. The Journal of Biological Chemistry. **275**, 34353-34358
65 Allen, R. J. and Kirk, K. (2004) The membrane potential of the intraerythrocytic malaria parasite *Plasmodium falciparum*. The Journal of Biological Chemistry. **279**, 11264-11272
66 Staines, H., Ellory, J.C., Kirk, K. (2000) Perturbation of the pump-leak balance for Na^+ and K^+ in malaria-infected erythrocytes. American Journal of Physiology. Cell Physiology. **280**
67 Spillman, N. J.*, et al.* (2013) Na^+ extrusion imposes an acid load on the intraerythrocytic malaria parasite. Molecular and Biochemical Parasitology. **189**, 1-4
68 Spillman, N. J.*, et al.* (2013) Na^+ regulation in the malaria parasite *Plasmodium falciparum* involves the cation ATPase PfATP4 and is a target of the spiroindolone antimalarials. Cell Host & Microbe. **13**, 227-237
69 Reader, J.*, et al.* (2021) Multistage and transmission-blocking targeted antimalarials discovered from the open-source MMV Pandemic Response Box. Nature Communications. **12**
70 Lee, P.*, et al.* (1988) X-Ray microanalysis of *Plasmodium falciparum* and infected red blood cells: effects of qinghaosu and chloroquine on potassium, sodium, and phosphorus composition. The American Journal of Tropical Medicine and Hygiene. **39**, 157-165

71 Ellekvist, P., Maciel, J., Mlambo, G., Ricke, C.H., Colding, H., Klaerke, D.A., Kumar, N. (2008) Critical role of a K^+ channel in *Plasmodium berghei* transmission revealed by targeted gene disruption. Proceedings of the National Academy of Science of the United States of America. **105**, 6398-6402
72 Gamo, F.-J.*, et al.* (2010) Thousands of chemical starting points for antimalarial lead identification. Nature. **465**, 305-310
73 Spillman, N. J. and Kirk, K. (2015) The malaria parasite cation ATPase PfATP4 and its role in the mechanism of action of a new arsenal of antimalarial drugs. International Journal for Parasitology – Drugs and Drug Resistance. **5**, 149-162
74 Flannery, E. L.*, et al.* (2015) Mutations in the P-type cation-transporter ATPase 4, PfATP4, mediate resistance to both aminopyrazole and spiroindolone antimalarials. ACS Chemical Biology. **10**, 413-420
75 Rottmann, M.*, et al.* (2010) Spiroindolones, a potent compound class for the treatment of malaria. Science. **329**, 1175-1180
76 Vaidya, A. B.*, et al.* (2014) Pyrazoleamide compounds are potent antimalarials that target Na^+ homeostasis in intraerythrocytic *Plasmodium falciparum*. Nature Communications. **5**, 5521
77 Jimenez-Diaz, M. B.*, et al.* (2014) (+)-SJ733, a clinical candidate for malaria that acts through ATP4 to induce rapid host-mediated clearance of *Plasmodium*. Proceedings of the National Academy of Sciences of the United States of America. **111**, E5455-5462
78 Zhang, R.*, et al.* (2016) A basis for rapid clearance of circulating ring-stage malaria parasites by the spiroindolone KAE609. Journal of Infectious Diseases. **213**, 100-104
79 White, N. J.*, et al.* (2014) Spiroindolone KAE609 for *falciparum* and *vivax* malaria. New England Journal of Medicine. **371**, 403-410
80 D'Alessandro, S.*, et al.* (2015) Salinomycin and other ionophores as a new class of antimalarial drugs with transmission-blocking activity. Antimicrobial Agents and Chemotherapy. **59**, 5135-5144
81 Waller, K. L.*, et al.* (2008) *Plasmodium falciparum*: growth response to potassium channel blocking compounds. Experimental Parasitology. **120**, 280-285
82 Miller, C. (2000) An overview of the potassium channel family. Genome Biology. **1**
83 Prole, D. L. and Marrion, N. V. (2012) Identification of putative potassium channel homologues in pathogenic protozoa. PLoS One. **7**, e32264
84 Heginbotham, L., Lu, Z, Abramson T, MacKinnon, R. (1994) Mutations in the K^+ channel signature sequence. Biophysical Journal. **66**, 1061-1067
85 Heil, B.*, et al.* (2006) Computational recognition of potassium channel sequences. Bioinformatics. **22**, 1562-1568
86 Herrington, J. and Arey, B. J. (2014) Chapter 6 - Conformational Mechanisms of Signaling Bias of Ion Channels. In Biased Signaling in Physiology, Pharmacology and Therapeutics (Arey, B. J., ed.). pp. 173-207, Academic Press, San Diego
87 Vergara, C., Latorre R., Marrion, N.V., Adelmant J.P. (1998) Calcium activated potassium channels. Current Opinion in Neurobiology. **8**
88 Wulff, H.*, et al.* (2009) Voltage-gated potassium channels as therapeutic targets. Nature Reviews Drug Discovery. **8**, 982-1001
89 Ashcroft, F. M. (2000) Ion Channels and Diseases. Academic Press, New York
90 Martin, R. E., Henry, R.I, Abbey, J.L, Clements, J.D, Kirk, K. (2005) The permeome of the malaria parasite. Genome Biology. **6**
91 Waller, K. L.*, et al.* (2008) Characterization of two putative potassium channels in *Plasmodium falciparum*. Malaria Journal. **7**, 19
92 Martin, R. E.*, et al.* (2009) Membrane transport proteins of the malaria parasite. Molecular Microbiology. **74**, 519-528
93 Zhang, M.*, et al.* (2018) Uncovering the essential genes of the human malaria parasite *Plasmodium falciparum* by saturation mutagenesis. Science. **360**
94 de Koning-Ward, T. F.*, et al.* (2015) Advances in molecular genetic systems in malaria. Nature Reviews Microbiology. **13**, 373-387

95 Pino, P. (2013) From technology to biology: a malaria genetic toolbox for the functional dissection of essential genes. Molecular Microbiol. **88**, 650-654
96 Shaw, P. J. A., A. (2017) Tools for attenuation of gene expression in malaria parasites. International Journal for Parasitology. **47**, 385-398
97 Collins, C. R.*, et al.* (2013) Robust inducible Cre recombinase activity in the human malaria parasite *Plasmodium falciparum* enables efficient gene deletion within a single asexual erythrocytic growth cycle. Molecular Microbiology. **88**, 687-701
98 Chen, P. B.*, et al. Plasmodium falciparum* PfSET7: enzymatic characterization and cellular localization of a novel protein methyltransferase in sporozoite, liver and erythrocytic stage parasites. Scientific Reports
99 de Azevedo, M. F.*, et al.* (2012) Systematic analysis of FKBP inducible degradation domain tagging strategies for the human malaria parasite *Plasmodium falciparum*. PLoS One. **7**, e40981
100 Jullien, N. (2003) Regulation of Cre recombinase by ligand-induced complementation of inactive fragments. Nucleic Acids Research. **31**, 131e-131
101 Lacroix, C.*, et al.* (2011) FLP/*FRT*-mediated conditional mutagenesis in pre-erythrocytic stages of *Plasmodium berghei*. Nature Protocol. **6**, 1412-1428
102 Kuang, D.*, et al.* (2017) Tagging to endogenous genes of *Plasmodium falciparum* using CRISPR/Cas9. Parasites and Vectors. **10**, 595
103 Straimer, J.*, et al.* (2012) Site-specific genome editing in *Plasmodium falciparum* using engineered zinc-finger nucleases. Nature Methods. **9**, 993-998
104 Meissner, M., Krejay, E., Gilson, P.R., de Koning-Ward, T.F., Soldati, D., Crabb, B.S. (2005) Tetracycline analogue-regulated transgene expression in *Plasmodium falciparum* blood stages using *Toxoplasma gondii* transactivators. Proceedings of the National Academy of Sciences of the United States of America. **102**, 2980-2985
105 Pino, P.*, et al.* (2012) A tetracycline-repressible transactivator system to study essential genes in malaria parasites. Cell Host Microbe. **12**, 824-834
106 Cui, L.*, et al.* (2015) Translational regulation during stage transitions in malaria parasites. Annals of the New York Academy of Sciences. **1342**, 1-9
107 Rajaram, K.*, et al.* (2020) Redesigned TetR-aptamer system to control gene expression in *Plasmodium falciparum*. mSphere. **5**
108 Winkler, W.*, et al.* (2004) Control of gene expression by a natural metabolite-repsonsive enzyme. Nature. **428**, 286-286
109 Breaker, R. R. (2011) Prospects for riboswitch discovery and analysis. Molecular Cell. **43**, 867-879
110 Ferre-D'Amare, A. R. (2010) The *glmS* ribozyme: use of a small molecule coenzyme by a gene-regulatory RNA. Quarterly Reviews of Biophysics. **43**, 423-447
111 Prommana, P.*, et al.* (2013) Inducible knockdown of *Plasmodium* gene expression using the *glmS* ribozyme. PLoS One. **8**, e73783
112 Kreidenweiss, A.*, et al.* (2013) 2A and the auxin-based degron system facilitate control of protein levels in *Plasmodium falciparum*. PLoS One. **8**, e78661
113 Nishimura, K.*, et al.* An auxin-based degron system for the rapid depletion of proteins in nonplant cells. Nature Methods
114 Philip, N. and Waters, A. P. (2015) Conditional degradation of *Plasmodium* calcineurin reveals functions in parasite colonization of both host and vector. Cell Host Microbe. **18**, 122-131
115 Ellekvist, P.*, et al.* (2004) Molecular cloning of a K^+ channel from the malaria parasite *Plasmodium falciparum*. Biochemical and Biophysical Research Communications. **318**, 477-484
116 Burda, P. C.*, et al.* (2020) Structure-based identification and functional characterization of a lipocalin in the malaria parasite *Plasmodium falciparum*. Cell Reports. **31**, 107817
117 Birnbaum, J.*, et al.* (2017) A genetic system to study *Plasmodium falciparum* protein function. Nature Methods. **14**, 450-456

118 Sonnhammer, E. L.*, et al.* (1998) A hidden Markov model for predicting transmembrane helices in protein sequences. Proceedings of the International Conference on Intelligent Systems for Molecular Biology. **6**, 175-182
119 Käll, L.*, et al.* (2004) A combined transmembrane topology and signal peptide prediction method. Journal of Molecular Biology. **14:338(5)**
120 Ikeda, M.*, et al.* (2003) TMPDB: a database of experimentally-characterized transmembrane topologies. Nucleic Acids Research. **31**, 406-409
121 Käll, L., Krogh, A, Sonnhammer, E.L.L. (2004) A combined transmembrane topology and signal peptide prediction method. Journal of Molecular Biology. **338**, 1027-1036
122 Hofmann, K., Stoffel, W. (1993) TMBASE - A database of membrane spanning protein segments. Biological Chemistry. **374**
123 Kyte J Fau - Doolittle, R. F. and Doolittle, R. F. A simple method for displaying the hydropathic character of a protein. Journal of Molecular Biology. **157(1)**, 105–132.
124 Gasteiger E., H. C., Gattiker A., Duvaud S., Wilkins M.R., Appel R.D., Bairoch A. (2005) Protein identification and analysis tools on the ExPASy server. In The Proteomics Protocols Handbook (Walker, J. M., ed.), Humana Press
125 Cibrowski, P. S., J. (2016) Proteomic profiling and analytical chemistry. Elsevier
126 Lu, S.*, et al.* CDD/SPARCLE: the conserved domain database in 2020. Nucleic Acids Research
127 Marchler-Bauer, A.*, et al.* (2017) CDD/SPARCLE: functional classification of proteins via subfamily domain architectures. Nucleic Acids Research. **45**, D200-D203
128 Marchler-Bauer, A.*, et al.* (2015) CDD: NCBI's conserved domain database. Nucleic Acids Research. **43**, D222-D226
129 Marchler-Bauer, A.*, et al.* (2011) CDD: a Conserved Domain Database for the functional annotation of proteins. Nucleic Acids Research. **39**, D225-D229
130 Waterhouse, A.*, et al.* (2018) SWISS-MODEL: homology modelling of protein structures and complexes. Nucleic Acids Research. **46**, W296-W303
131 Bienert, S.*, et al.* (2016) The SWISS-MODEL Repository—new features and functionality. Nucleic Acids Research. **45**, D313-D319
132 Studer, G.*, et al.* (2019) QMEANDisCo—distance constraints applied on model quality estimation. Bioinformatics. **36**, 1765-1771
133 Bertoni, M.*, et al.* (2017) Modeling protein quaternary structure of homo- and hetero-oligomers beyond binary interactions by homology. Scientific Reports. **7**, 10480
134 Ramachandran, G. N. and Sasisekharan, V. (1968) Conformation of polypeptides and proteins. In Advances in Protein Chemistry Volume 23. pp. 283-437
135 Painter, H. J.*, et al.* (2017) Capturing in vivo RNA transcriptional dynamics from the malaria parasite *Plasmodium falciparum*. Genome Research. **27**, 1074-1086
136 van Biljon, R.*, et al.* (2019) Hierarchical transcriptional control regulates *Plasmodium falciparum* sexual differentiation. BMC Genomics. **20**, 920
137 Reader, J.*, et al.* (2015) Nowhere to hide: interrogating different metabolic parameters of *Plasmodium falciparum* gametocytes in a transmission blocking drug discovery pipeline towards malaria elimination. Malaria Journal. **14**, 213
138 Trager, W. and Jensen, J. (1976) Human malaria parasites in continuous culture. Science. **193**, 673-675
139 Schuster, F. L. (2002) Cultivation of *Plasmodium* spp. Clinical Microbiology Reviews. **15**, 355-364
140 Lambros, C. and Vanderberg, J. (1979) Synchronization of *Plasmodium falciparum* erythrocytic stages in culture. Journal of Parasitology. **65**, 418-420
141 Green, M. R. and Sambrook, J. (2019) Screening bacterial colonies using X-Gal and IPTG: alpha-Complementation. Cold Spring Harbor Protocols. **2019**
142 Green, M. R. and Sambrook, J. (2016) Preparation of plasmid DNA by alkaline lysis with sodium dodecyl sulfate: minipreps. Cold Spring Harbor Protocols. **2016**
143 Buck, J. M.*, et al.* (2018) Blasticidin-S deaminase, a new selection marker for genetic transformation of the diatom *Phaeodactylum tricornutum*. PeerJ. **6**, e5884

144 Rug M., M. A. G. (2012) Transfection of *Plasmodium falciparum*. In Malaria. (R, M., ed.), Humana Press, Totowa, NJ
145 Martin, R.*, et al.* (2005) The 'permeome' of the malaria parasite: an overview of the membrane transport proteins of *Plasmodium falciparum*. Genome Biology. **6**
146 Kuang, Q.*, et al.* (2015) Structure of potassium channels. Cellular and Molecular Life Science. **72**, 3677-3693
147 Moller, S., Croning, M.D.R., Apweiler, R. (2001) Evaluation of methods for the prediction of membrane spanning regions. Bioinformatics. **17**, 646-653
148 Cuthbertson, J. M.*, et al.* (2005) Transmembrane helix prediction: a comparative evaluation and analysis. Protein Engineering, Design & Selection. **18**, 295-308
149 Machery-Nagel. (2017) Instruction NucleoSpin gel and PCR clean up. ed.)^eds.), Machery-Nagel, Düren · Germany
150 Crabb, B. S., Cooke, B.M., Rheeder, J.C., Waller, R.F., Caruana, S.R., Davern, K.M, Wickman, M. E., Brown, G.V., Coppel, R.L., Cowman, A.F. (1997) Targeted gene disruption shows that knobs enable malaria-infected red cells to cytoadhere under physiological shear stress. Cell. **89**
151 O'Donnel, R. A. O., Freitas-Junior, L.H., Preiser, P.R., Williamson, D.H., Duraisingh, M., McElwain, T.F., Scherf, A, Cowman, A.F., Crabb, B.S. (2002) A genetic screen for improved plasmid segregation reveals a role for Rep20 in the interaction of *Plasmodium falciparum* chromosomes. The EMBO Journal. **21**, 1231-1239
152 van Dijk, M. R., Janse, C.J., Waters, A. P. (1996) Expression of a *Plasmodium* gene introduced into subtelomeric regions of *Plasmodium berghei* chromosome. Science. **271**, 662
153 Alonso, P. L.*, et al.* (2011) A research agenda to underpin malaria eradication. PLoS Medicine. **8**, e1000406
154 Joet, T., Eckstein-Ludwig, U., Morin, C., Krishna., S. (2003) Validation of the hexose transporter of *PIasmodium falciparum* as a novel drug target. PNAS. **100**, 7476-7479
155 Erler, H.*, et al.* (2018) The intracellular parasite *Toxoplasma gondii* harbors three druggable FNT-type formate and l-lactate transporters in the plasma membrane. Journal of Biological Chemistry. **293**, 17622-17630
156 Martin, R. E. (2019) The transportome of the malaria parasite. Biological reviews of the Cambridge Philosophical Society. **95**, 305-332
157 Kirk, K. and Lehane, A. M. (2014) Membrane transport in the malaria parasite and its host erythrocyte. Biochemical Journal. **457**, 1-18
158 Molbaek, K.*, et al.* (2020) Purification and initial characterization of *Plasmodium falciparum* K^+ channels, PfKch1 and PfKch2 produced in *Saccharomyces cerevisiae*. Microbial Cell Factories. **19**, 183
159 Ellekvist, P.*, et al.* (2017) Functional characterization of malaria parasites deficient in the K^+ channel Kch2. Biochemical and Biophysical Research Communications. **493**, 690-696
160 Gomes, A. R.*, et al.* (2015) A genome-scale vector resource enables high-throughput reverse genetic screening in a malaria parasite. Cell Host Microbe. **17**, 404-413
161 Aroonsri, A.*, et al.* (2019) Validation of *Plasmodium falciparum* deoxyhypusine synthase as an antimalarial target. PeerJ. **7**, e6713
162 Jankowska-Dollken, M.*, et al.* (2019) Overexpression of the HECT ubiquitin ligase PfUT prolongs the intraerythrocytic cycle and reduces invasion efficiency of *Plasmodium falciparum*. Scientific Reports. **9**, 18333
163 Crabb, B.*, et al.* (2004) Transfection of the human malaria parasite *Plasmodium falciparum*. Methods in Molecular Biology. **270**, 263-276

7 Supplementary information

Generate recombinant plasmids of pGFP_*glmS* and pSLI_*glmS* with *k1* and *k2* gene fragments

Preparation of pGFP_*glmS* and pSLI_*glmS* plasmids for cloning procedures

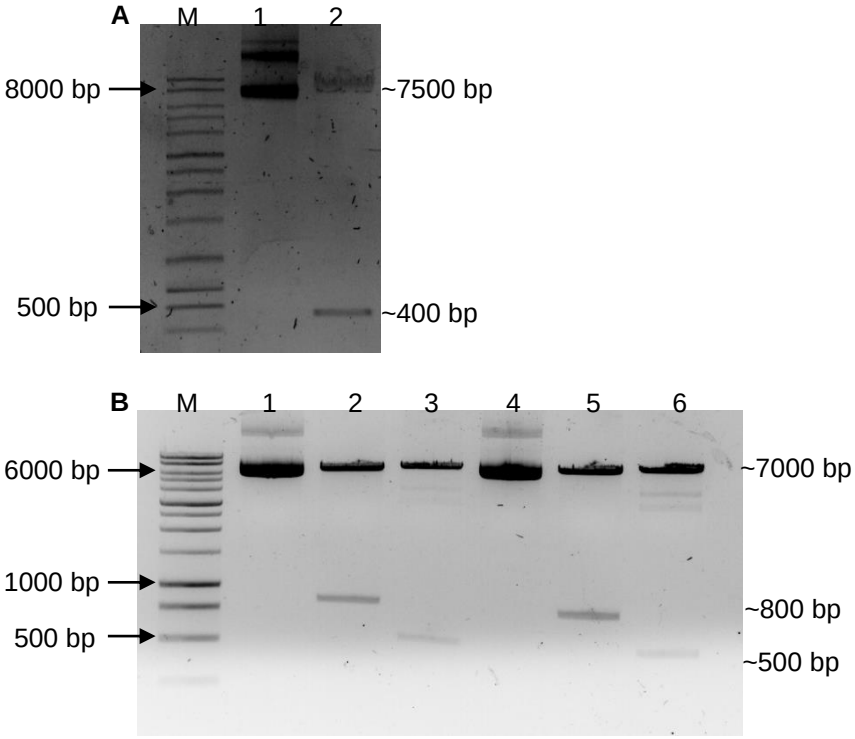

Supplementary Figure 1 associated with Figure 14 A) pGFP_*glmS* plasmid. M: 1 kb ladder (Promega™, Madison, USA). Lane 1: Uncut pGFP_*glmS* plasmid. Lane 2: Plasmid digested with *Bam*HI and *Hind*III B) pSLI_*glmS* WT & pSLI_*glmS* M9 plasmid. M: 1 kb ladder (Promega™, Madison, USA). Lane 1: Uncut pSLI_*glmS* WT plasmid. Lane 2: pSLI_*glmS* WT plasmid digested with *Not*I and *Mlu*I. Lane 3: pSLI_*glmS* WT plasmid digested with *Bam*HI and *Hind*III. Lane 4: Uncut pSLI_*glmS* M9 plasmid. Lane 5: pSLI_*glmS* M9 plasmid digested with *Not*I and *Mlu*I. Lane 6: pSLI_*glmS* M9 plasmid digested with *Bam*HI and *Hind*III. The DNA was separated with 1 % (w/v) agarose/TAE gel and visualised with EtBr (1.2 mg/mL) under UV light.

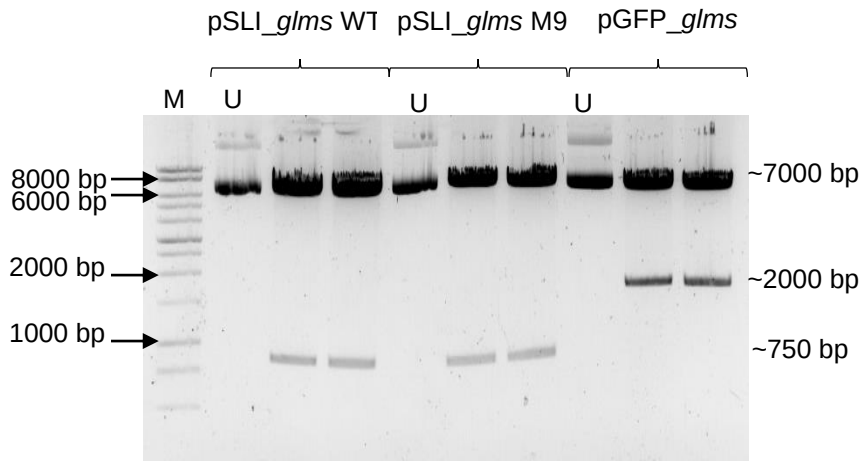

Supplementary Figure 2 associated with Figure 15 M: 1 kb ladder (Promega™, Madison, USA). U: Uncut plasmid. pSLI_*glmS* WT & pSLI_*glmS* M9 plasmid was digested with *Not*I and *Mlu*I. pGFP_*glmS* plasmid was digested with *Afl*II and *Kpn*I. The DNA was separated with 1 % (w/v) agarose/TAE gel and visualised with EtBr (1.2 mg/mL) under UV light.

Cloning of *k1* gene fragment into pGFP_*glmS*, pSLI_*glmS* WT and pSLI_*glmS* M9 to generate pGFP_*glmS_k1,* pSLI_*glmS* WT_*k1* and pSLI_*glmS* M9_*k1.*

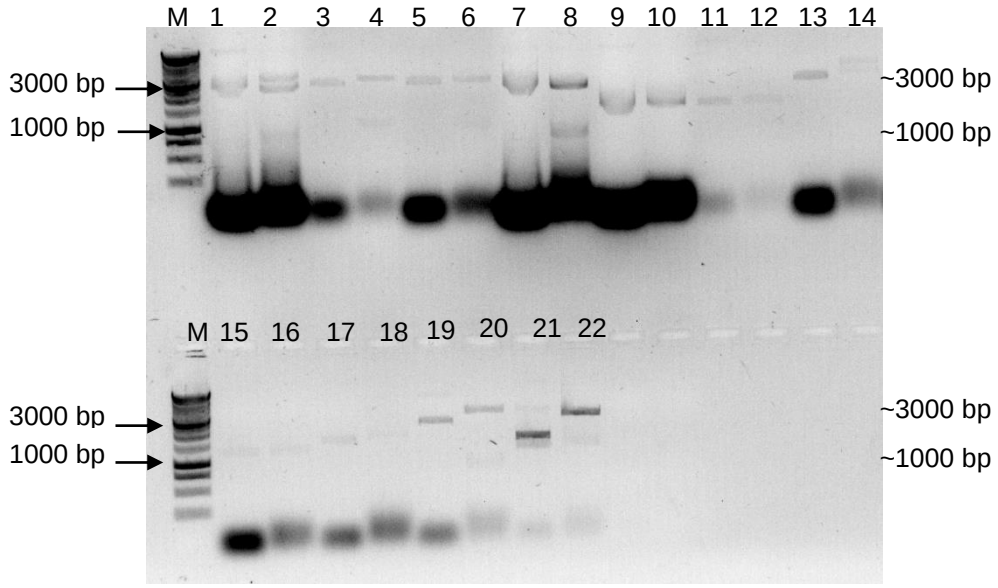

Supplementary Figure 3 associated with Figure 16 M: 1 kp ladder (Promega™, Madison, USA). Lane 1-22: pGEM T-Easy plasmid *k1* insert for pGFP_*glmS* digested with *Eco*RI. The DNA was separated with 1 % (w/v) agarose/TAE gel and visualised with EtBr (1.2 mg/mL) under UV light.

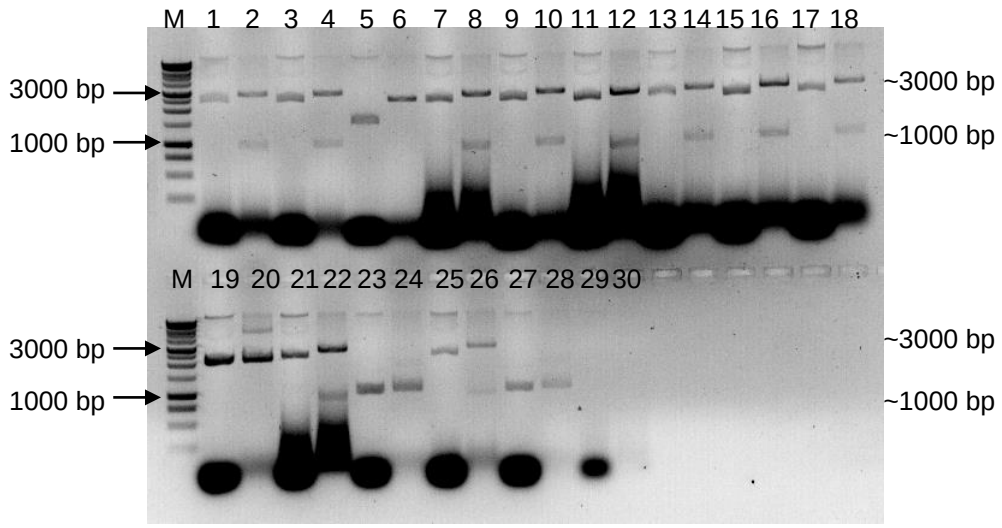

Supplementary Figure 4 associated with Figure 16. M: 1 kp ladder (Promega™, Madison, USA). Lane 1-30: pGEM®-T Easy plasmid *k1* insert for pSLI_*glmS* digested with *Eco*RI. The DNA was separated with 1 % (w/v) agarose/TAE gel and visualised with EtBr (1.2 mg/mL) under UV light.

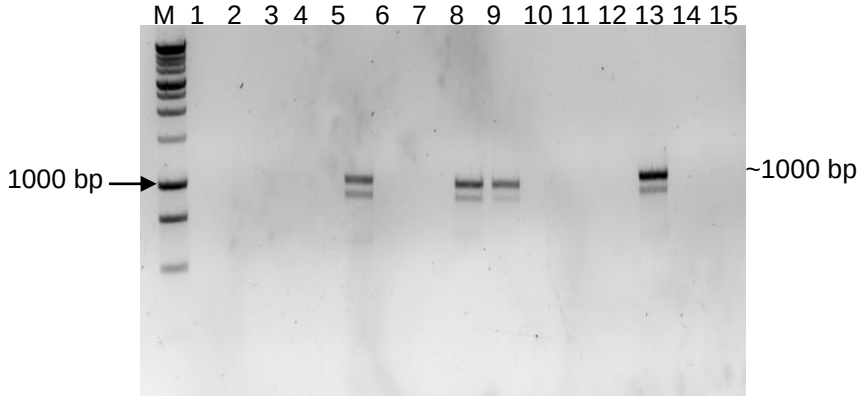

Supplementary Figure 5 associated with Figure 17. M: 1 kb ladder (Promega™, Madison, USA). Lane 1-5: Screening for positive clones containing pGFP_*glmS*, with C-terminal fragment. Lane 6-10: Screening for positive clones containing pSLI_*glmS* WT, with C-terminal fragment. Lane 11-15: Screening for positive clones containing pSLI_*glmS* M9, with C-terminal fragment. The DNA was separated with 1 % (w/v) agarose/TAE gel and visualised with EtBr (1.2 mg/mL) under UV light.

Cloning of *k2* gene fragment into pGFP*_glmS* and pSLI*_glmS* WT and pSLI*_glmS* M9 to generate pGFP*_glmS_k2,* pSLI*_glmS* WT*_k2* and pSLI*_glmS* M9*_k2.*

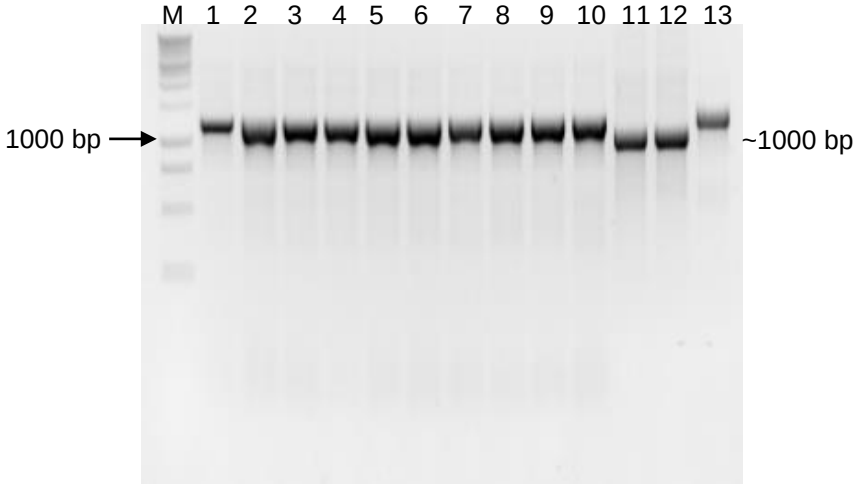

Supplementary Figure 6 associated with Figure 18. Colony screening PCR for positive clones containing the *k2* gene fragment in pSLI*_glmS* WT plasmid. M: 1 kb ladder (Promega™, Madison, USA). Lane 1-13: Screening for positive clones containing pSLI*_glmS* WT, with C-terminal fragment. The DNA was separated with 1 % (w/v) agarose/TAE gel and visualised with EtBr (1.2 mg/mL) under UV light.

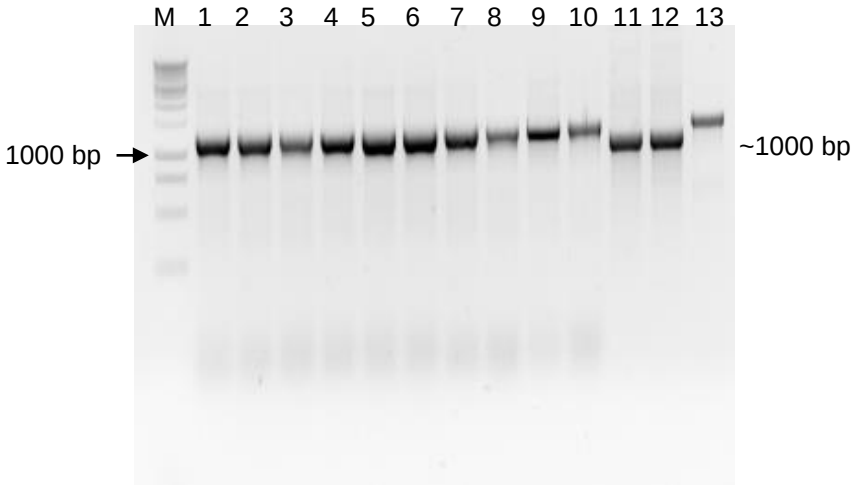

Supplementary Figure 6 associated with Figure 17. Colony screening PCR for positive clones containing the *k2* gene fragment in pSLI*_glmS* M9 plasmid. M: 1 kb ladder (Promega™, Madison, USA). Lane 1-13: Screening for positive clones containing pSLI*_glmS* WT, with C-terminal fragment. The DNA was separated with 1 % (w/v) agarose/TAE gel and visualised with EtBr (1.2 mg/mL) under UV light.